JRC Scientific and Technical Reports

Development of a data set for continental hydrologic modelling

Input layers related to topography, channel geometry, land cover and soil characteristics of European and African river basins

Katalin Bódis

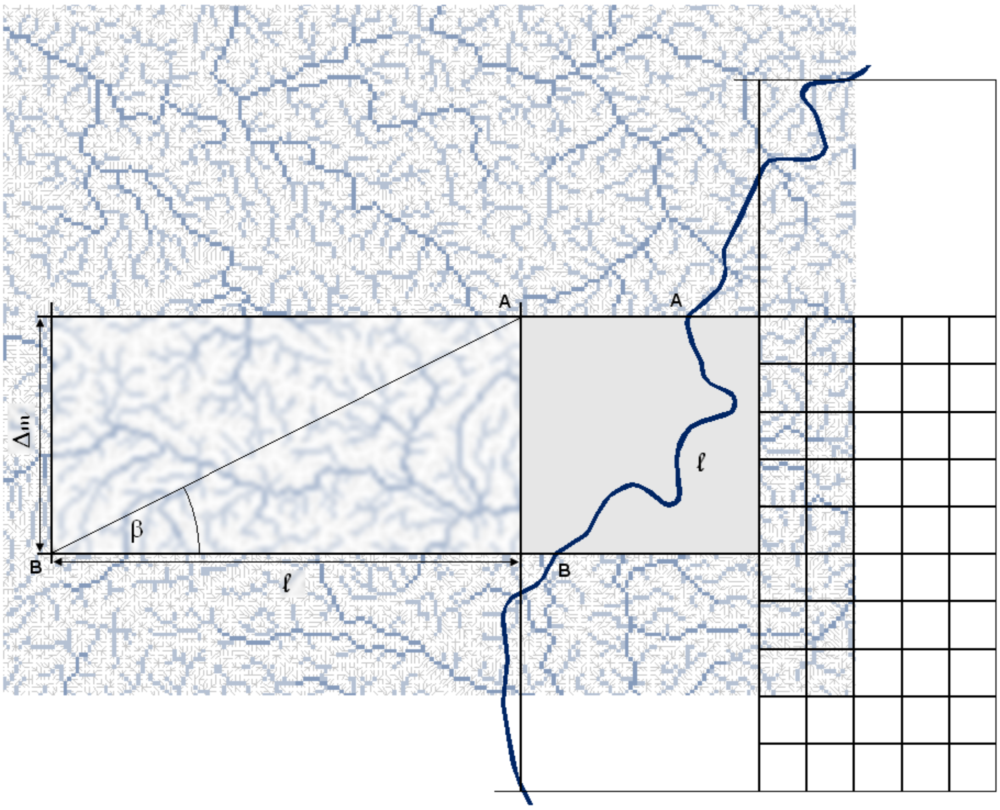

EUROPEAN COMMISSION

Institute for Environment and Sustainability

EUR 24087 EN - 2009

Development of a data set for continental hydrologic modelling

Input layers related to topography, channel geometry, land cover and soil characteristics of European and African river basins

The mission of the Institute for Environment and Sustainability is to provide scientific-technical support to the European Union's Policies for the protection and sustainable development of the European and global environment.

European Commission
Joint Research Centre
Institute for Environment and Sustainability

Contact information

Address:
Joint Research Centre, Via Enrico Fermi 2749, TP 261, 21027 Ispra (VA) Italy

E-mail: katalin.bodis@jrc.ec.europa.eu
Tel.: +39 0332 785009
Fax: +39 0332 786653

http://ies.jrc.ec.europa.eu/
http://www.jrc.ec.europa.eu/
http://floods.jrc.ec.europa.eu/

Legal Notice
Neither the European Commission nor any person acting on behalf of the Commission is responsible for the use which might be made of this publication.

Europe Direct is a service to help you find answers to your questions about the European Union

Freephone number (*):

00 800 6 7 8 9 10 11

(*) Certain mobile telephone operators do not allow access to 00 800 numbers or these calls may be billed.

A great deal of additional information on the European Union is available on the Internet. It can be accessed through the Europa server http://europa.eu/

JRC 55283

EUR 24087 EN
ISBN 978-92-79-14149-2
ISSN 1018-5593
doi:10.2788/46925

Luxembourg: Publications Office of the European Union

© European Union, 2009

Reproduction is authorised provided the source is acknowledged.

The cover figure symbolizes the methodology followed for definition of flow length in cell-based model. The background shows a section of modelled river network in Central Europe.

Printed in Italy

Development of a data set for continental hydrologic modelling

Input layers related to topography, channel geometry, land cover and soil characteristics of European and African river basins

Katalin Bódis

Institute for Environment and Sustainability

Land Management and Natural Hazards Unit

Action FLOOD

EUR 24087 EN - 2009

Table of Contents

List of Figures

List of Tables

List of Acronyms

Acronym	Description
CCM	Catchment Characterisation and Modelling
CIS	Catchment-based Information System
CLC2000	CORINE land cover 2000
D8	Deterministic 8 one-dimensional flow routing algorithm
DEM	Digital elevation model
DEM100	SRTM-based processed DEM in 100 m spatial resolution
DEM1KM	SRTM-based processed DEM in 1000 m spatial resolution
DEM5KM	SRTM-based processed DEM in 5000 m spatial resolution
EEA	European Environment Agency
ESDAC	European Soil Data Centre
ETC-LUSI	European Topic Centre on Land Use and Spatial Information
ETRS	European Terrestrial Reference System
FAO	Food and Agriculture Organization of the United Nations
GEM	Global Environment Monitoring unit of the European Commission, JRC
GIS	Geographical Information Systems
GISCO	Geographic Information System of the European Commission
GTOPO30	Global 30 Arc-Second Elevation Data Set
HWSD	Harmonized World Soil Database
IFSAR	Interferometric Synthetic Aperture Radar
IIASA	International Institute for Applied Systems Analysis
ISRIC	International Soil Reference and Information Centre
ISSCAS	Institute of Soil Science, Chinese Academy of Science
JRC	Joint Research Centre of the European Commission
LAEA	Lambert Azimuthal Equal Area
LCCS	Land Cover Classification System
LDD	Local Drain Direction
NASA	National Aeronautics and Space Administration of the United States
NGA	National Geospatial-Intelligence Agency of the United States
SGDBE	Soil Geographical Database of Eurasia
SMU	Soil Mapping Unit
SOTER	The global SOils and TERrain database
SRTM	Shuttle Radar Topography Mission
STU	Soil Typological Unit
UNESCO	United Nations Educational, Scientific and Cultural Organization
UPS	Upstream area, contributing area above a cells in a grid based on LDD
USGS	United States Geological Survey
WFD	Water Framework Directive
CGIAR-CSI	Consultative Group on International Agricultural Research - Consortium for Spatial Information

1 Introduction

The data set was created for the purpose of updating/processing static input layers for LISFLOOD model. The new data set contains gridded numerical and descriptive information related to topography, channel geometry, land cover and soil characteristics of European and African river basins. This document gives a brief summary of the source geo-spatial data sets, the applied methodology and main characteristics of the resulted data.

1.1 Model Requirements - Data Format, Geographical Extent, Spatial Resolution

The LISFLOOD model is a hydrological rainfall-runoff model that is capable of simulating hydrological processes that occur in a catchment. The model can be used in large and trans-national catchments for a variety of applications (flood forecasting, assessing the effects of river regulation measures, assessing the effects of land-use change, assessing the effects of climate change). LISFLOOD has been developed by the Floods group of the Natural Hazards Project of the Joint Research Centre (JRC) of the European Commission (van der Knijff and de Roo, 2008).

The LISFLOOD model is implemented in the PCRaster Environmental Modelling language (Wesseling et al., 1996). PCRaster is a raster GIS environment that has its own binary format raster called PCRaster map. Since the LISFLOOD model requires the spatial input data in this format (van der Knijff and de Roo, 2008), all the new geographic layers resulted by GIS operations within other software environments had to be converted into PCRaster map format.

A complete set of LISFLOOD base maps covering Europe have been compiled at 1 km and 5 km spatial resolution, thus the new input maps were created using the same cell-sizes. The resolution of new African data layers is 0.1 degree. The exact geographic extent of processed data is shown in maps in chapters 4 and 5 and given with coordinates in *Annex 6*.

1.2 Projection and Coordinate System

The reference systems of source data are usually different from the target system. Global layers (e.g. topography, global land cover, global soil database) are given in geographic coordinates, while European GIS layers are stored in the Lambert Azimuthal Equal Area (LAEA) projection with the ETRS 1989 datum. Data preparation and pre-processing of high resolution national data also included integration of geo-reference systems (Gierk et al., 2008). Since the modelled area extends over several administrative regions and countries it was necessary to specify a common reference system, which is also corresponding to the European standards (Annoni et al., 2001). Based on available data and map projections, the Lambert Azimuthal Equal Area Coordinate Reference System used by EUROSTAT-GISCO (Annoni et al., 2001) has been selected as a common reference system of the elaborated European data set. The GISCO Lambert Azimuthal Equal Area projection is characterised by the following parameters:

Projection Name: .... GISCO_LAEA
Projection Type: .... Lambert Azimuthal Equal Area
Spheroid: .... Sphere
Radius of sphere of reference: 6378388
Units: .... meters
Longitude of centre of projection: ... 09° 00' 00"
Latitude of centre of projection: ...... 48° 00' 00"
False easting: 0.0
False northing: 0.0

The African data set is kept in the source geographic coordinates with the WGS 1984 datum. PCRaster map format does not store the definition or parameters of the applied projection; the geographic location is given only by coordinates related to the mentioned reference systems.

2 Source European and Global Data Sets

The aim of this chapter is to provide background information about the main characteristics of source geo-spatial data sets that were further processed in order to update/create input data layers for LISFLOOD model. The brief summary contains important details about the original reference systems, original scales and spatial resolution, the date of surveying and publishing. Developers and users can equally find useful the indicated references to the available data sources; becoming aware of advantages and limitations of applications. Future improvements of LISFLOOD input data set could be done using the updated versions of data presented in the following pages.

2.1 Shuttle Radar Topography Mission (SRTM)

The Shuttle Radar Topography Mission (SRTM) obtained elevation data on a near-global scale (between N60 and S57 degree) to generate the most complete high-resolution digital topographic database of Earth. The project was a joint endeavour of NASA, the U.S. National Geospatial-Intelligence Agency (NGA), and the German and Italian Space Agencies, and flew in February 2000. It used dual radar antennas to acquire interferometric radar data (IFSAR), processed to digital topographic data at 1 arc-sec resolution (Farr et al., 2007).

Calibration, verification and detailed error analysis (errors resulted by calibration, absolute and relative altitude error, errors resulted by the geographical location, random errors, error distribution) of SRTM data have been completed in the NASA Jet Propulsion Laboratory (Rodriguez et al., 2005, Rodriguez et al., 2006). Following a longer period of processing the first version of digital topographic data was published in January 2003. Since the release of the public version the data was significantly improved and published as new versions of the original terrain elevation data (Slater et al., 2006).

According to the NASA-NGA agreement on data distribution the SRTM tiles have been released in 3 arc-sec (~90 m) resolution for areas outside the United States and full resolution 1 arc-sec (~30 m) for the area of the United States. The vertical resolution of the data is a metre. Specified accuracy requirements for the released final product (SRTM V2) were 16 m absolute vertical error (90 percent linear error, with respect to the reflective surface), 20 m absolute horizontal error (90 percent circular error) and 10 m relative vertical error (90 percent linear error). Estimated vertical accuracy values fall between 3 and 15 meters, with 99.4 percent of the cells having absolute vertical accuracies of 10 m or less (Slater et al., 2006). Further editing processes eliminated many of the voids in the unfinished data through interpolation and by defining water bodies (Grohman et al., 2006; Luedeling et al., 2007; Reuter et al., 2007; Vogt et al., 2007; Vrščaj et al., 2007).

The files of SRTM data as a public topographic database may be obtained through the Internet (URL: http://dds.cr.usgs.gov/srtm). Besides elevation data, appropriate documentation and references are also available. The “highest quality SRTM data set” is available from the website of the Consortium for Spatial Information (CGIAR-CSI): http://srtm.csi.cgiar.org.

The tiles of SRTM data were processed and applied for upgrading the previously used digital elevation model and its derivatives which originally based on the GTOPO30 - Global 30 Arc-Second Elevation Data Set (USGS 2009).

2.2 Catchment-based Information System (CIS) – Flow Network

The 1 km gridded flow network developed in the frame of research activity to design and implement a Catchment-based Information System (CIS) forms an essential component in the development of catchment-scale and European-wide flood simulation and forecasting models (Hiederer and de Roo, 2003).

The main input data of the LISFLOOD model regarding the graph of flow network and flow direction of the analysed surface is the so-called Local Drain Direction map (van der Knijff and de Roo, 2008). In cell-based models this data layer contains flow directions from each cell to its steepest downward neighbour using the Deterministic 8 (D8) one-dimensional flow routing algorithm (O'Callaghan and Mark, 1984), however this method shows an obvious bias towards the cardinal (orthogonal) directions against the intermediate (diagonal) directions (*Figure 1*). This essential layer of river routing network was provided by the CIS. The river routing network defines neighbourhood relations of all elements in a gridded data set. A catchment is determined by the array of cells, which are connected by an uninterrupted thread of neighbouring cells (Hiederer and de Roo, 2003). This concept fulfils the requirements against flow path and channel network representation/simulation of LISFLOOD where each cell of the catchment shall be characterised by runoff attributes and for each flow path, the routing stops at the first downstream pixel that is part of the channel network (the flow network has no loops nor intersections).

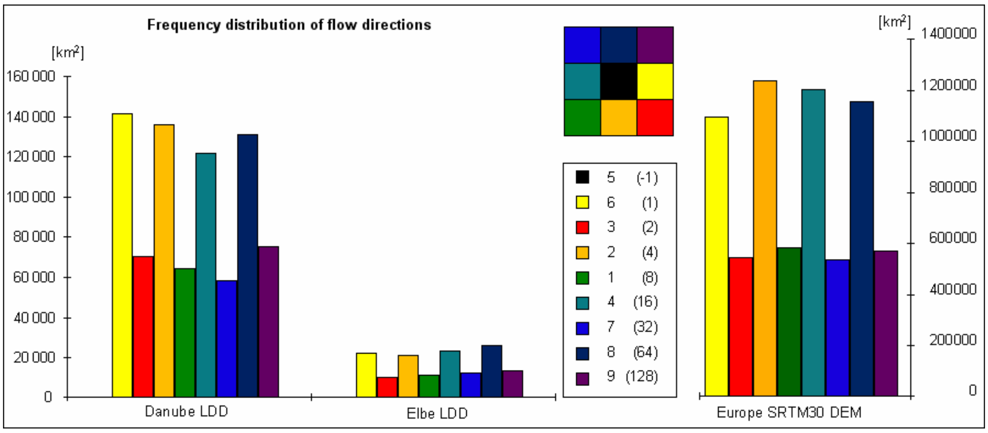

Figure 1 Frequency distribution of flow directions (D8) in the Danube and the Elbe Basins, compared to the pattern of frequency of flow directions calculated for Europe. (Numerical codes: LDD in PCRaster. Numbers between brackets: flow directions in Arc/Info)

For the determination of river routing network and for the delineation of catchments and sub-catchments a "stream burning" method was applied involving a digital elevation model and a reference river network developed for the purposes of the Catchment-based Information System. The vector-based auxiliary network was built starting with commercially available data sets. The river data was further developed to ensure connectivity of rivers within a river system, separation of different systems in the raster representation and a single defined outlet (Hiederer and de Roo, 2003).

Among other applications the 1 km gridded flow network developed in the CIS has been being applied in the LISFLOOD hydrological rainfall-runoff model in large trans-national catchments and European-wide flood simulation and forecasting (Hiederer and de Roo, 2003). The 5 km resolution flow network of LISFLOOD model was generated based on the CIS 1 km gridded data set, using the modelled flow directions, flow accumulation and derived streams in the generalization procedure.

2.3 Pan-European River and Catchment Database

The Pan-European River and Catchment Database was developed by the Catchment Characterisation and Modelling (CCM) activity of the Joint Research Centre (JRC) (Vogt et al., 2007a).

In order to derive high quality river networks and catchment boundaries, the 3 arc-second digital elevation model from the Space Shuttle Radar Topography Mission (SRTM) has been processed. The original one degree tiles have been projected, re-sampled and tessellated into a Lambert Azimuthal Equal Area projection with a grid-cell resolution of 100 metres. In order to cover the area north of 60 degrees latitude, which is not covered by SRTM, the processed data has been extended with national DEMs from Norway, Sweden, and Finland at 100 metre grid-cell resolution and USGS GTOPO30 data at 1000 metre grid-cell resolution for Iceland and the Russian territory (Vogt et al., 2007b).

The 100 m gridded flow network has been extracted from the DEM using algorithms based on the concepts of mathematical morphology (Soille, 2004a). Spurious pits have been removed by an optimal combination of carving and pit filling procedures (Soille, 2004b). River positioning in flat areas have been implemented by a developed adaptive drainage enforcement algorithm (Soille et al., 2003). For the advanced “stream burning” method in flat areas a so-called reference layer was applied. The applied reference layer consisted of a compilation of Water Framework Directive (WFD) Article 3 data (main rivers), GISCO river data at 1:3,000,000 scale. Both data sets were edited and completed by in-house digitised rivers from Image2000 (Vogt et al., 2007b).

The CCM database covers the entire European continent, including the Atlantic islands, Iceland and Turkey. It includes a hierarchical set of river segments and catchments, a lake layer and structured hydrological feature codes based. The CCM data are freely available for non-commercial use. The data and information on the development and characteristics of the database are available from the JRC website: Catchment Characterisation and Modelling, URL: http://desert.jrc.ec.europa.eu/action/php/index.php?action=view&id=23

The generated seamless pan-European digital elevation model with the resolution of 100 metres and the derived cell-based flow network provide the topographical and hydrographical background for LISFLOOD for flood extent and depth-damage calculations for flood hazard and flood risk evaluation based on predefined projections of climate change (Vogt et al., 2007a). The Local Drain Direction maps in PCRaster format were transformed from the CCM flow direction layers which were computed by using the traditional D8 algorithm. Since the coding of directions are different in different systems, besides the data format the value-set of the raster has been altered too (*Figure 2*).

7	8	9
4	5	6
1	2	3

a) PCRaster

32	64	128
16	-1	1
8	4	2

b) Arc/Info GRID

7	8	1
6		2
5	4	3

c) SAGA

5	3	7
1		2
6	4	8

d) CCM

Figure 2 Coding of flow directions in three cell-based GIS and the codes in CCM

In a raster system the assigned flow directions usually do not indicate the geographical four cardinal and four intermediate quarters of the globe. Depending on the applied projection, the location of the point of origin of the coordinate system and the location of the given cell, the flow-direction codes signify only relative directions comparing to the central pixel.

2.4 CORINE Land Cover

LISFLOOD input maps related to land use (land cover map with land cover classes, map with forest fraction for each cell and map with fraction of urban area) were created using the European 'Corine land cover 2000 (CLC2000) 100 m - version 12/2009' data set. The source data was processed by the European Topic Centre on Land Use and Spatial Information (ETC-LUSI) and published by the European Environment Agency (EEA) in September 2009.

The CORINE data classifies the land cover types into 44 classes using the methodology described in the 'CORINE land cover technical guide – Addendum 2000' (EEA, 2000). The spatial resolution of the gridded CLC2000 is 100 m. The data is available in the Lambert Azimuthal Equal Area (LAEA) projection with the ETRS 1989 datum.

The CLC2000 data covers the European territories of the member states of the European Union extended by the area of Albania, Bosnia and Herzegovina, Croatia, Kosovo, former Yugoslav Republic of Macedonia, Iceland, Liechtenstein, Montenegro, Norway, San Marino, Serbia (*Figure 3a*). In order to carry out European-wide hydrological modelling by LISFLOOD the land cover types of river basins not covered by CORINE (e.g. Upper-Rhine and Upper-Rhone in Switzerland, Danube sub-catchments in Ukraine and Moldova, other catchments in Belarus, Russia, Turkey and Norway) had to be defined using an additional land cover database.

2.5 Global Land Cover

The Global Land Cover 2000 (GLC2000) database (GEM, 2003) has been chosen to extend the missing areas of the European land cover database. The general objective of the GLC2000 was to provide a harmonized land cover database covering the whole globe for the year 2000 to the International Convention on Climate Change, the Convention to Combat Desertification, the Ramsar Convention and the Kyoto Protocol. The GLC2000 product and documentation are available from the website of the producer Global Environment Monitoring Unit (GEM) of the European Commission, Joint Research Centre (GEM, 2003).

The GLC2000 project used the FAO Land Cover Classification System (LCCS) which differs from the classes applied in CORINE. The source data is defined by geographic coordinates (Lat/Lon, WGS84). The spatial resolution is ~1km at the Equator (0.00833 decimal degrees). *Figure 3b* shows the GLC2000 using the "statistically corresponding" land cover classes of CORINE.

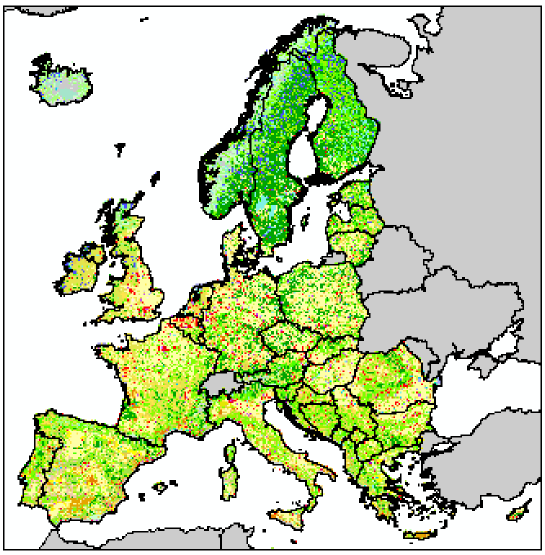

Figure 3a Geographical coverage of CORINE land cover (version 12/2009, EEA)

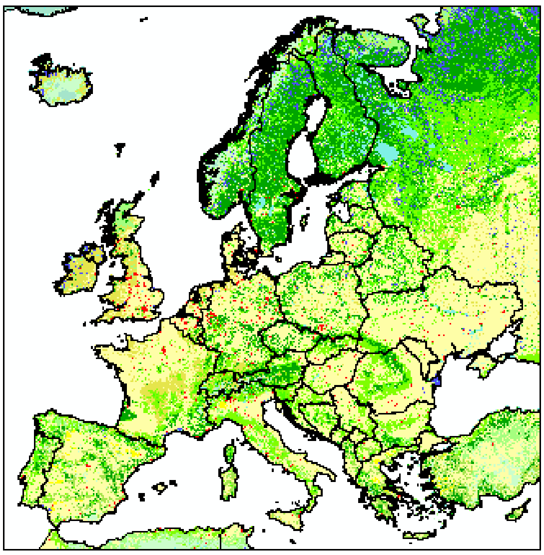

Figure 3b Global Land Cover 2000 (Source of data: GEM, 2003)

2.6 Soil Geographical Database of Eurasia

The Soil Geographical Database of Eurasia (SGDBE) forms the core of the European Soil Information System (Lambert et al., 2003; Panagos 2006, van Liedekerke et al. 2007), developed by the Land Management and Natural Hazards Unit of the Institute for Environment and Sustainability of the Joint Research Centre. The database is managed in the European Soil Data Centre (ESDAC) by the action 'Soil Data and Information Systems' (Action SOIL).

The database contains a list of Soil Typological Units (STU), characterizing distinct soil types that have been identified and described. The STU are described by attributes (variables) specifying the nature and properties of the soils, for example the texture, the moisture regime, the stoniness, etc. The scale selected for the geographical representation of the SGDBE is the 1:1,000,000. For easy GIS applications of the database a data set conversion has been performed. Based on the non-spatial components of the SGDBE a new data set was created for further analyses (Tóth et al., 2008). The polygon attribute table of SGDBE (the attribute table of the spatial component) was extended by the stored information of all the occurring Soil Typological Units (STUs) within the given Soil Mapping Unit (SMU) using sequential table-operations in SQL (Tóth et al., 2008).

The detailed instruction guide (Lambert et al., 2003) of the inventory as well as the data and documentation are available from the EU Soil Portal: http://eusoils.jrc.ec.europa.eu.

The Soil Geographical Database of Eurasia provided the basis for the gridded European soil layers (soil textures, soil depth) as input maps of LISFLOOD model.

2.7 World Harmonised Soil Database

Input maps of LISFLOOD model related to soil information of non-European territories were generated based on the Harmonized World Soil Database (HWSD) developed by the Land Use Change and Agriculture Program of IIASA (LUC) and the Food and Agriculture Organization of the United Nations (FAO).

The HWSD is a 30 arc-second raster database with over 16000 different soil mapping units that combines existing regional and national updates of soil information worldwide – the European Soil Database (ESDB), the 1:1 million soil map of China, various regional SOTER databases (SOTWIS Database), and the Soil Map of the World – with the information contained within the 1:5000000 scale FAO-UNESCO Soil Map of the World. The resulting raster database consists of 21600 rows and 43200 columns, which are linked to harmonized soil property data (FAO/IIASA/ISRIC/ISSCAS/JRC, 2009).

In order to prepare a data set of African river basins the soil layers were produced based on the Harmonized World Soil Database v 1.0 in the required 0.1 degree grid resolution (See more: Chapter 3.10, Soil Map). The WHSD v 1.1 was published in March, 2009.

2.8 High Resolution Data from Member States of the European Union

The LISFLOOD input maps related to channel geometry were improved using high resolution geo-data provided by the responsible national institutes. The master data of gauging stations containing their geographical locations in coordinates as well as in river kilometres, spatial attributes of reservoirs and cross-sections describing the riverbed geometry in high resolution enabled a more realistic estimation of gridded geometric parameters of main rivers in the 1 km and 5 km resolution model. The original data formats and reference systems were very different. The data integration and harmonization involved error detection, error correction (if it was possible) and re-projections (Wachter, 2006; Gierk et al., 2008).

3 Methodology and Data

Different sources, types and characteristics of input data required different processing methodologies. Most of the GIS operations and described processes were completed within the Arc/Info Workstation 9.3 environment. Raster data were analysed and processed in 'Grid' module of Arc/Info 9.3, while the tabular data were analysed and processed in 'Tables' module of Arc/Info and ArcView GIS 3.2. Automatized calculations were carried out using Arc Macro Language (AML) within Arc/Info, Avenue within ArcView GIS 3.2 and Linux shell scripts with embedded GDAL utilities (Geospatial Data Abstraction Library).

3.1 Overview of the Methodology

The European and the African data sets were processed using similar spatial operations. The most significant dissimilarity between the two data sets is that while the European data set was processed in the metre-based LAEA reference system, the African data set was kept in the source geographic coordinate system. This feature had to be taken into consideration in all the calculations using/resulting values in metrical scale (horizontal length calculations on the spheroid, gradient estimations, area-definitions, etc.). The characteristics and differences of given spatial value sets also predefined the allowed numerical and spatial operations. The input data could be classified in three measuring scales.

a) Nominal Scale

A nominal scale is a list of categories to which objects can be classified. No quantitative information can be conveyed and no ordering of the items can be implied. E.g. land cover classes and the classified D8 flow directions are belonging to this type. It makes no sense to do arithmetical operation using the arbitrary numerical codes of the classes.

b) Ordinal Scale

Measurements with ordinal scales are ordered in the sense that higher numbers represent higher values. However, the intervals between the numbers are not necessarily equal. E.g. the soil texture classes (coarse, medium, medium fine, fine, very fine) are measured in ordinal scale. The assigned values to classes based on their ranking with respect to one another, but no further arithmetical operation can be performed.

c) Ratio Scale

A ratio scale is defined as a measurement scale in which a certain distance along the scale means the same thing no matter where on the scale we are. There is a natural zero point of the scale. Physical measurements of height, length, weight are typically ratio variables. Arithmetical operations including taking ratios among ratio scaled variables are allowed. Values of digital elevation models, gradient maps, maps of river length, etc. are measured in ration scale.

The raster input data can be treated as gridded information of 'continuous phenomena' (e.g. ground surface) or 'discrete phenomena' (e.g. polygons of land cover classes). Accordingly resampling of data can be completed by different strategies; central sampling, taking the mean of the input values or defining the spatially dominant phenomenon. Other, predefined resampling rules (e.g. calculating the standard deviation or skewness of distribution) can be followed too.

3.2 Digital Elevation Model (DEM)

In the previous phases of hydrological modelling of large river basins a GTOPO30-based global digital elevation model was processed (projection, resampling to 1km and 5 km resolutions) and expanded by available higher resolution DEMs from a few regions of Europe (Hiederer and de Roo, 2003). This data set contained visible errors (*Figure 4*) and artifacts (e.g. edges of maps, terrain stairs) but provided a more or less uniform coverage of the continent.

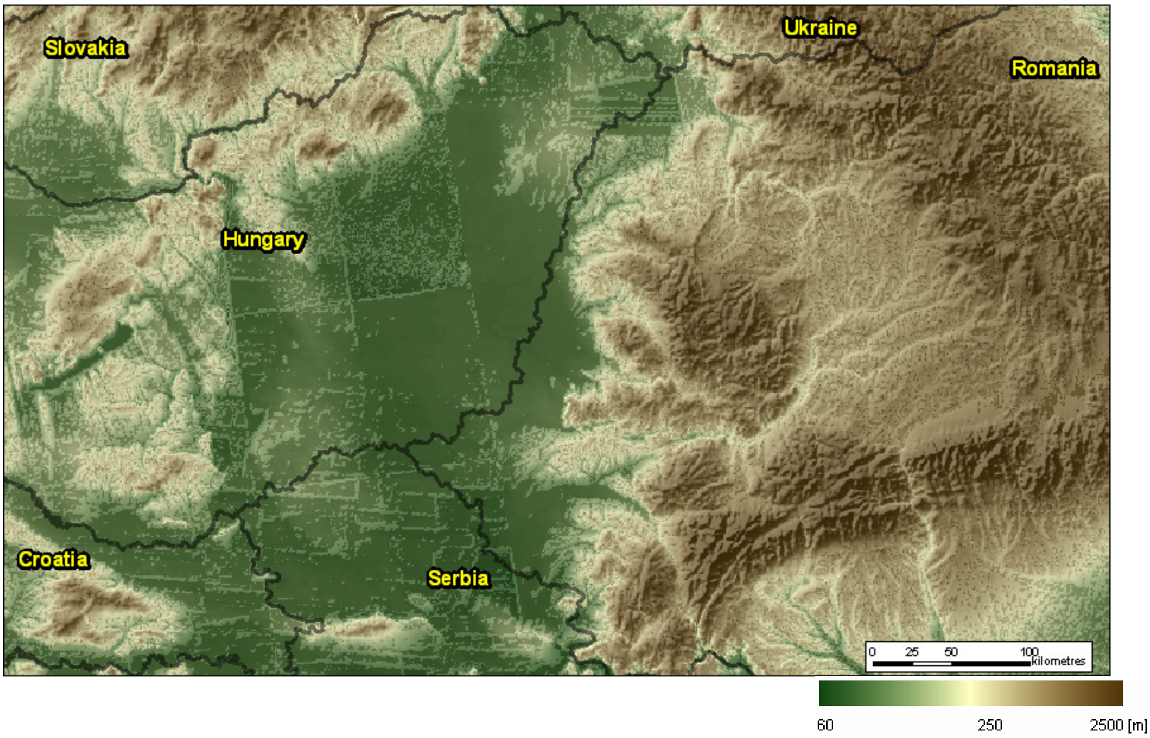

Figure 4 The Central and Easter Carpatian Basin presented in GTOPO30 DEM (horizontal resolution is 1 km, vertical resolution is 1 m)

The GTOPO30-based 1 km resolution data was changed to an SRTM-based DEM (*Figure 5*) that was prepared (format conversion, void filling, projection, resampling) within the Institute for Environment and Sustainability of the Joint Research Centre (Vogt et al., 2007a). The resulted DEM in 100 m resolution was re-projected again into the GISCO Lambert Azimuthal Equal Area projection and that product (DEM100) formed the basis of further operations.

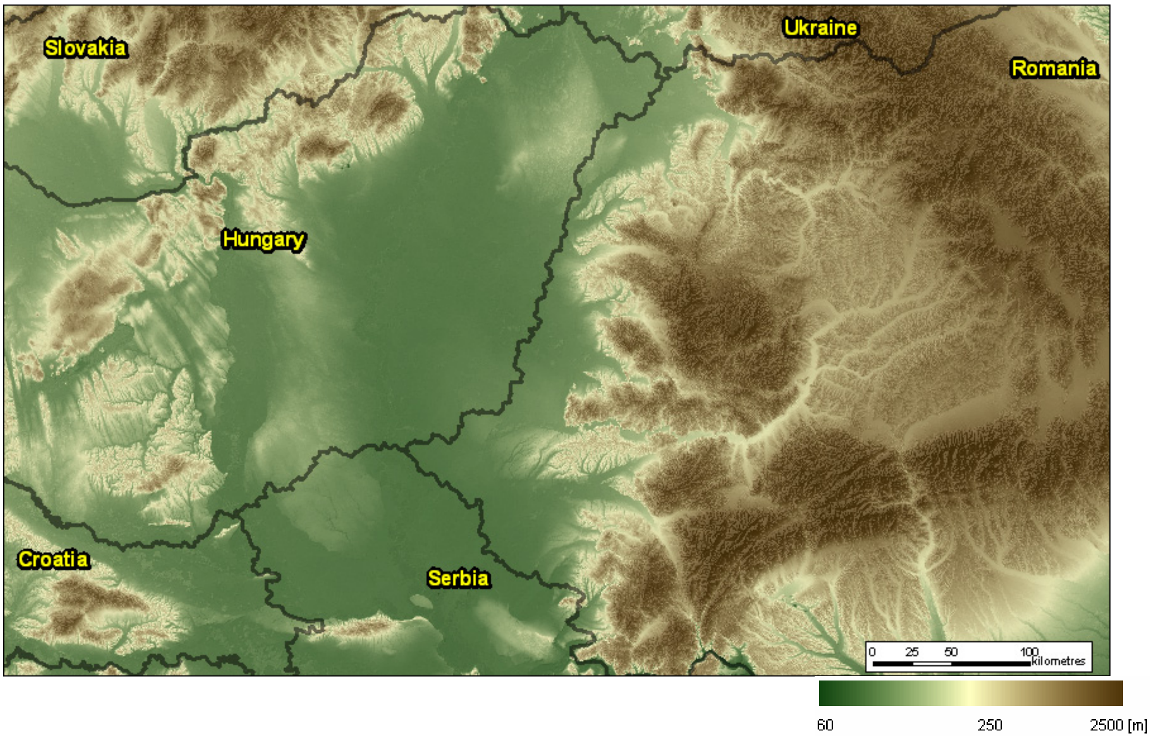

Figure 5 The Central and Easter Carpatian Basin presented in SRTM3 DEM (horizontal resolution is 100 m, vertical resolution is 1 m)

3.2.1 Regular Resampling – Central Phenomenon

The pre-processed DEM100 was resampled to 1 km and 5 km gridded data using two methodologies. Continouos surfaces (as the terrain is considered apart overhanging rock walls) are frequently represented by regularly spaced points. Resampling 10x10 (50x50) elevation values from the DEM100 into DEM1KM (DEM5KM) the corresponding methodology is to select a well-defined location (e.g. lower left cell, central cell) within the finer grid and assign its value to the cell from the coarser grid. When there are even-numbered finer cells within the coarser cell, an additional rule can be implemented, e.g. the lowest right value closest to the centre is assigned to the larger pixel. This method was applied to create the DEM1KM_CENT and DEM5KM_CENT elevation models in 1 km and 5 km resolutions. The spatial resampling has naturally altered the cardinality of the input value set and the range of values (*Table 1*).

Table 1 *Comparison of the value sets of the source and resampled DEMs*

	DEM100	DEM1KM_CENT	DEM5KM_CENT
Number of Values	4508	3661	2835
Minimum Value	-10.000	-10	-10.000
Maximum Value	4669.000	4562.000	4092.000
Mean	331.305	331.304	331.314
Standard Deviation	375.737	375.703	375.928

3.2.2 Resampling by Average Values

Some applications of digital terrain models in coarser resolution (e.g. snow accumulation and melt modelling) require the information of mean altitude of the modelled area by averaging the heights of all grid points of the finer surface model. This operation certainly smoothes the terrain and modifies the value set of the source elevation model (*Table 2*).

Table 2 *Comparison of the value sets of the source and averaged DEMs*

	DEM100	DEM1KM_MEAN	DEM5KM_MEAN
Minimum Value	-10.000	-10.000	-9.250
Maximum Value	4669.000	4443.010	3539.372
Mean	331.305	327.019	318.149
Standard Deviation	375.737	373.552	363.295

In order to provide additional information to the averaged elevation, three auxiliary grids were generated using aggregate functions that partition the input higher resolution grid into blocks, calculate the new values for the specified cells within the blocks, and send it to the cell-locations in the corresponding blocks on the output coarser grid. The standard deviation, the relative relief and the skewness of distribution of values were calculated for each cell for a fixed set of non-overlapping windows. The defined neighbourhood parameters were 10x10 and 50x50 cell-sized blocks corresponding to the target 1 km and 5 km resolution.

3.2.3 Standard Deviation

The map of standard deviation of averaged values was calculated in order to present how widely the values are dispersed from the arithmetic mean value in each resampled cell.

The standard deviation (σ) was computed using the following formula, where N is equal to 100 or 2500 depending on the output resolutions (1 km or 5 km).

$$\sigma = \sqrt{\frac{1}{N}\sum_{i=1}^{N}(x_i - \bar{x})^2}$$

x_i - individual cell-values of the source DEM100,

$\bar{x}$ - arithmetic mean of the represented 100 (2500) values.

3.2.4 Relative Relief

The relative relief is defined as the biggest vertical difference within a given area. As relative relief express the potential energy available for downslope transport, it is also called relief energy (Hagedorn, 1985). It can be calculated from the difference between the maximum and minimum altitude within a moving window or for a fixed set of non-overlapping windows accordingly to the output resolution (1 km - DEM1KM_RR, 5 km - DEM5KM_RR). *Table 3* summarizes the main statistical characteristics of resulted value sets.

Table 3 *Comparison of relative relief data in 1 km and 5 km resolution*

	DEM100	DEM1KM_RR	DEM5KM_RR
Number of Values	4508	1198	2110
Minimum Value	-10.000	0.000	0.000
Maximum Value	4669.000	1791.000	2999.000
Mean	331.305	75.493	220.272
Standard Deviation	375.737	107.175	290.973

The relative relief map is equal to the 'elevation range map' required by LISFLOOD describing the difference between maximum and minimum elevation within a modelled pixel in metre (van der Knijff and de Roo, 2008).

The same methodology was applied on a subset of the DEM100 representing the gridded flow network in 100 m resolution. The relative relief within the river segments provided the maximum difference in elevation to calculate the channel gradient.

3.2.5 Skewness

The skewness of a distribution characterizes the degree of asymmetry of a distribution around its mean. Positive skewness indicates a distribution with an asymmetric tail extending toward more positive values (relatively few large data values). Negative skewness indicates a distribution with an asymmetric tail extending toward more negative values (relatively few low data values).

For a sample of *n* values the sample skewness (γ) is defined and calculated as:

$$\gamma = \frac{1}{(N-1)\sigma^3} \sum_{i=1}^{N} (x_i - \bar{x})^3$$

where x_i is the i^th individual cell-value of the source DEM100, $\bar{x}$ is the arithmetic mean of the represented 100 (2500) values (*N*) and σ is the standard deviation of the sampled values.

The main characteristics of the calculated skewness values are the followings:

skw_srtm_1km.map - Minimum= -9.949, Maximum= 9.949, Mean=0.160, StdDev=0.730
skw_srtm_5km.map - Minimum=-18.026, Maximum=35.327, Mean=0.294, StdDev=0.814

Since the elevation data is strongly generalized due to the coarse resolution (1 km and 5 km) of the digital elevation models, the additional statistical information of the aggregated finer elevation values was produced on purpose to provide auxiliary information for estimations of further input data related to topography, e.g. altitude correction in temperature interpolation, definition of sub-pixel elevation zones for snow accumulation and melt modelling (van der Knijff and de Roo, 2008).

3.3 Slope Gradient

Slope gradient shows the maximum rate of change in value from each cell to its neighbours. The applied slope function calculates the slope gradient for each cell on basis of the digital elevation model fitting a plane to the z values of a 3x3 cell neighbourhood around the processing or centre cell. The direction the plane faces is the aspect for the processing cell. The slope gradient for the cell is calculated from the 3x3 neighbourhood using the average maximum technique (Burrough, 1986). An output slope gradient grid can be calculated as percent slope or degree of slope. Slope function using the described algorithm is usually available in every GIS software application.

The previous surface gradient map inherited the errors from the source GTOPO30 DEM. In spite of the gradient values of some areas were replaced by values derived from more accurate national data (*Figure 6*) it did not provide a consistent European coverage.

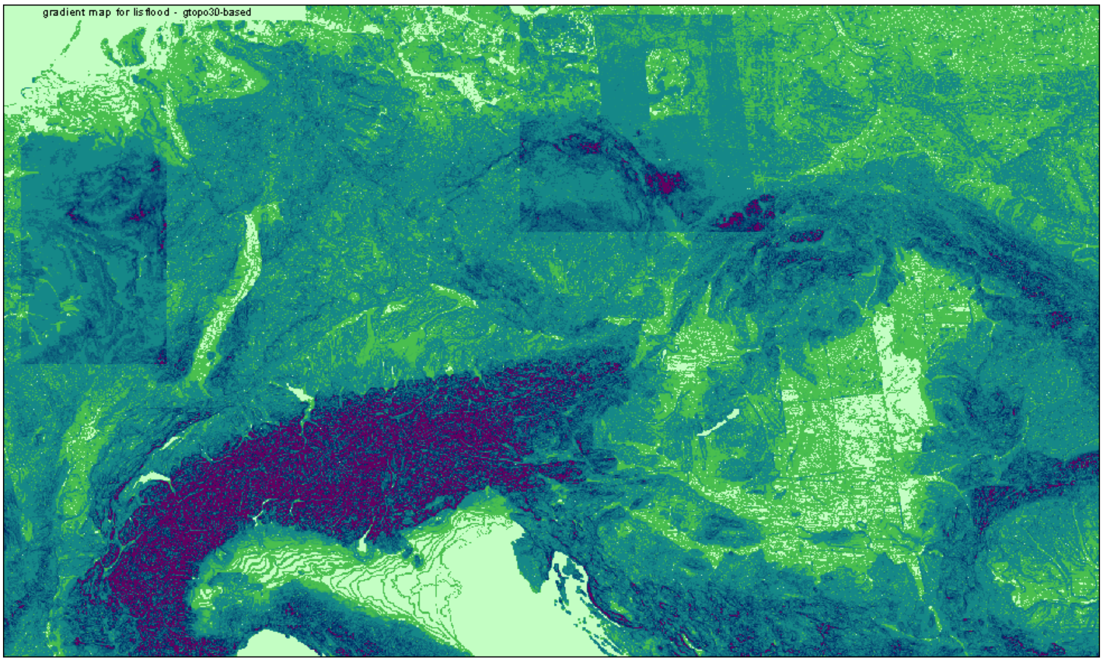

Figure 6 Surface gradient map (1km) as a derivative of GTOPO30 and national DEMs

Preparing slope gradient maps in 1 km and 5 km resolution grid using SRTM-based 100 m resolution digital elevation model (DEM100) as input data, first the gradient value of each cell in 100 m resolution was calculated, then those values were aggregated (averaged) in order to define the cell-values of the coarser resolution (1 km, 5 km) grids (*Figure 7*). According to the model requirements the final slope gradient is given as the tangent of slope in degrees (van der Knijff and de Roo, 2008).

The main characteristics of the processed gradient values are the followings:

gradient_1km.map - Minimum=0.000, Maximum=1.362, Mean=0.079, StdDev=0.107
gradient_5km.map - Minimum=0.000, Maximum=0.698, Mean=0.079, StdDev=0.097

In case of the African river basins the calculation of the input slope gradient map has been done within the degree-based geographic coordinate system. Since the horizontal and the vertical map units were not the same (degree and metre) in the source high resolution elevation data, a so-called z-factor was applied for each defined circle of latitude (see also *Annex 1*). This attribute was taken into consideration during the calculations compensating the changes of cell-size in metrical scale getting farther from the Equator. The resulted slope values were averaged and resampled to the target 0.1x0.1 degree resolution gradient map.

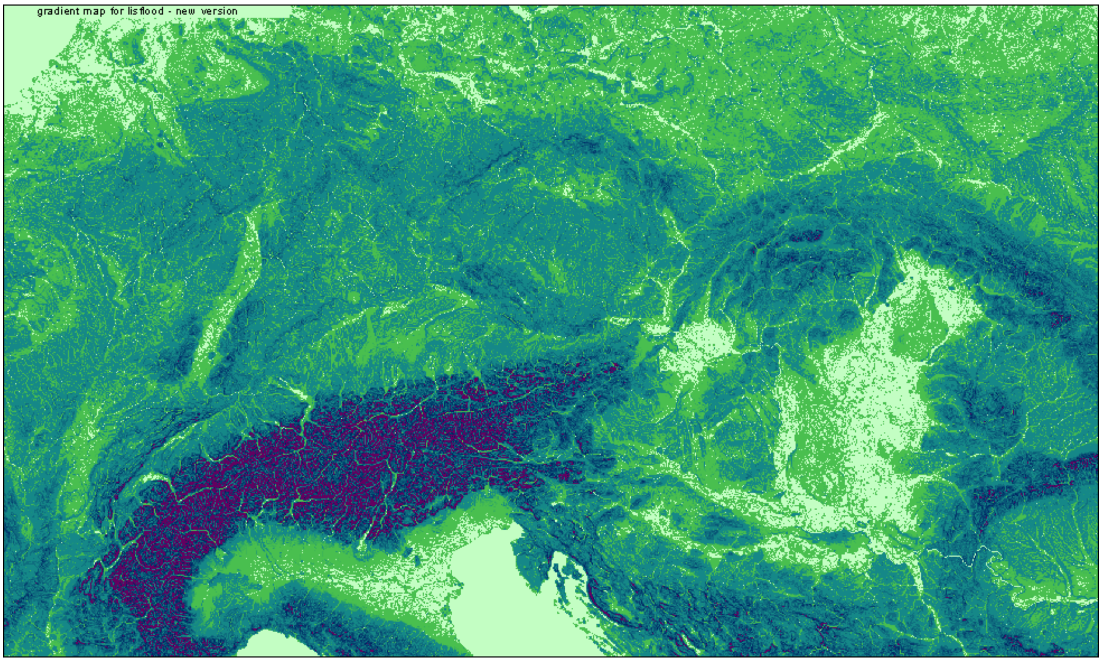

Figure 7 Catch of the surface gradient map derived from SRTM100 DEM

3.4 Channel Gradient

Two components must be defined in order to approximate the channel gradient for each cell of the flow network model in the resolution of 1 km and 5 km. The first component is the terrain-based 'difference in elevation' while the second component is the flow length within a cell estimated by length of vectors in a proper river network data set (*Figure 8*).

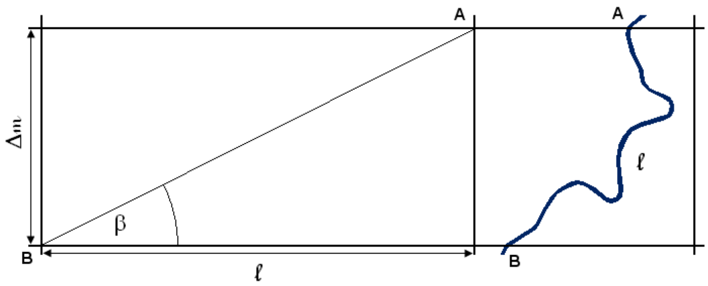

Figure 8 Diagram of parameters defined in order to approximate cell-based channel gradient, A - highest point, B - lowest point, Δm - difference in elevation between A and B (DEM), l – length of river, β - channel gradient

3.4.1 Estimation of Difference in Elevation using Interpolated Channel Elevation Model

Without having adequately accurate alternative data source and assuming that the water level and the natural riverbeds are more or less parallel with the neighbouring surface, the relative difference in elevation between the highest and the lowest points of the channel within one pixel has been derived from SRTM-based 100 m resolution digital elevation model (DEM100). The next initial assumption was that the riverbeds are located at the bottom of the valleys following the steepest slope towards the lowest points of their closer surroundings. Thus the starting (upstream, highest) and ending (downstream, lowest) points were computed for each river segment based on the local minimum values (aggregate function, searching blocks are 1 and 5 square kilometre) of the nodes (sources and inflows).

The auxiliary channel elevation model and elevation differences were calculated in three main phases:

a) Section identification and node selection

Based on the model river network representing a raster linear network and the related flow direction maps (Local Drain Direction, LDD) a unique ID was assigned to each section of a raster linear network between intersections (from-points, to-points). Since the structure of the network (nodes and edges in between, no loops) was a directed acyclic graph the from-points could be selected by the lowest upstream area (UPS) values within one river section and similarly the inflow points downstream had the highest UPS value within a section.

b) Channel elevation model by linear interpolation

Linear interpolation has been done within the river sections between the elevation values of nodes (*Figure 9*). The result is the calculated ideal elevation model of the channel network where the pixels with greater UPS should have lower or equal altitude within one segment, the river is consistently descending.

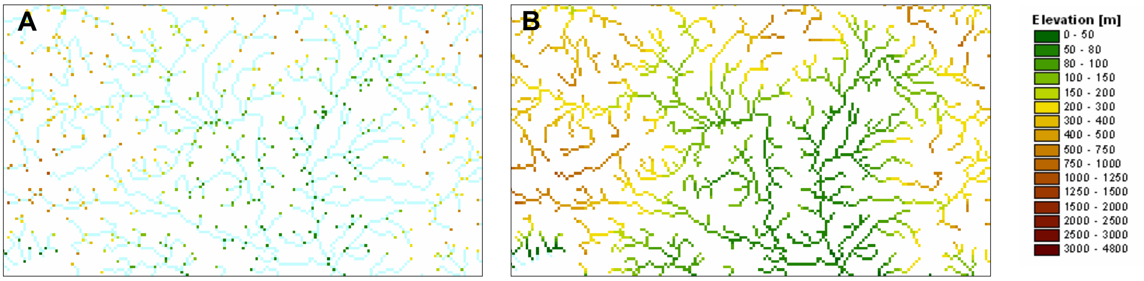

Figure 9 Nodes of river network in 1 km resolution with associated elevation values (A) and interpolated channel elevation model (B) based on local minimum values of DEM100

c) Shifting the model values along the flow directions

Since the general slope functions apply a third-order finite difference method based on the 3x3 neighbourhood using the average maximum technique they are not suitable in a situation where only the upstream and downstream values are available (1Dimension). In order to calculate the gradient the whole system was shifted with one cell-value downstream along the LDD, so the cells have got the value of the adjacent downstream cell.

The simple difference of the interpolated and shifted channel DEM resulted in a grid containing the differences in elevation between the neighbouring channel pixels.

3.4.2 Estimation of Flow Length within Each Cell of the Model River Network

The flow length could be approximated roughly by the cell-size of the gridded model taking the length of orthogonal and diagonal directions into account; in the orthogonal directions the length is equal to the cell size (1000 and 5000 metres), and in the diagonal directions the flow length is equal to the diagonal of the cell (sqrt2 * cellsize, 1414.2135 and 7071.0678 metres). In case no additional input data regarding the flow- or river length was available, this simple geometrical estimation was applied.

The roughly estimated flow length was replaced by calculated flow length based on the method explained in the chapter 3.5 'Channel Length' where the cell-based flow length was estimated using an appropriate vector river data set developed formerly in the frame of the CIS-project (Catchment-based Information System, (Hiederer and de Roo, 2003).

The channel gradient was calculated using the two right-angle sides of the slope (*Figure 8*):

Channel gradient (β) = Grid with differences in elevation (Δm) / Grid with flow length (l)

The result map contains the calculated stream gradient values (*Figure 10*).

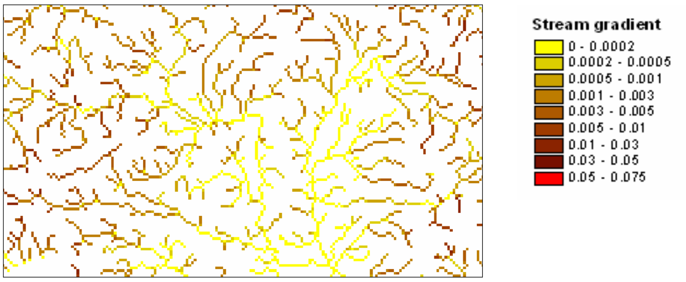

Figure 10 Channel gradient map based on SRTM (DEM100) and vector river network

SRTM (DEM100) and river network-based gradient map was improved and refined by additional information from national hydrological institutes. The gradient values of Danube River were corrected based on descriptive data from the responsible national water authorities. The gradient values of the German part of the main Elbe River were corrected by data derived from high resolution cross-section data (Gierk et al., 2008).

According to an experimental comparison between the surveyed and processed national cross-section data and the generally applied SRTM-based digital elevation model (DEM100) there is an obvious absolute difference between the surveyed mean of bottom values derived from the cross-sections and the remote sensed surface DEM. On the other hand the relative differences in elevation which were required for the calculations, and the derived gradient values are acceptable from further hydrological modelling point of view (Gierk et al., 2008).

3.5 Channel Length

The former maps of channel length contained uniform values; in 1 km resolution the model channel length was defined in 1500 metres, in 5 km resolution each pixel had the value of 7095 metres. Geometrically this is not a bad estimation but the generalized values and pattern did not express the spatial diversity of the river network. More realistic vector-based river data and coordinates of gauging stations from the national institutes enabled to upgrade the data set. The new channel length maps were created in two main steps depending on the resolution.

The calculations were based on known river kilometres (Danube and Elbe Basin) and vector data from the Catchment-based Information System data set (Hiederer and de Roo, 2003).

3.5.1 Channel Length Map 1 km Data Set Based on Reference Data

The 1 km data set was upgraded first. In the case of the Danube Basin and the Czech part of the Elbe Catchment the location of gauging stations were defined by two reference systems; they were given in geographic coordinates and in river kilometres (*Figure 11*). Length of river sections between the gauging stations were calculated based on the river kilometre distances and the rounded integer values were assigned to each river section as an attribute data. This calculated distance was divided by the number of river pixels belonging to each section. In the case of the German part of the Elbe the dense cross-section data provided the information to the calculations.

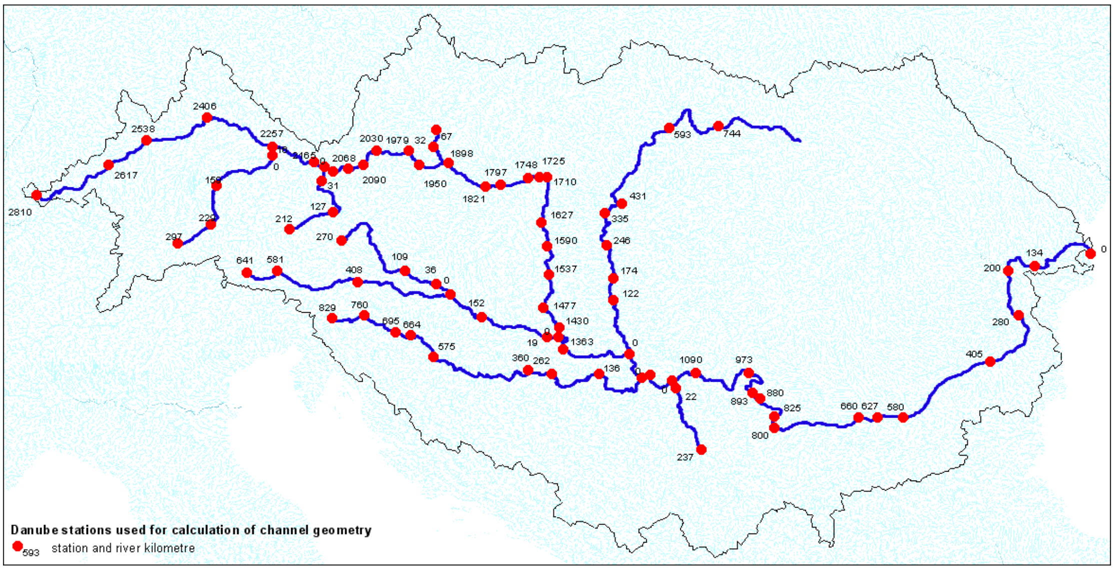

Figure 11 Gauging stations of Danube and its main tributaries used for parameter definition of channel geometry. The numbers indicate the location of gauging station in river kilometres. This information was used to estimate channel length within cells between the stations

Simple statistical comparison showed that the distances based on surveying (river kilometres) were longer averagely with 8 % than the geometrical length of the necessarily generalized vector river sections. Using this information all the other river pixels of the 1 km model network were modified where there were corresponding vector river. Because of missing input data in the case of pixels of other, smaller rivers/channels (out of the vector river network) an averaging has been done based on the calculated values: cell-value of unknown cells = the average cell-value of calculated length (1188 m).

The sketch of calculated river length shows spatial diversity (*Figure 12*). The values can naturally exceed the grid size because of meandering rivers. The cell-values of final 1 km resolution model river network are between 600 m and 1600 m.

3.5.2 Channel Length Map 5 km Data Set Based on the 1 km Calculation

The sources of the 5 km resolution channel length map were the calculated 1 km map of river length (*Figure 12*) based on national data (river km, cross-section of the Danube and Elbe system), the vector-based river network from the CIS data set and the corrected local drainage direction map in 5 km resolution.

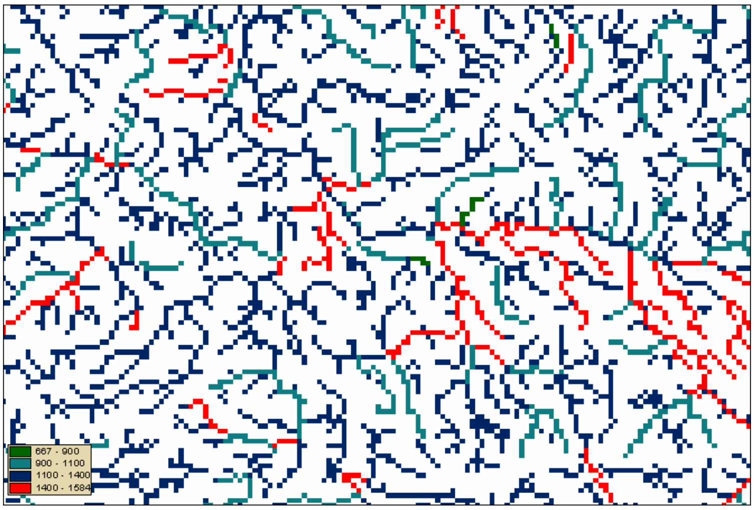

Figure 12 Calculated river lengths in 1 km resolution model show spatial diversity (the dimension of the legend is metre)

In the low (5 km) resolution the pattern of the flow network is strongly generalized and the details and linear characteristics of the natural flow network are not recognisable. Thus a methodology distinct from the previously presented one has been developed as follows:

a) Calculate the length where there is a reference,

b) Calculate the average based on directions of references.

Where only one river belonged to a 5x5 km-sized pixel the new cell-value was defined as the total length of the inside river segment in 1 km resolution (*Figure 13*).

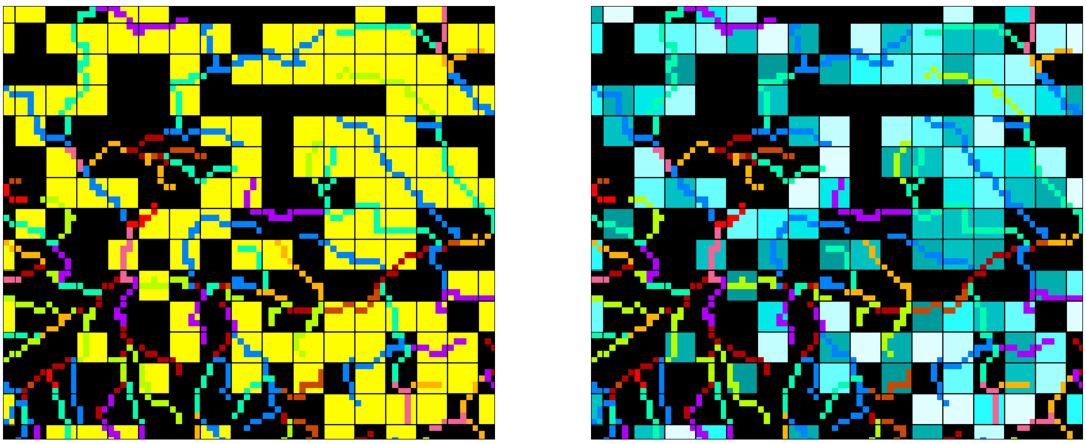

Figure 13 Selection of the 5 km pixels belonging only to one river (yellow cells) and the summarized length of 1km pixels (bluish cells). There is more than one river or there is no river in the black cells

The flow network in 5 km resolution does not represent the ‘real rivers’, but the ‘flow direction’ defines the pattern of possible material transport through the neighbouring cells. Thus the flow length of undefined cells in 5 km resolution cannot be the sum of length of smaller confluent rivers, but can be approximated by the flow direction-based average length of cells were unambiguously defined in the previous step.

The calculation of the direction-based average length was done based on the 1 km data modified by an experimental multiplicator expressing the difference between the measured and vector-geometry based values (*Figure 14*).

$Diagonal_{5km} = Diagonal_{1km} * 5[km] * c_{vector/raster} = 1112.83 * 5 * 1.08 \approx 6010$ m (*Figure 14a*)

$Orthogonal_{1km} = Orthogonal_{1km} * 5[km] * c_{vector/raster} = 1098.2 * 5 * 1.08 \approx 5881$ m (*Figure 14b*)

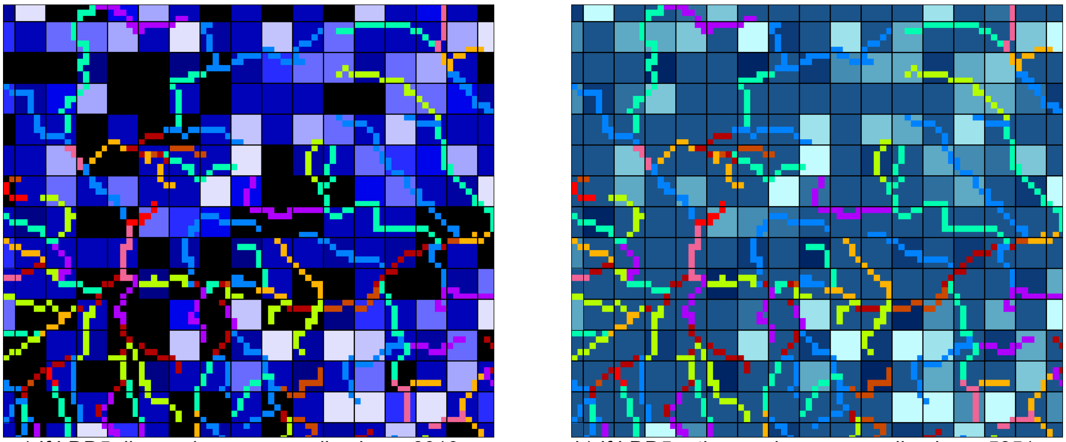

a) If LDD5 diagonal ==> new cell-value = 6010 m   b) If LDD5 orthogonal ==> new cell-value = 5851 m

Figure 14 Length assignment to the undefined cells of flow network in 5 km resolution based on averaged values of 1 km network and local drainage direction (LDD) in 5 km resolution

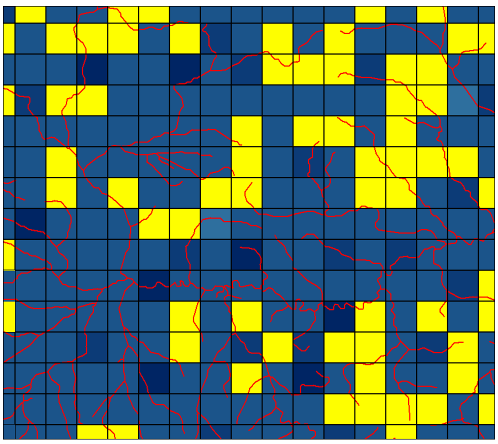

The result map contains channel length values between 768 m and 7637 m (*Figure 15*).

Minimum Value = 768.000
Maximum Value = 7637.000
Mean = 5371.625
Standard Deviation = 1524.303

Figure 15 The result map (red lines show the reference vector network based on CIS data set, the yellow pixels highlight where the defined channel length value is less than 5 km)

The channel length values formed the second component for calculations of channel gradient described in Chapter 3.4.

3.6 Channel Bottom Width

A previous data set of channel bottom widths usually contained high values (30-50 % larger values than the measured values at control points). The preliminary results of model calibration also required the improvement of the data set. However there are available automatic or semi-automatic techniques to estimate 'river width' based on representative river discharge with the assumption of rectangular cross sections and using digital elevation models (e.g. Pistocchi and Pennington, 2006), the presented corrections have been done based on high resolution cross-section data and digital image interpretation (Image2000) under a similar assumption of rectangular cross sections.

The channel bottom width values were interpolated between measured information within the main river basins being in the focus of model calibration (Danube, Elbe). Representative channel with values had been defined at the location of gauging stations then intermediate values were evenly distributed along the river segments between the stations (*Figure 16*). The calculation has been completed by linear interpolation.

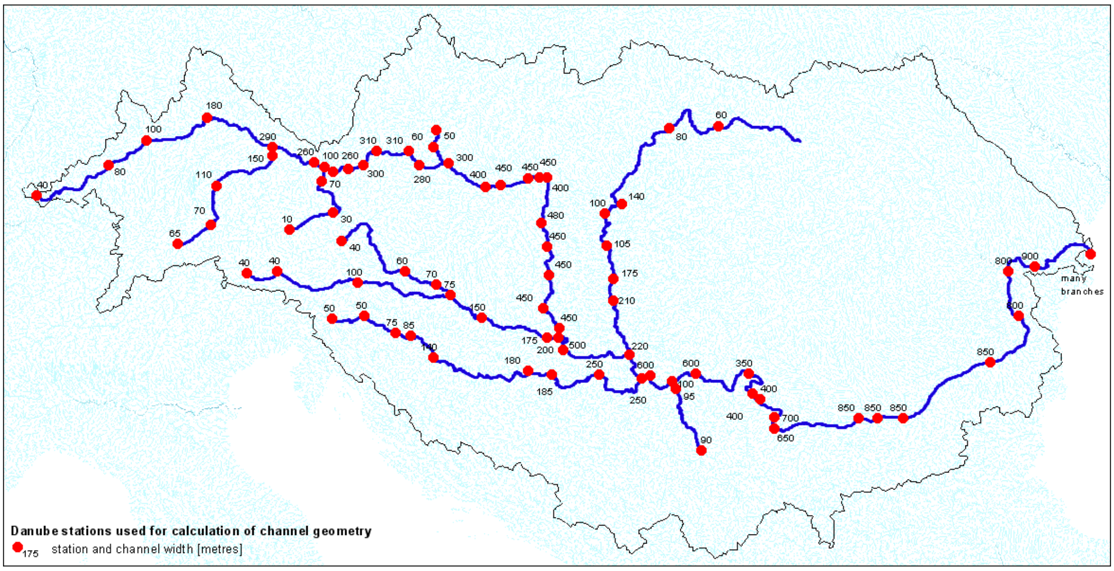

Figure 16 Gauging stations of Danube and its main tributaries used for parameter definition of channel geometry. The numbers indicate the representative channel width at the stations. This information was used to estimate channel bottom width within cells between the stations

The values along the Tisza River (Danube Basin) and Elbe River were obtained from cross-section evaluation. The channel width values of Saale River (Elbe Basin) were defined by measurements on geo-referenced aerial imageries (Gierk et al., 2008). Comparison between the aggregated values of previously used channel bottom widths and the estimated new values indicates the overestimation of the old channel bottom width model (*Table 4*). Modifications were completed along the indicated rivers only, in both (1km, 5 km) data sets. All the other values were kept from the previous maps.

Table 4 *Comparison between the aggregated values (old and new data set, channel width)*

River	Source	Method	Sum of old values	Sum of new values
Danube and main tributaries	cross-sections	interpolation between measured values	2692 km	1383 km
Tisza	cross-sections	interpolation between measured values	219 km	85 km
German Elbe	cross-sections	interpolation between measured values	201 km	142 km
Saale	Image2000	measurement and interpolation	11 km	6 km

3.7 Channel Depth and Manning Values

Similarly to channel with, estimates of channel depth and Manning's roughness coefficient for channels were obtained from available river cross sections and tables from scientific literature; within the Elbe Basin using high resolution cross-section information (Gierk et al., 2008) and descriptive profile-data in the Danube Basin (*Figure 17*). The new values were defined using linear interpolation between representative channel depth values of gauging stations.

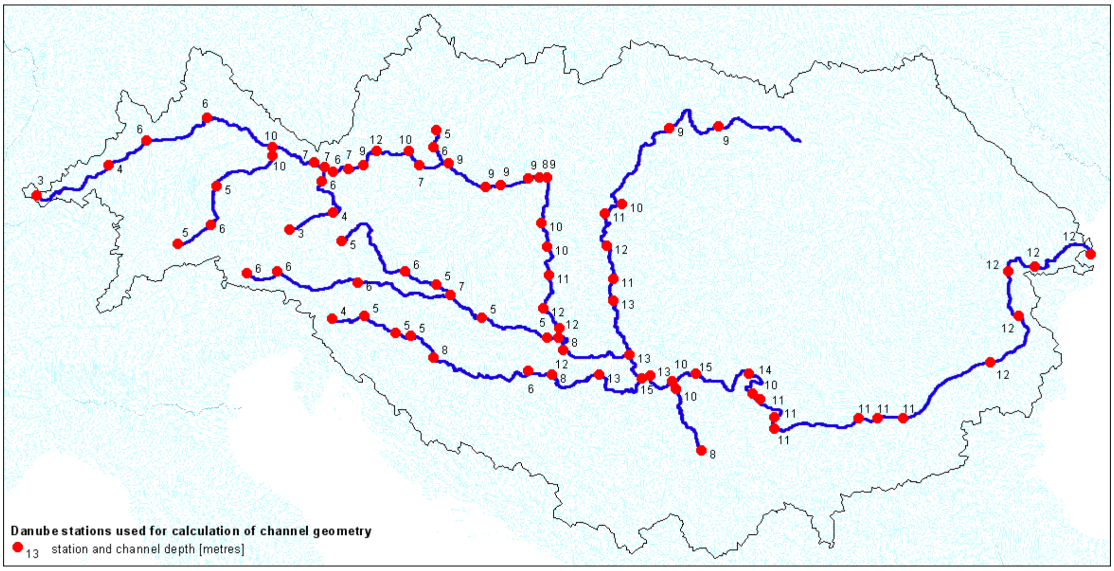

Figure 17 Gauging stations of Danube and its main tributaries used for parameter definition of channel geometry. The numbers indicate the representative channel depth at the stations. This information was used to estimate channel depth within cells between the stations

For the African layers, the channel depth can be estimated by a routine based on the defined local drain direction and calculated upstream area. The Manning value was set to the constant 0.04.

3.8 Local Drain Direction (LDD)

The Local Drain Direction map forms an essential component in continental-wide hydrological modelling expressing flow (transport) directions from each cell to its steepest downslope neighbour.

The European 1 km gridded flow network has been developed in the frame of research activity to design and implement a Catchment-based Information System (CIS). For the determination of river routing network a "stream burning" method was applied involving a digital elevation model and a reference river network developed for the purposes of the CIS (Hiederer and de Roo, 2003). The CIS 1 km flow network has been proved to be adequate to represent the real flow-pattern (*Figure 18*) and to obtain realistic model-results.

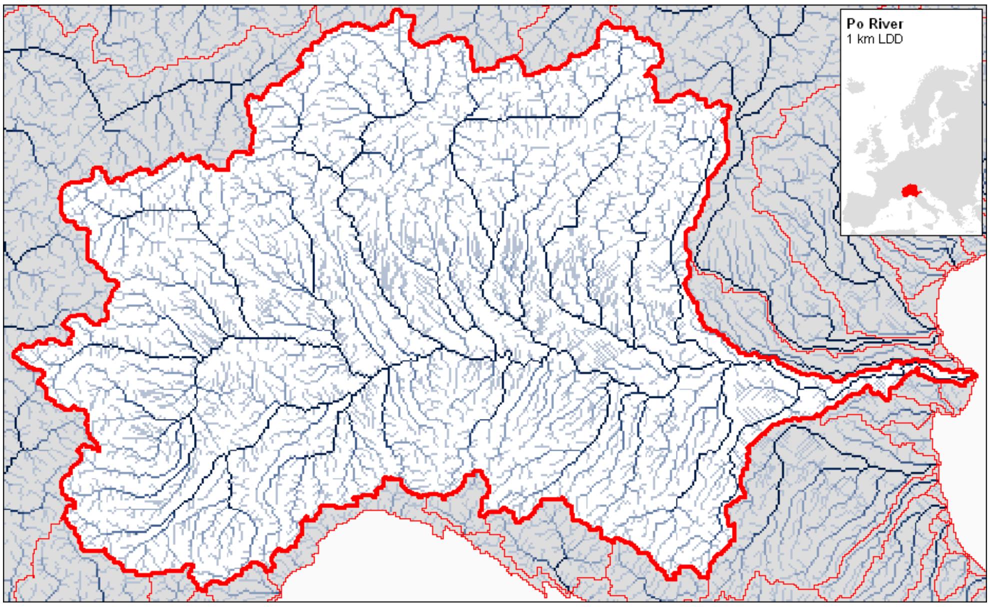

Figure 18 Example of LDD-based flow network in spatial resolution of 1 km (Po Basin)

The European 5 km resolution flow network of LISFLOOD model was generated based on the CIS 1 km gridded data set, using the modelled flow directions, flow accumulation and derived streams in the generalization procedure (*Figure 19*).

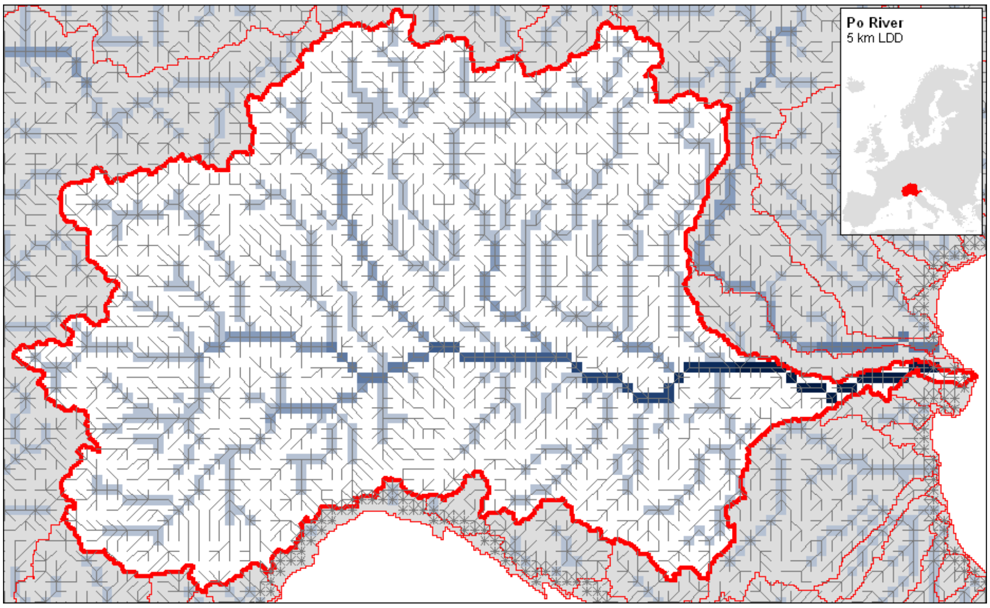

Figure 19 Example of LDD-based flow network in spatial resolution of 5 km (Po Basin)

The generalized 5 km Local Drain Direction map has been modified at several crucial locations (catchment borders, outlets, confluences, flat areas). The major difficulty of error recognition and correction is that there is no related Digital Elevation Model or reference river network in this coarse resolution, thus inconsistencies/deficiencies in the flow network can be discovered excursively. Calibration tests of the hydrological model assist the development of model flow network; too high or too low predicted values in model response at given river segments indicate not realistic area of upstream sub-catchments. Most errors were discovered visually or tracing back the strange model responses.

The *Figure 20* shows a typical case in the Danube Basin where a tributary of the upstream area flows backwards into another tributary and thus the connection of that region is partly lost or misleading to the main river. The red lines represent the realistic river network which was developed within the CIS project (Hiederer and de Roo, 2003) and forms the basis of the 1 km LDD. The bluish squares represent the river cells in the 5 km model before and after the modifications. Code numbers of D8 flow direction model indicate the direction of discharge from a given cell as showed previous by the *Figure 2a*.

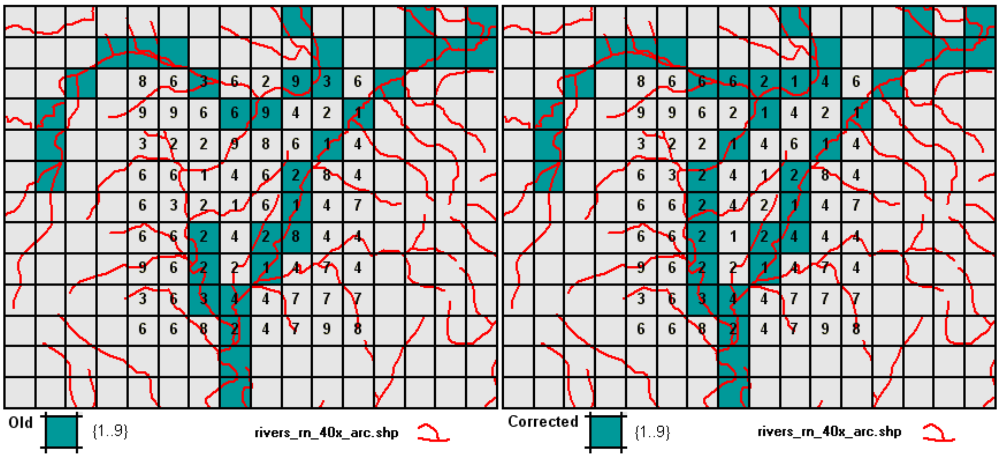

Figure 20 River segment in the Danube Basin before and after correction

The errors have been corrected manually. Flow directions of more than 400 locations were modified, mainly in the Danube Basin (250 cells, *Figure 21*), in the Rhine Basin (75), in the Po Basin (33) and along other main rivers (Elbe, Rhone, Garonne, Isonzo, Marica, Dniester, Vistula, etc., 79 cells).

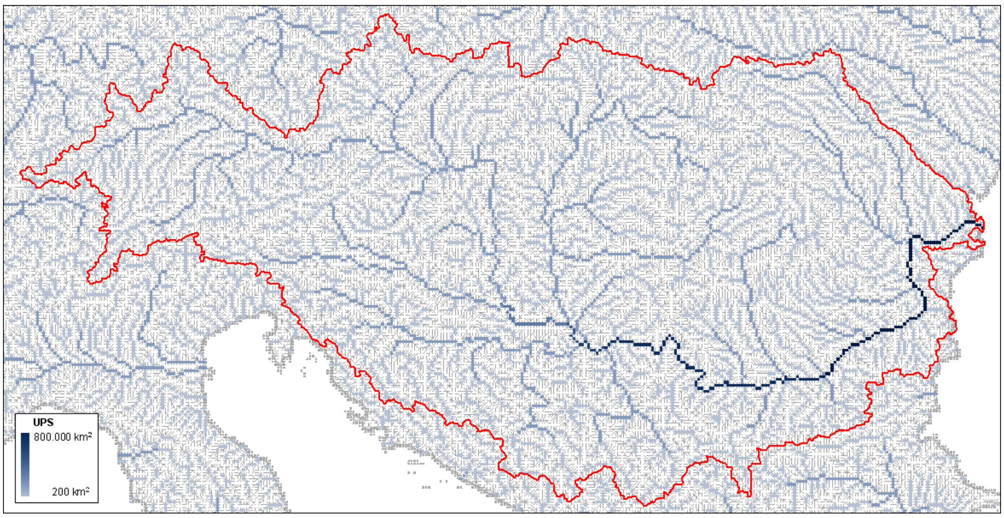

Figure 21 The Danube Basin and its surroundings after the LDD-corrections. Legend shows the calculated catchment area (upstream area, ups) above each cell of the model flow network in 5 km spatial resolution

3.8.1 Development of Local Drain Direction Map in Coarser Spatial Resolution

The Local Drain Direction maps of the African river basins were developed by a sequence of upscaling operations performed on flow network derived from high resolution digital elevation model.

Automatically generated high resolution flow networks obtained from solely a DEM are usually not realistic, especially not in a flat terrain, but these model networks can provide sufficient input data for generation of a coarser flow direction model. Assuming that the representative discharge happens along the network elements (cells) characterised by higher upstream area, upscaling the high resolution network using an iterative algorithm results in a flow network which corresponds to the main pattern of the finer flow network.

The DEM-based methodology was developed and tested in the well-known Danube Basin. The flow network generated by the upscaling procedure was then used to delineate sub-basins and the borders of watersheds were compared to reference data (*Figure 22*). The size of the test area is 800.000 km^2, the area of modelled sub-catchments are between 55.000 km^2 and 280.000 km^2. The details of the generated network obviously show some differences from the high resolution pattern, but even so, the applied methodology resulted in promising outputs. Significant errors in derived flow directions should be corrected manually.

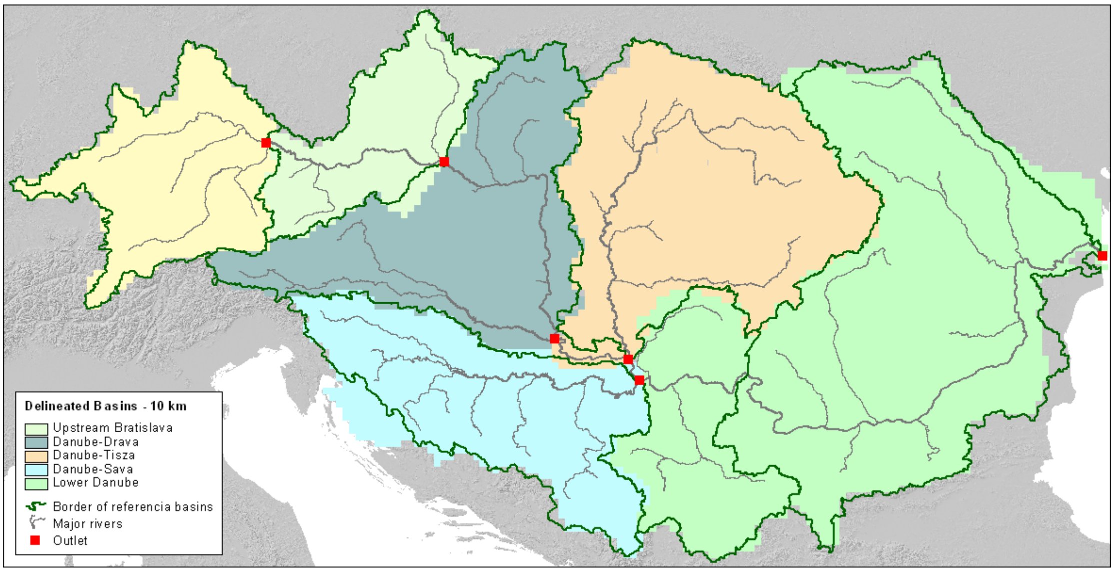

Figure 22 Delineated sub-catchments based on a generated flow network in 10 km resolution. Border zones in 10 km are more or less similar to reference catchment borders (green line)

In the first processing steps the flow directions and the corresponding flow network with area of upstream watershed for each cell were calculated from the high resolution, SRTM-based DEM100. These operations do not result in an accurate flow network and the product contains significant local inconsistencies, but the generated models provide sufficient input information for further grid operations aiming to develop a data layer of large area with representative flow directions in a low spatial resolution. The derived flow network is not a representation of the 'river network', but it approaches the flow directions of main routing on the terrain.

The first model result in high resolution was iteratively scaled into lower and lower resolution by resampling the source upstream area values and ordering always the maximum values to the new pixels. The original grid size was set to 100 metres then enlarged from 500 metres to 50 kilometres. *Figure 23a-e* show the flow pattern of intermediate steps in different spatial resolutions. The green line indicates the Danube sub-catchment border above Passau.

In order to define the flow direction within the network an artificial surface was generated using the inverse values of maximal contributing areas in each cell. The lowest point of this generated surface is the pour point of the watershed which has the highest UPS value. A standard GIS function calculating flow directions based on D8 model then was applied to approach the direction of main discharge. The result is presented by red lines in *Figure 23f*. The yellow line shows the sub-catchment delineated using the generated 10 km flow network.

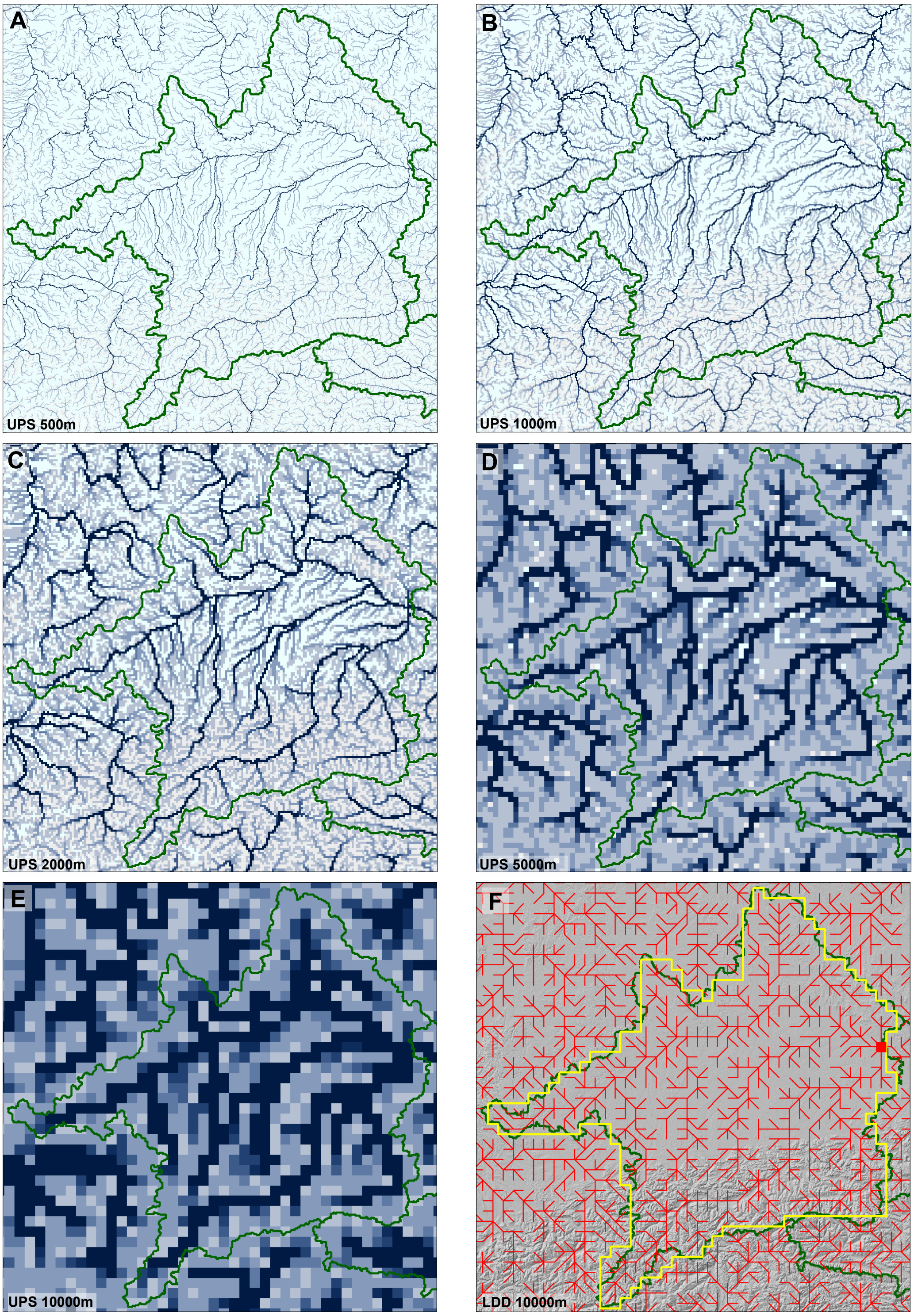

Figure 23 Definition of flow directions in low resolution based on high resolution DEM (detailed description of the methodology and the figures is given in the text)

The presented methodology was implemented on SRTM-based elevation model of Africa.

3.8.2 Development of Local Drain Direction Map of African River Basins

The first version of African LDD in 0.1 degree spatial resolution was created based on digital elevation modelling and was then manually modified at several crucial locations (*Figure 24*).

The source of applied digital elevation model is the SRTM data set sampled at 3 arc-seconds, which is 1/1200th of a degree of latitude and longitude, or about 92-93 meters at the equator (see more: Chapter 2.1 Shuttle Radar Topography Mission). An approximated flow direction map in 0.1 degree resolution was derived using complex GIS-operations in several processing steps. The main working phases with comments were the followings:

1) Download the needed SRTM tiles

- Useful data from CGIAR-CSI website: http://srtm.csi.cgiar.org.

2) Merge the tiles into larger blocks according to predefined processing windows

- The African data set was initially processed in nine analyzing windows;
- The maximal data size within the applied software environment has to be taken into consideration (which is about 2 Gb in Arc/Info Grid).

3) Create a grid of flow direction from each cell to its steepest downslope neighbour

- Inbuilt functions of commercial or open source GIS packages can be applied;
- Local inconsistencies between 'real' and derived network can be ignored.

4) Create a grid of accumulated flow to each cell

- Inbuilt functions of commercial or open source GIS packages can be applied;
- Accumulated number of upstream cells only approaches the contributing area of upstream cells, since the regular grid-spacing in degree scale does not mean regular tessellation in a metric system.

5) Resample the higher resolution grid into the target resolution

- Supposing that higher upstream area indicates the main direction of discharge;
- Preferably the target resolution is not larger than the size of modelled phenomenon;
- Suggested resampling method is ordering the maximum values to the processed cell;
- Recursive checking of network pattern is recommended during the iterative process.

6) Generate an artificial surface of the derived flow network

- Ensure that the surface is continuously descending along the flow path;
- Easy way of generating such surface is taking the inverse of the UPS grid;
- The lowest point of this generated surface is the pour point of the watershed which has the highest UPS value.

7) Calculate the flow directions based on D8 model

- Inbuilt functions of commercial or open source GIS packages can be applied;
- All cells at the edge of the surface grid can be forced to flow outward;
- Cells with undefined flow direction can be flagged as sinks;
- If a cell has the same change in elevation in multiple directions and is not part of a sink the code of direction should be defined/corrected manually.

8) Quality check and error correction

- The generated flow direction data set can be tested using the standard procedure of delineating flow network and sub-catchments;
- Generate a grid of accumulated flow to each cell based on the derived flow directions;
- Compare the calculated values against the UPS data used as input earlier;
- In case of significant differences in UPS and flow path, manual correction is required.

The procedure above is a quick emergency solution if there is no auxiliary data available.

If validation data, details of the river basins, the hierarchical flow network and the terrain are available (e.g. accurate and consistent reference river database) a more sophisticated methodology could be followed as suggested in the relevant literature on development of continental-wide networks or evaluating global drainage direction data (e.g. Maidment, 1996; Döll and Lehner, 2002; Hiederer and de Roo, 2003; Soille et al., 2003; Vogt et al., 2007a).

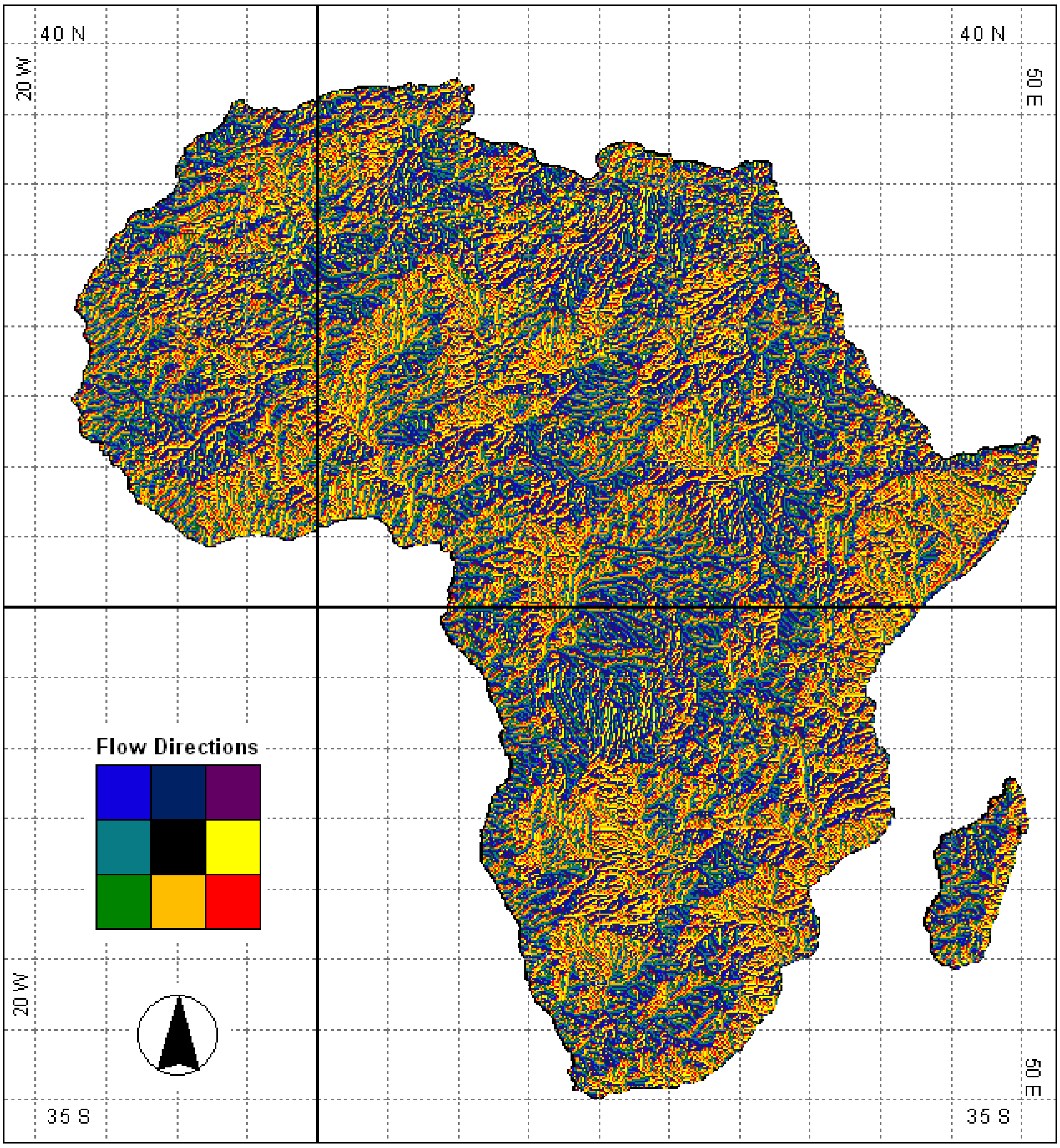

Figure 24 Derived flow directions of African river basins based on D8 model

As mentioned, the presented methodology does not result in a very accurate flow network in a high resolution and the product can contain significant local inconsistencies which have to be corrected manually. The generated flow models, on the other hand, provide sufficient input information for further grid operations. Since the derived flow network does not intend to be a representation of the 'river network' in that scale, but it approaches the flow directions of main routing on the terrain, the product forms an acceptable input data for large-scale hydrological modelling.

3.8.3 Development of Local Drain Direction Map of African Pilot Areas

For the African study auxiliary data (several analogue maps and hydrological stations with their estimated upstream area, source: internet) were collected in the case of two pilot areas.

a) Pilot area: Juba Basin, Shabelle Basin, Lag Badana Basin

The automatically derived flow network of international river basins at the border zone of Somalia, Ethiopia and Kenya was corrected by data of gauging stations on the main rivers. The inconsistency between reference data and calculated upstream contributing area, and the size of total watersheds indicated the need of further processing. The resulted flow network in that coarser resolution (0.1 degree) satisfactorily represents the realistic flow path (*Figure 25*).

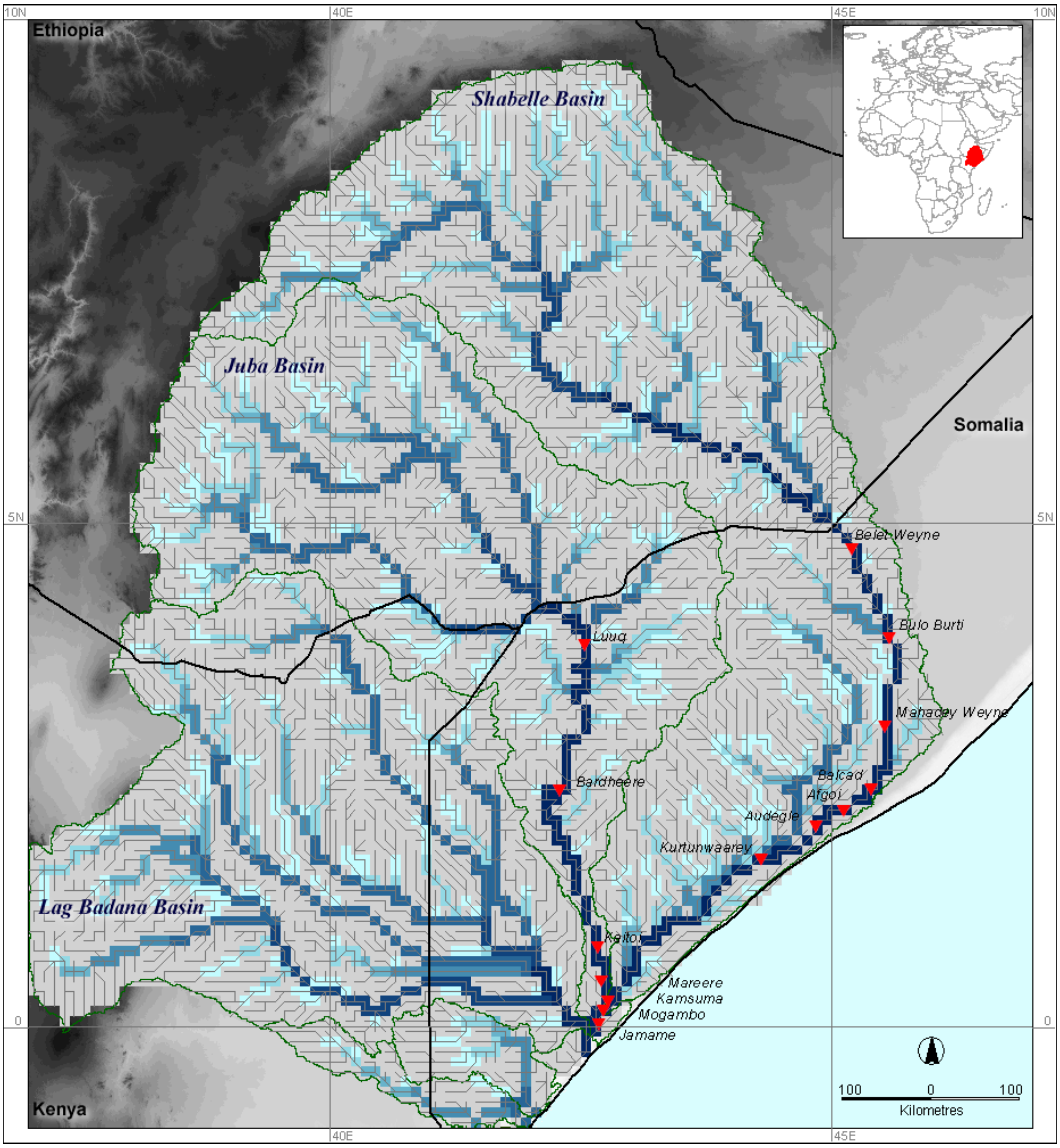

Figure 25 Overview of LDD and modelled rivers. Juba-Shabelle-Lag Basins. Outlet in Somalia

b) Pilot area: Zambezi Basin (and sub-basins) Save River, Limpopo, Okavango Basin

Similarly to the Somalia river basins a flow direction data set of Southern-African basins was created in 0.1 degree resolution based on SRTM elevation data. Scanned topographic maps were used to improve the automatically derived flow direction values (*Figure 26*).

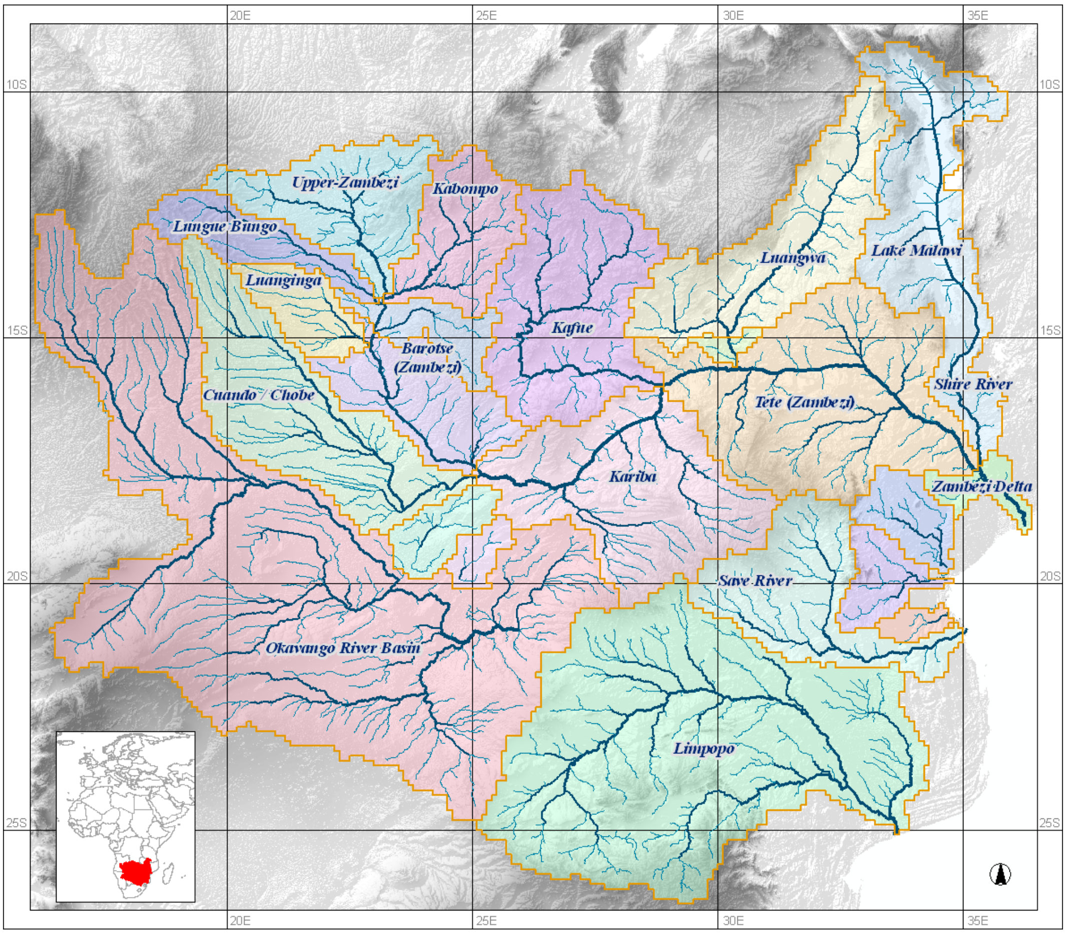

Figure 26 Overview of modelled rivers and basins in Southern-Africa

The local drain direction maps of both pilot areas were created additionally to the continental-wide flow model and integrated then with the previously presented African flow direction data.

3.9 Land Use – Land Cover

LISFLOOD input maps related to land use (land cover map with land cover classes, map with forest fraction for each cell and map with fraction of urban area) were created using the European 'Corine land cover 2000 (CLC2000) 100 m - version 12/2009' data set and the Global Land Cover 2000 (GLC2000) data.

The source land cover data was resampled to the modelling resolution used in LISFLOOD hydrological model. The grid size of output data was set then to 1km and 5 km. Since the classes of the new land cover data set for LISFLOOD had to be harmonised, the two data sets were merged into one using a simple statistical approach. For the African study the GLC2000 data set was resampled to 0.1 degree resolution.

3.9.1 Merging CLC2000 and GLC2000

The CLC2000 data covers the European territories of the member states of the European Union extended by the area of other European countries (*Figure 3a*). In order to carry out European-wide hydrological modelling by LISFLOOD the land cover types of river basins not covered by CLC2000 were defined using the GLC2000 data (see also *Annex 2, Annex 3*).

The CLC2000 data was extended by values from the GLC2000 data and the result has a value-set using the nomenclature of CORINE classes. The reclassification of GLC2000 values was done based on the dominant, spatially corresponding land cover class of the CLC2000. Similar methodology was applied creating the previous land cover layer based on 250 m resolution CORINE data (Laguardia, 2005). *Table 5* shows the reclassified land cover classes and the nominal correspondence between the two source land cover data sets.

Table 5 *Statistical correspondence between the GLC2000 and the CLC2000 data sets*

Code GLC2000	Land Cover Type GLC2000	Code CLC2000	Land Cover Type CLC2000
1	Tree Cover, broadleaved, evergreen	28	Sclerophyllous vegetation
2	Tree Cover, broadleaved, deciduous, closed	23	Broad-leaved forest
3	Tree Cover, broadleaved, deciduous, open	25	Mixed forest
4	Tree Cover, needle-leaved, evergreen	24	Coniferous forest
5	Tree Cover, needle-leaved, deciduous	25	Mixed forest
6	Tree Cover, mixed leaf type	25	Mixed forest
7	Tree Cover, regularly flooded, fresh water	24	Coniferous forest
8	Tree Cover, regularly flooded, saline water	28	Sclerophyllous vegetation
9	Mosaic: Tree Cover / Other natural vegetation	24	Coniferous forest
10	Tree Cover, burnt	12	Non-irrigated arable land
11	Shrub Cover, closed-open, evergreen	28	Sclerophyllous vegetation
12	Shrub Cover, closed-open, deciduous	27	Moors and heathland
13	Herbaceous Cover, closed-open	18	Pastures
14	Sparse herbaceous or sparse shrub cover	32	Sparsely vegetated areas
15	Regularly flooded shrub and/or herbaceous cover	36	Peat bogs
16	Cultivated and managed areas	12	Non-irrigated arable land
17	Mosaic: Cropland / Tree Cover / Other natural vegetation	12	Non-irrigated arable land
18	Mosaic: Cropland / Shrub and/or grass cover	12	Non-irrigated arable land
19	Bare Areas	32	Sparsely vegetated areas
20	Water Bodies	41	Water bodies
21	Snow and Ice	34	Glaciers and perpetual snow
22	Artificial surfaces and associated areas	2	Discontinuous urban fabric
23	Irrigated Agriculture	13	Permanently irrigated land

The missing area of CLC2000 data set was completed by using land cover information from the reclassified land cover grid.

The combined product (*Figure 27*) as a European Land Cover (ELC2000) in 100 m resolution forms an input data to the MOLAND model - Monitoring Land Use/Cover Dynamics (Kasanko, et al., 2006a; Kasanko, et al., 2006b; Engelen et al., 2007; Petrov, el al., 2009). The MOLAND land cover data was delivered in 100 m spatial resolution in the coordinate system of Lambert Azimuthal Equal Area (LAEA) projection with the ETRS 1989 datum.

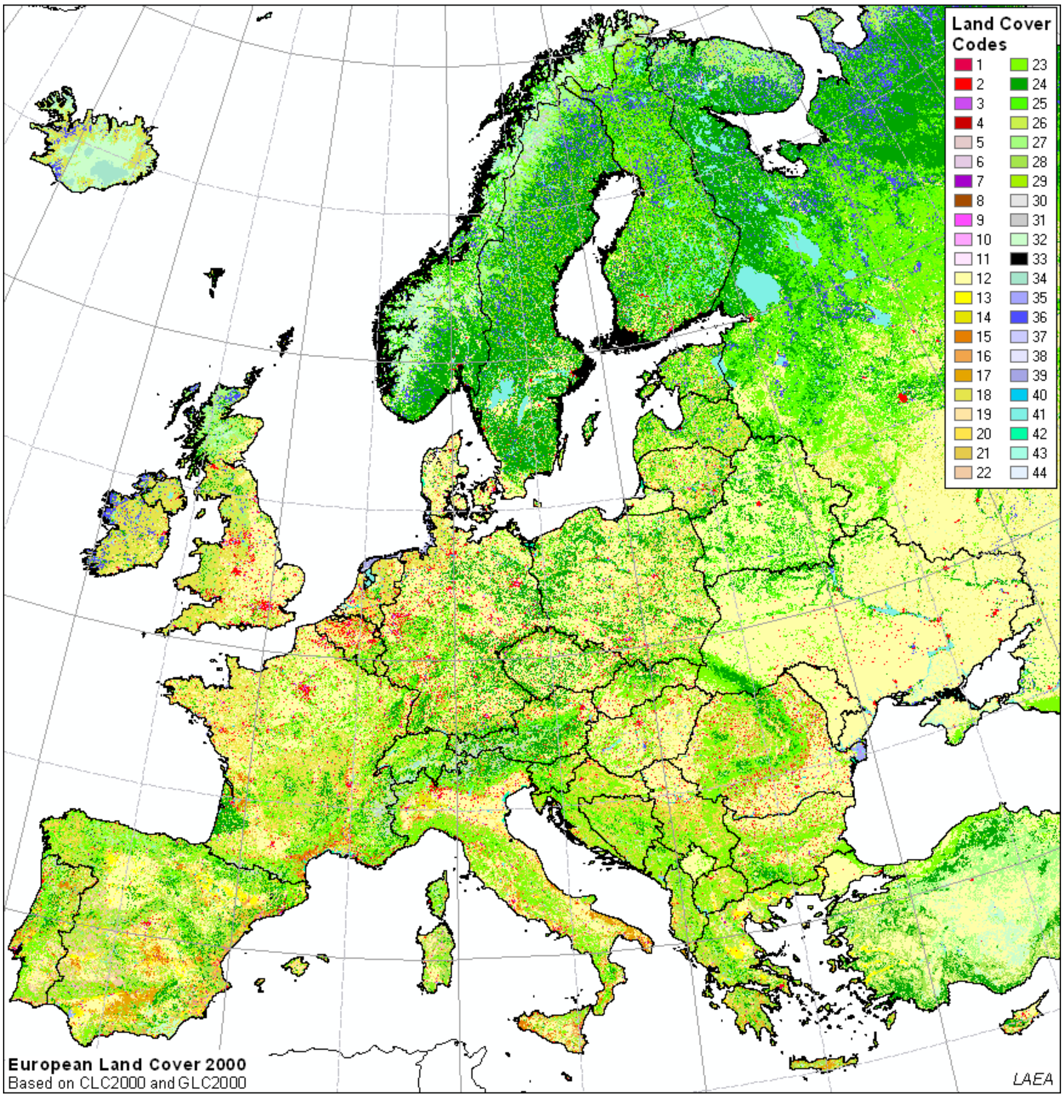

Figure 27 A combined European land cover layer based on CLC2000 and GLC2000 data set. Codes of applied CORINE land cover classes are given in Annex 2

The developed ELC2000 provided the input spatial information to rescaling operations and development of required European data layers for hydrological modelling. The LISFLOOD model inputs were resampled to 1 km and 5 km spatial resolution and re-projected into GISCO LAEA system.

3.9.2 Rescaling from 100 m Resolution to 1 km and 5 km

Land cover classes belong to the nominal scale of values. The codes are given arbitrarily and only examination if a nominal scale value is equal to some particular value or counting the number of occurrences of each value is allowed. This principal had been taken into consideration when the source ELC2000 was resampled to 1 km and 5 km gridded data using three methodologies.

a) Regular sampling

Each cell of the 1 km (5 km) grid inherits its value from the central (lowest right cell closest to the centre) 100x100 m pixel. After the evenly distributed sampling the resulted grid shows not the most important or dominant land cover type of the surface represented by the pixel. Pattern of obtained land surfaces can have mosaic structure or shows discontinuity on originally homogeneous or connected surfaces (e.g. water body, forest belt).

b) Spatially dominant value

The method finds the majority value (the value that appears most often) for the specified area such as the grid size of the resampled data. The technique similarly can break continuous linear surfaces but the new values reflect the main characteristics of the area better than after the regular sampling.

c) Spatial proportion of classes

The spatial distribution and frequency of each class is defined and ordered as percentage of the whole represented area of the new pixel. Addition of all proportional land cover grids should result in 100 (or 1, depending on the applied scale).

The spatial resampling has naturally altered the cardinality of the input value set and there are areal differences in aggregated classes using the different techniques (see also *Annex 4*).

Since there are number of model parameters used in the LISFLOOD hydrological model and read through tables that are linked to the classes on the land use (land cover), the product resulted by the spatially dominant value-method is recommended to use. Cell-based definition of crop coefficient, rooting depth or Manning's roughness for each land use (land cover) class are better represented by aggregated classes than by regularly sampled definition.

The other two maps related to land cover have been generated by the spatial proportions.

3.9.3 Forest Coverage

The gridded data contains the forest fraction for each cell. Values range from 0 (no forest at all) to 1 (pixel is 100% forest). CORINE classes 'broad-leaved forest' (23), 'coniferous forest' (24) and 'mixed forest' (25) were merged then the areal proportion of forest coverage defined for each cell in 1 km and 5 km grid.

3.9.4 Impermeable Surfaces Based on Land Cover Classes

Similarly to the forest maps, the fraction of urban area was defined for each cell. Values range from 0 (no urban area at all) to 1 (pixel is 100% urban). In addition to the areal statistics a classification of permeability was applied assigning also the other land cover classes to five permeability classes (Laguardia, 2005) and calculating then the average permeability for each 1 km and 5 km pixel (see also *Annex 5*).

3.9.5 Land Cover Data of African River Basins

The data source of the resampled African land cover layer was the Global Land Cover 2000 data (GEM, 2003).

The spatially dominant land cover type and the variety of the classes (max 12) within the ~100 km^2 pixels were calculated and rescaled to 0.1 degree resolution (*Figure 28*). The land cover is classified in 25 classes (see also *Annex 3*).

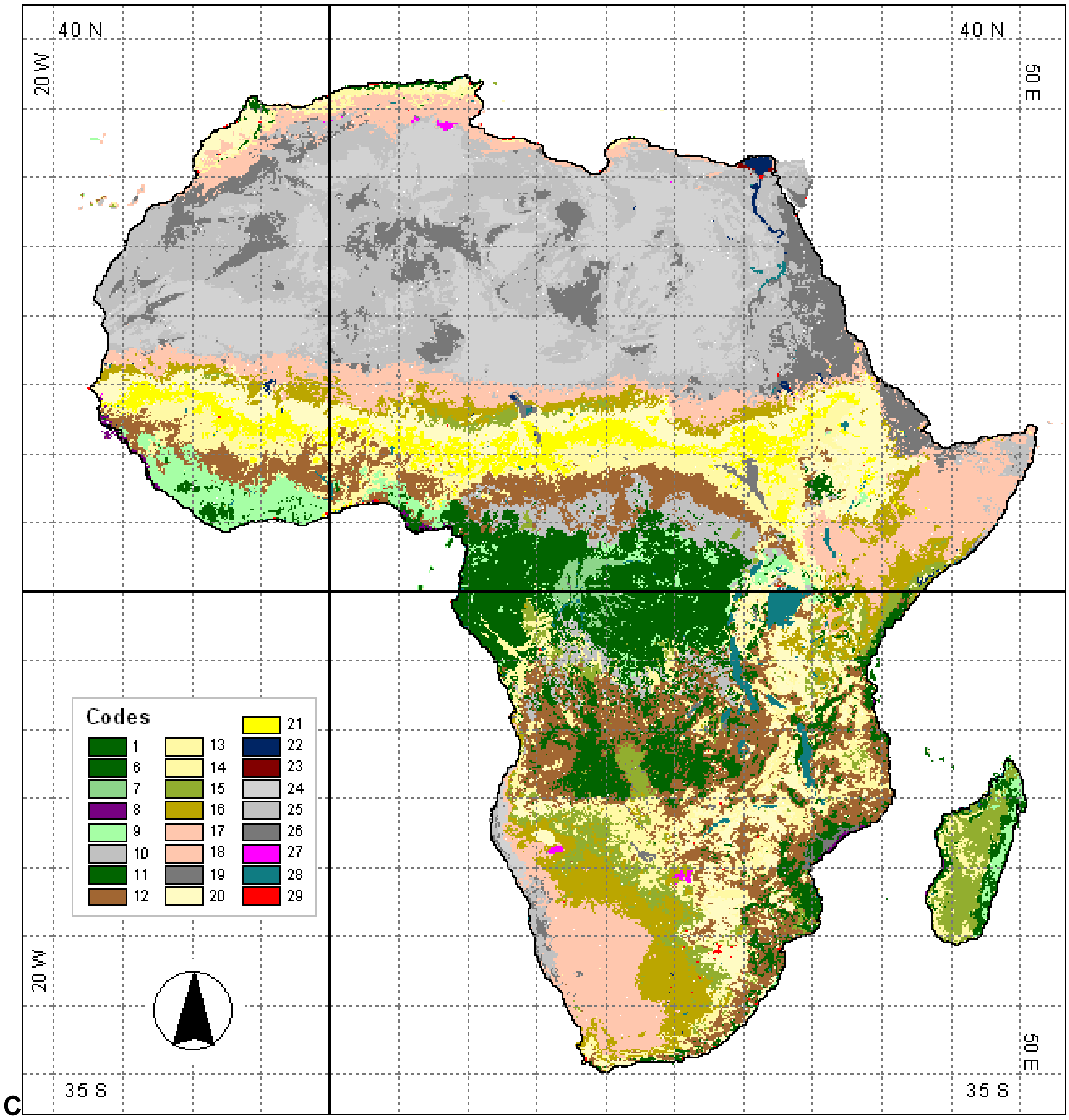

Figure 28 Resampled land cover classes in 0.1 degree spatial resolution based on GLC2000 Codes of applied land cover classes are given in Annex 3

The area-percentage of 25 individual classes was also calculated and stored in the corresponding PCRaster files. The model layers regarding forest coverage and urban area can be derived from the data using a predefined reclassification of the original land cover classes.

3.10 Soil Map

The LISFLOOD hydrological model distinguishes between soil texture in two soil layers; soil texture class layer 1 and 2 (upper layer and lower layer). These layers are corresponding to the topsoil and subsoil classification in the source soil databases (SGDBE - Soil Geographical Database of Eurasia, HWSD - Harmonized World Soil Database).

3.10.1 Soil Texture Map

The soil texture maps of Europe were created based on the gridded values of soils that classified as dominant in the SGDBE. This data set was available for the LISFLOOD hydrological model.

New layers for Africa related to soil texture were set up accordingly to the dominant soils based on the Harmonized World Soil Database v 1.0 (HWSD). The grid size was set to 0.1 degree. Sand, silt and clay content in percentage was derived on topsoil and subsoil levels with the condition that the sum of the three components was 100%. In case there was no mineral structure or information available ‘no data’ was assigned to the pixel (*Figure 29*).

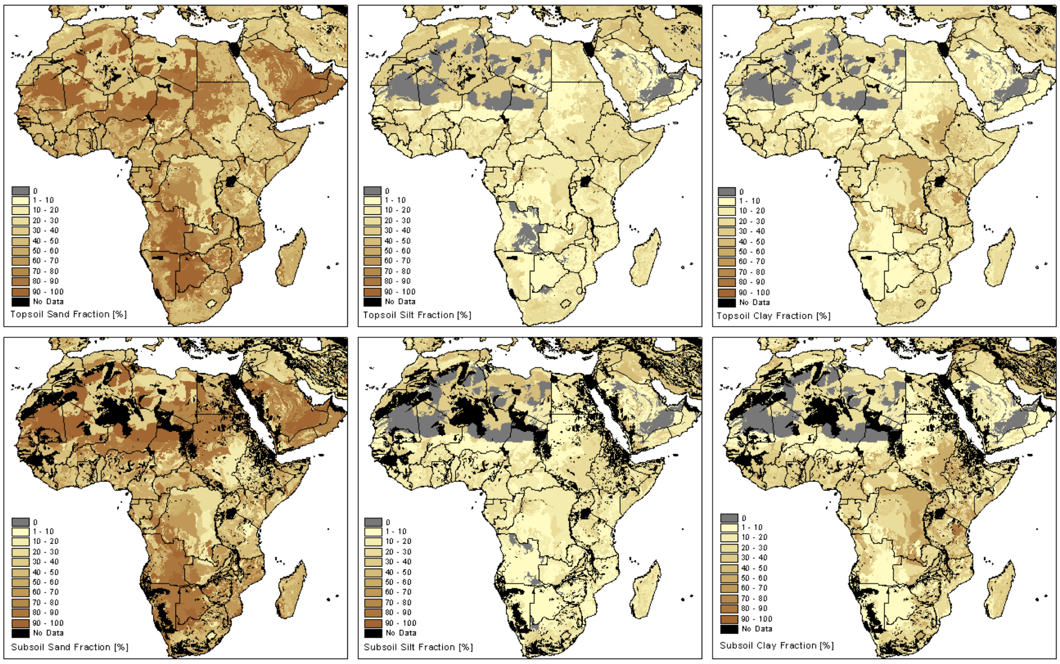

Figure 29 Overview of soil texture information derived from the HWSD v 1.0

Thus six data layers (topsoil, subsoil and sand, silt and clay content in both) were created and reclassified then based on the requirements of the LISFLOOD hydrological model against classes and codes of soil texture (*Table 6*).

***Table 6** Soil texture classification applied in LISFLOOD*

Class Codes	Description	Values for clay and sand contents
0	No mineral texture	peat soils, rocks, etc.
1	Coarse	clay ≤ 18 % and sand > 65 %
2	Medium	18 % < clay < 35 % and sand ≥ 15 %, or clay ≤ 18 % and 15 % ≤ sand ≤ 65 %
3	Medium fine	clay < 35 % and sand < 15 %
4	Fine	35 % ≤ clay ≤ 60 %
5	Very fine	clay > 60 %

3.10.2 Soil Depth Map

The soil depth layer of LISFLOOD contains the soil depth to bedrock or groundwater given in centimetre (van der Knijff and de Roo, 2008). Similarly to the European texture maps, the soil depth map of Europe was created based on the gridded values of soils that classified as dominant in the SGDBE. This data set was available for the LISFLOOD hydrological model.

The source of the African soil data was the WHSD. According to the model requirements the most frequently occurring value of Reference Soil Depth [cm] was extracted and assigned to the new pixel (*Figure 30*).

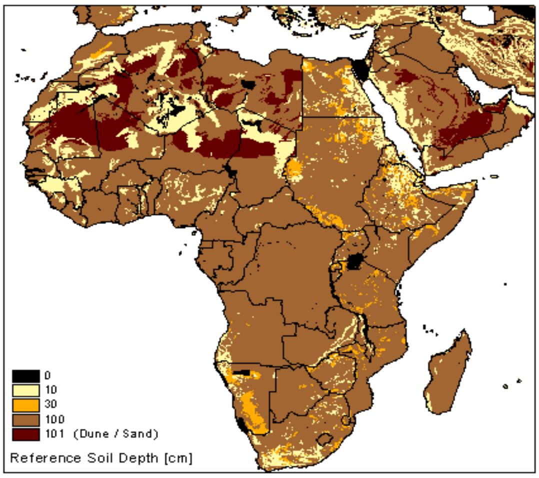

Figure 30 Soil depth layer

In the WHSD the reference soil depth of all soil units is set at 100 cm, except for Rendzinas and Rankers of FAO-74 and Leptosols of FAO-90, where the reference soil depth is set at 30 cm, and for Lithosols of FAO-74 and Lithic Leptosols of FAO-90, where it is set at 10 cm (FAO/IIASA/ISRIC/ISSCAS/JRC, 2009).

In the case of SAND DUNES the Topsoil Sand Fraction and the Topsoil Sand Fraction is 100%, the other values are 0, and the soil depth in these cases is set to 101 (exceeding the other deepest value which is 100 cm). The values of 0.1 degree resolution grid were defined

3.10.3 Modelling of Soil Parameters and Further Model Development

The presented methodology of creating new data layers and upscaling other complex spatial data sets from higher resolution to a coarser one is an approach among different possible processing techniques. The results are the strongly generalized models of the reality.

The future European input soil layers of LISFLOOD could be defined based on the methodology suggested for the development of a spatial European soil property data set, attempting to avoid the potential bias in the representation of soil properties when mapping only the characteristics of the dominant soil typological unit (Hiederer and Jones, 2009).

For the African data set, the use of latest version (version 1.1, March, 2009) of WHSD would probably improve even the coarse (0.1 degree grid) data since the already existing data set was extended by SOTWIS information for Burundi, the Democratic Republic of the Congo, Gambia, Senegal, and Rwanda.

4 Results – New European Input Maps

Most of the GIS operations and described processes were completed within the Arc/Info Workstation 9.3 environment using the binary raster data format of the 'Grid' module. According to the LISFLOOD model requirements against the input file formats, all the resulted grid data have been converted into the also binary PCRaster map format.

The complete list of LISFLOOD input maps is given in the User Manual (van der Knijff and de Roo, 2008). Only the updated/new data layers developed lately are listed in *Table 7, 8*. The physical parameters and description of processed PCRaster maps are given in *Annex 6*.

Table 7 *New European data layers related to topography, channel geometry and land cover (1 km)*

Name of New PCRaster Map	Default Name in LISFLOOD	Description
chanbnkf_1km.map	chanbnkf.map	Bankfull channel depth [m]
chanbw_1km.map	chanbw.map	Channel bottom width [m]
changrad_1km.map	changrad.map	Channel gradient [m m^{-1}]
chanleng_1km.map	chanleng.map	Channel length [m]
chanman_1km.map	chanman.map	Manning's roughness coefficient for channels
dem_cent_1km.map		Digital elevation model, central value [m]
dem_mean_1km.map		Digital elevation model, average of values [m]
dem_rr_1km.map		Digital elevation model, relative relief [m]
dem_skw_1km.map		Digital elevation model, skewness of distribution
dem_std_1km.map		Digital elevation model, standard deviation [m]
directrf_1km.map	directrf.map	Direct runoff fraction map [%]
forest_1km.map	forest.map	Forest fraction for each cell
gradient_1km.map	gradient.map	Slope gradient [m m^{-1}]
landuse_cent_1km.map		Map of land cover classes (CLC2000), central value
landuse_domi_1km.map	landuse.map	Map of dominant land cover classes (CLC2000)

Table 8 *New European data layers related to topography, channel geometry and land cover (5 km)*

Name of New PCRaster Map	Default Name in LISFLOOD	Description
chanbnkf_5km.map	chanbnkf.map	Bankfull channel depth [m]
chanbw_5km.map	chanbw.map	Channel bottom width [m]
changrad_5km.map	changrad.map	Channel gradient [m m^{-1}]
chanleng_5km.map	chanleng.map	Channel length [m]
dem_cent_5km.map		Digital elevation model, central value [m]
dem_mean_5km.map		Digital elevation model, average of values [m]
dem_rr_5km.map		Digital elevation model, relative relief [m]
dem_skw_5km.map		Digital elevation model, skewness of distribution
dem_std_5km.map		Digital elevation model, standard deviation [m]
directrf_5km.map	directrf.map	Direct runoff fraction map [%]
forest_5km.map	forest.map	Forest fraction for each cell
gradient_5km.map	gradient.map	Slope gradient [m m^{-1}]
landuse_cent_5km.map		Map of land cover classes (CLC2000), central value
landuse_domi_5km.map	landuse.map	Map of dominant land cover classes (CLC2000)
ldd_5km.map	ldd.map	Local drain direction map (with value 1-9)
ups_5km.map		LDD-based upstream area map for each cell [km^2]

4.1 Digital Elevation Model

The main technical parameters of the derived digital elevation models are listed in *Annex 6*. The value set is variant using different resampling techniques and different grid sizes. *Figure 31* illustrates the DEM in 1 km resolution using central resampling method.

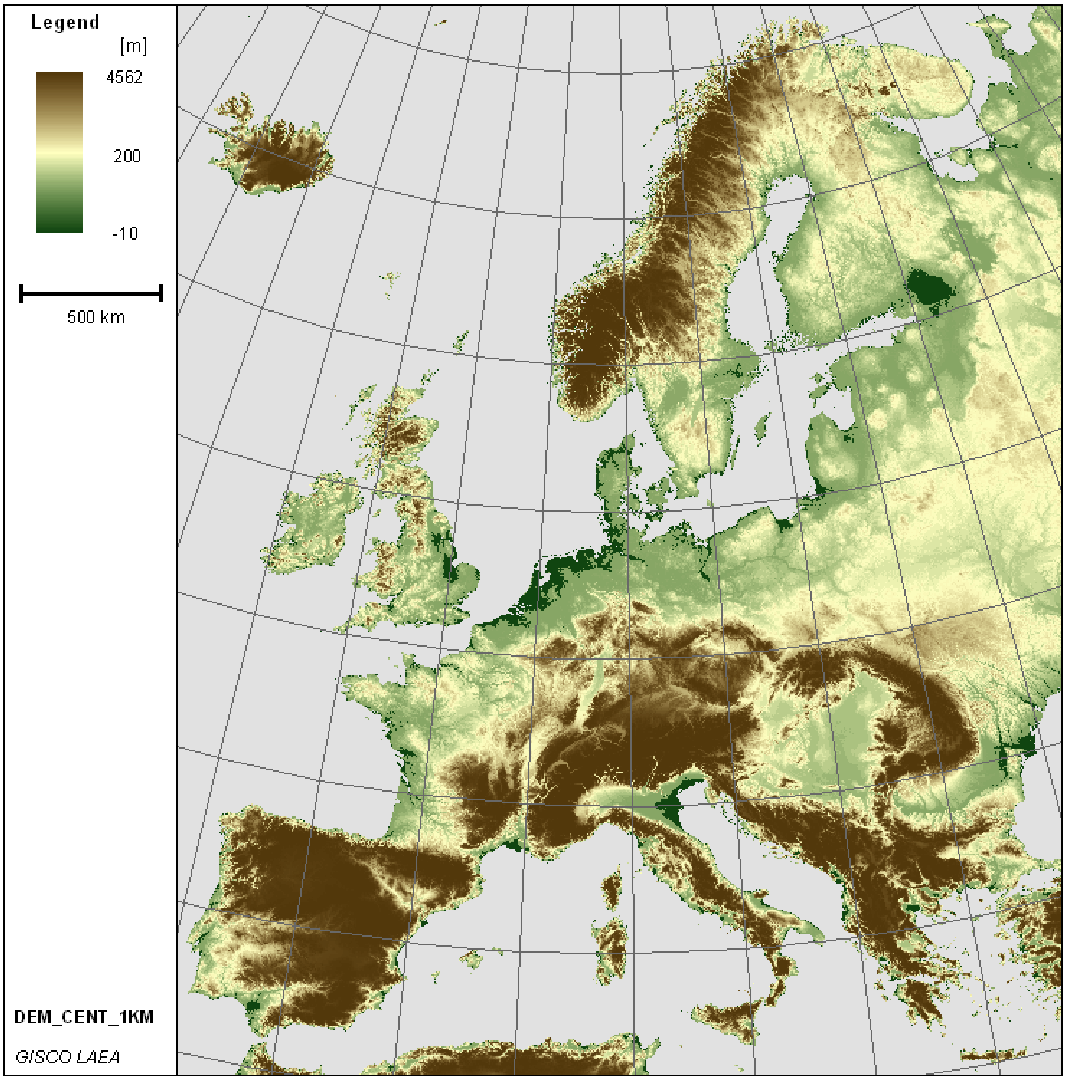

Figure 31 DEM in 1 km resolution using central resampling method

DEM_CENT_1KM.MAP

Format: PCRaster/PCRaster Raster File
Size is 3400, 4050
Coordinate System is GISCO LAEA 0948
Origin = (-1700000.000000000000000,2700000.000000000000000)
Pixel Size = (1000.000000000000000,-1000.000000000000000)
Metadata:
  PCRASTER_VALUESCALE=VS_SCALAR
Corner Coordinates:
Upper Left (-1700000.000, 2700000.000)
Lower Left (-1700000.000,-1350000.000)
Upper Right (1700000.000, 2700000.000)
Lower Right (1700000.000,-1350000.000)
Center   (0.000, 675000.000)
Band 1 Block=3400x1 Type=Float32, ColorInterp=Undefined
  Min=-10.000 Max=4562.000
  Minimum=-10.000, Maximum=4562.000, Mean=331.304, StdDev=375.703
  NoData Value=-3.40282346638529e+38

4.2 Relative Relief Map

The relative relief is defined as the biggest vertical difference within a given area. As relative relief express the potential energy available for downslope transport, it is also called relief energy (Hagedorn, 1985). The relative relief map (*Figure 32*) is equal to the 'elevation range map' required by LISFLOOD describing the difference between maximum and minimum elevation within a modelled pixel in metre (van der Knijff and de Roo, 2008).

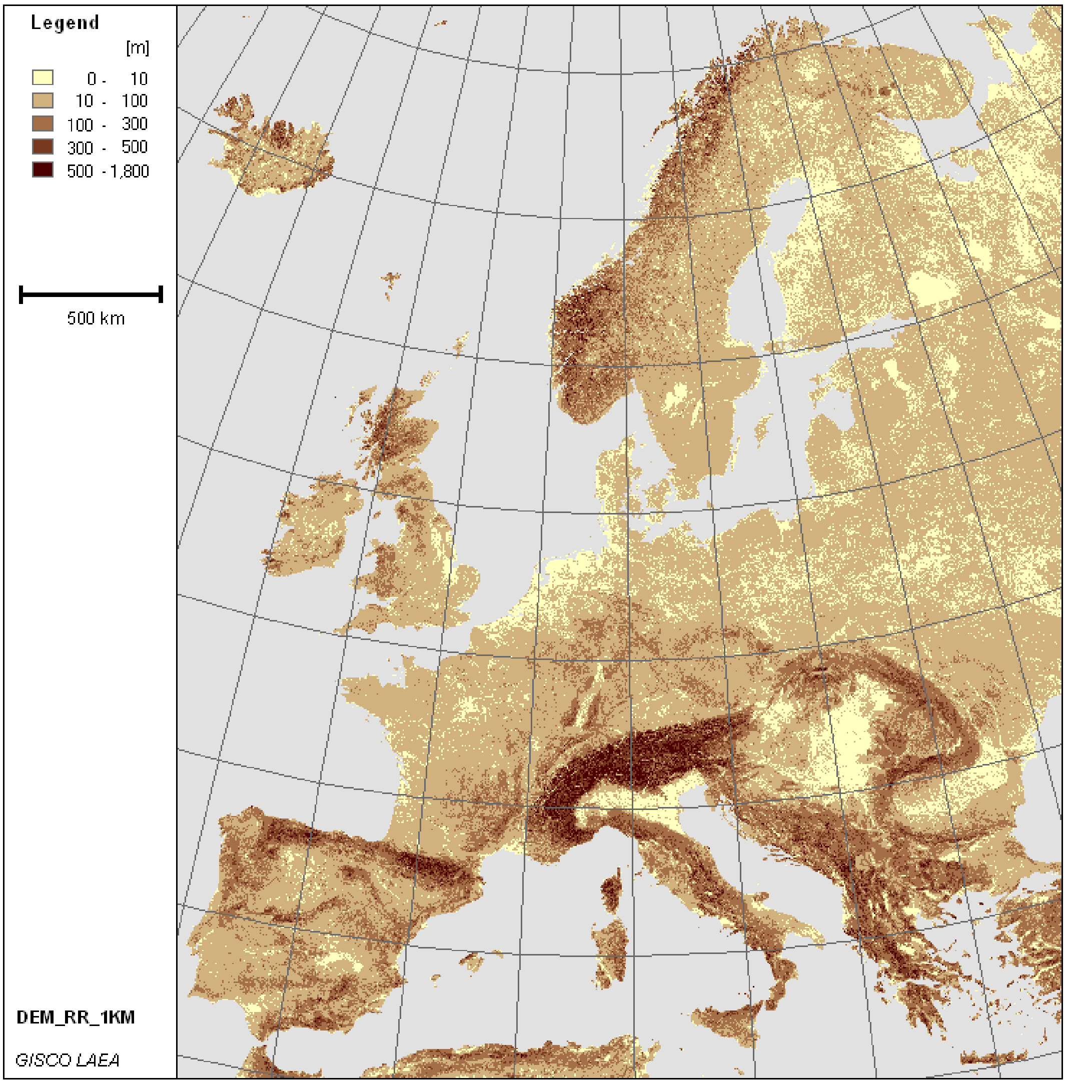

Figure 32 Relative relief map in 1 km resolution based on SRTM elevation model

The main characteristics of the processed relative relief maps [m] are the followings:

DEM_RR_1KM.MAP - Minimum=0.000, Maximum=1791.000, Mean= 75.493, StdDev=107.175
DEM_RR_5KM.MAP - Minimum=0.000, Maximum=2999.000, Mean=220.272, StdDev=290.973

Since the applied DEM100 data is an SRTM-based merged product of elevation data from different sources (SRTM and GTOPO30 and some other sources at higher latitudes), the derived maps are amplifying the edges between different data sets.

4.3 Standard Deviation Map

The map of standard deviation of averaged values was calculated in order to present how widely the values are dispersed from the arithmetic mean value in each resampled cell (*Figure 33*).

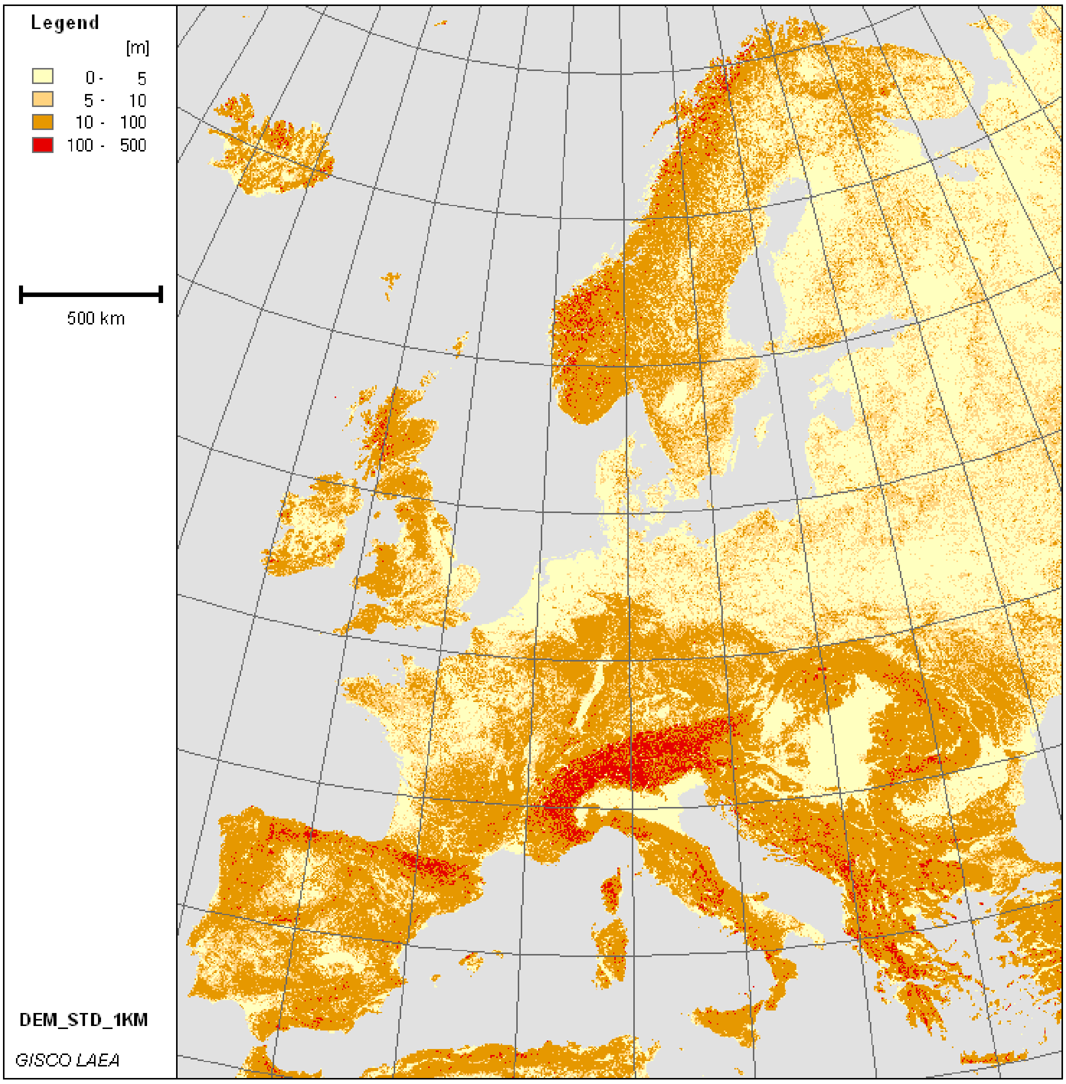

Figure 33 Standard deviation map in 1 km resolution based on SRTM elevation model

The main characteristics of the processed standard deviation maps [m] are the followings:

DEM_STD_1KM.MAP - Minimum=0.000, Maximum=524.997, Mean=18.860, StdDev=27.458
DEM_STD_5KM.MAP - Minimum=0.000, Maximum=709.146, Mean=48.305, StdDev=67.467

The purpose of this map is to provide additional information about the distribution of elevation values based on the higher resolution data. The obtained information is going to be used in definition of sub-pixel elevation zones for snow accumulation and melt modelling.

4.4 Skewness Map

The skewness of a distribution characterizes the degree of asymmetry of a distribution around its mean (*Figure 34*). Positive skewness indicates a distribution with an asymmetric tail extending toward more positive values (relatively few large data values). Negative skewness indicates a distribution with an asymmetric tail extending toward more negative values (relatively few low data values).

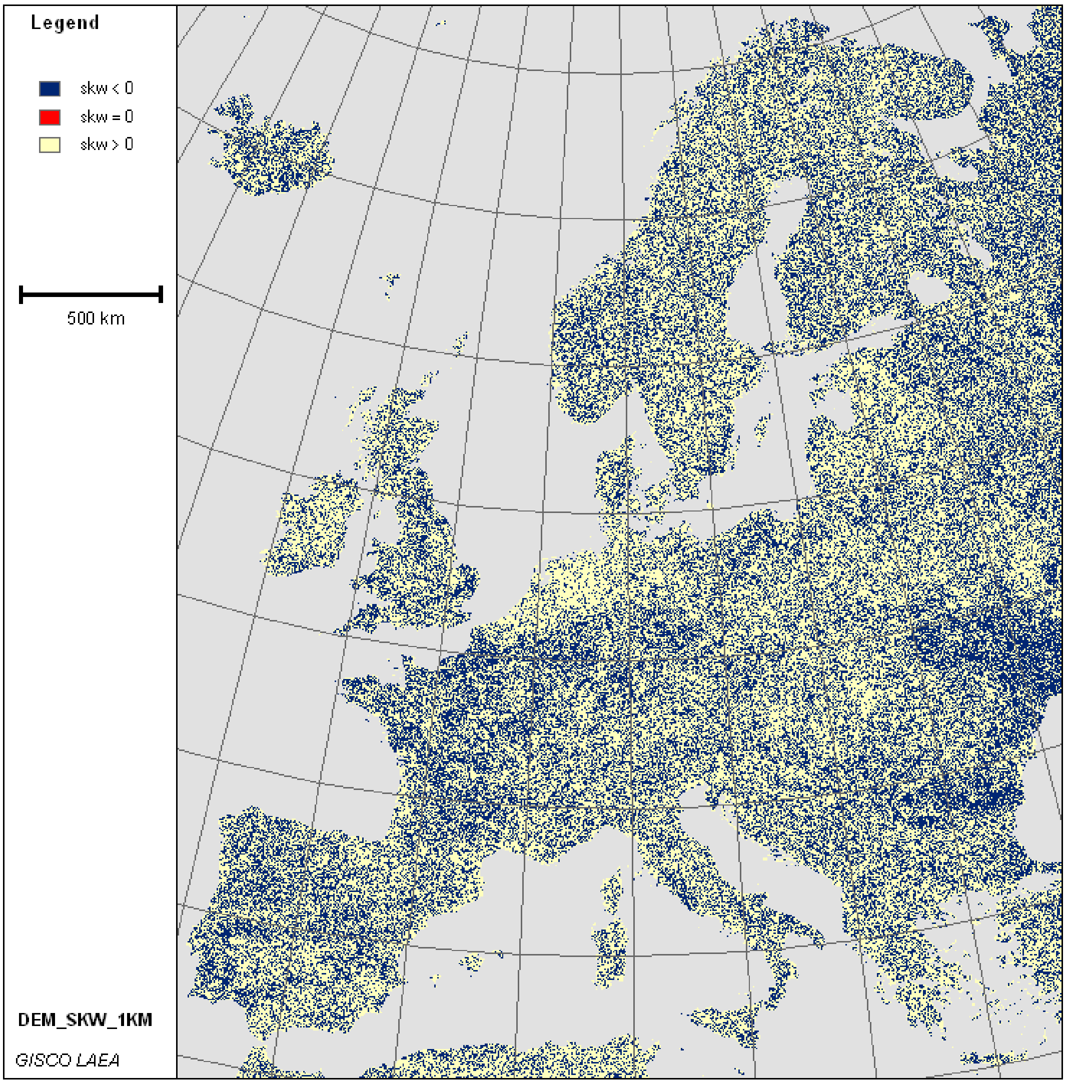

Figure 34 Skewness map in 1 km resolution based on SRTM elevation model

The main characteristics of the processed skewness maps are the followings:

DEM_SWK_1KM.MAP - Minimum= - 9.949, Maximum= 9.949, Mean=0.160, StdDev=0.730
DEM_SKW_5KM.MAP - Minimum= -18.026, Maximum=35.327, Mean=0.294, StdDev=0.814

Similarly to the previously presented standard deviation map, the skewness map was created in order to provide additional information about the distribution of elevation values based on the higher resolution data. The obtained information is going to be used in definition of sub-pixel elevation zones for snow accumulation and melt modelling.

4.5 Slope Gradient Map

Slope gradient shows the maximum rate of change in value from each cell to its neighbours. According to the model requirements the final slope gradient (*Figure 35*) is given as the tangent of slope in degrees (van der Knijff and de Roo, 2008).

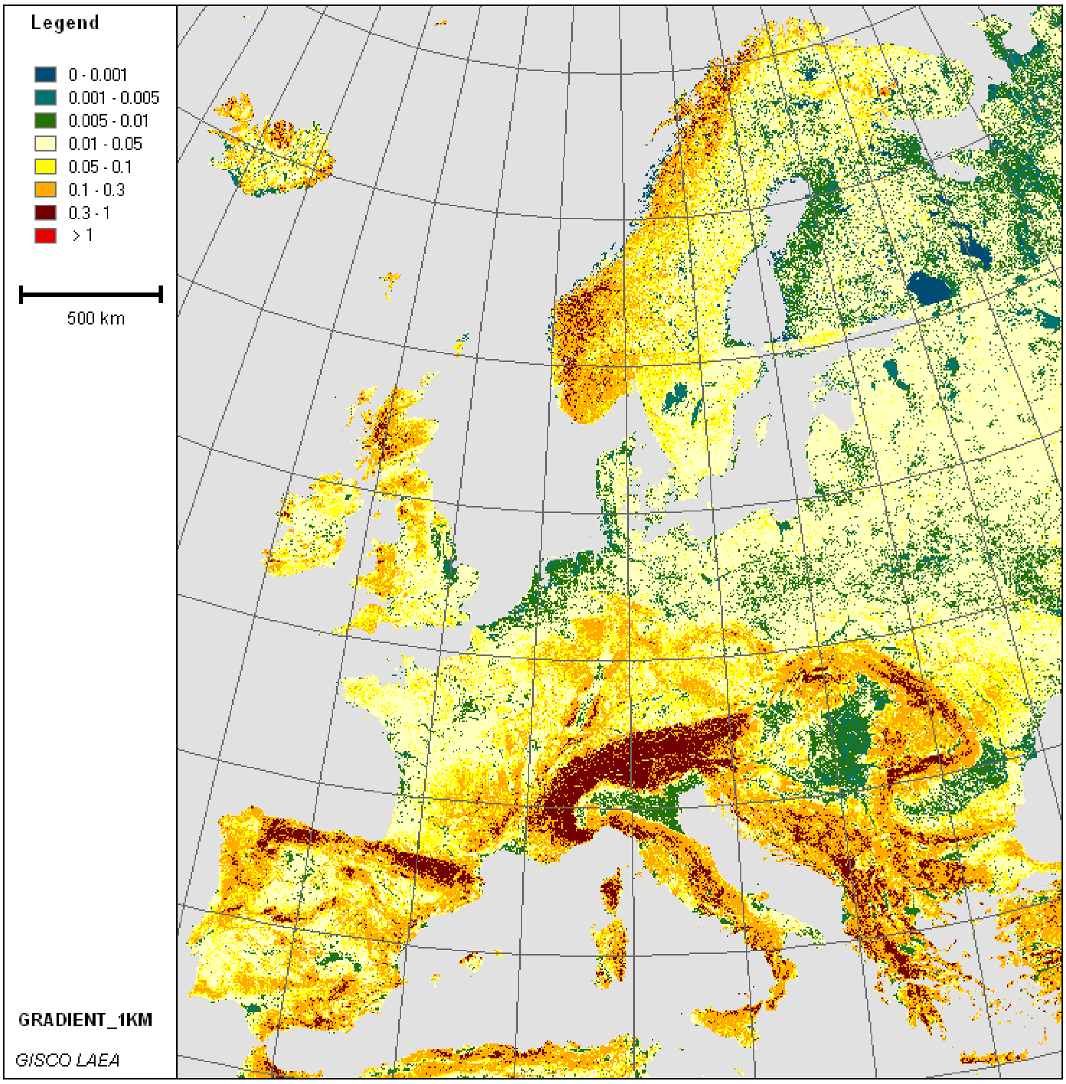

Figure 35 Gradient map in 1 km resolution based on SRTM elevation model

The main characteristics of the processed slope gradient values are the followings:

GRADIENT_1KM.MAP - Minimum=0.000, Maximum=1.362, Mean=0.079, StdDev=0.107
GRADIENT_5KM.MAP - Minimum=0.000, Maximum=0.698, Mean=0.079, StdDev=0.097

4.6 Channel Gradient Map

The channel gradient maps sampled in both, 1 km and the 5 km resolution grids naturally show lower values than the steepness of surface slopes (*Figure 36*).

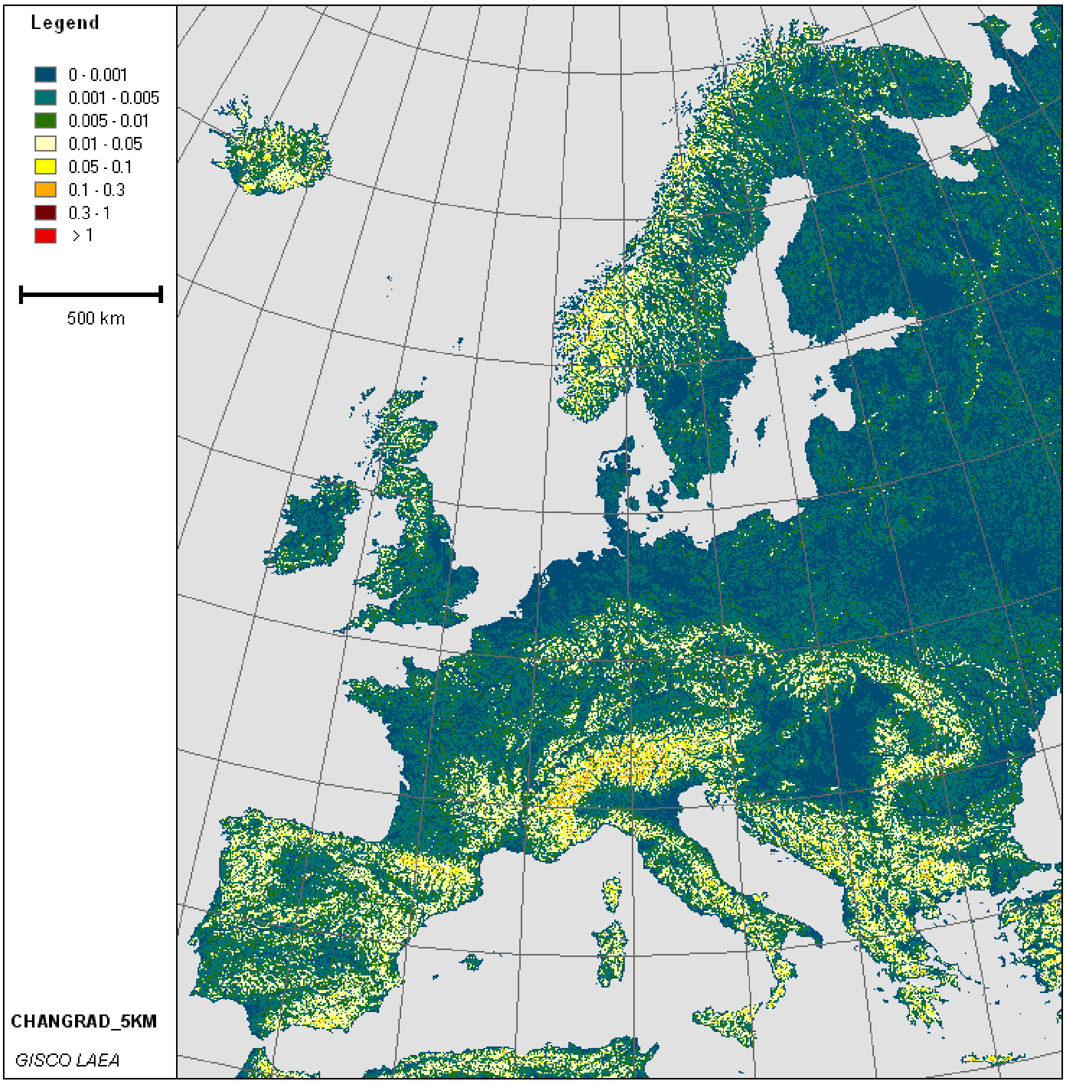

Figure 36 Channel gradient map in 5 km resolution based on SRTM elevation model

The main characteristics of the processed channel gradient values are the followings:

CHANGRAD_1KM.MAP - Minimum=0.000, Maximum=0.656, Mean=0.016, StdDev=0.032
CHANGRAD_5KM.MAP - Minimum=0.000, Maximum=0.522, Mean=0.006, StdDev=0.014

4.7 Channel Length Map

The new channel length maps reflect the flow pattern more realistically than the previously applied unique values given by the cell size and a standard multiplier (*Figure 37*).

The main characteristics of the processed channel length values [m] are the followings:

CHANLENG_1KM.MAP - Minimum=667, Maximum= 1584, Mean=1187.593, StdDev= 114.127
CHANLENG_5KM.MAP - Minimum=768, Maximum=11669, Mean=5371.818, StdDev=1524.804

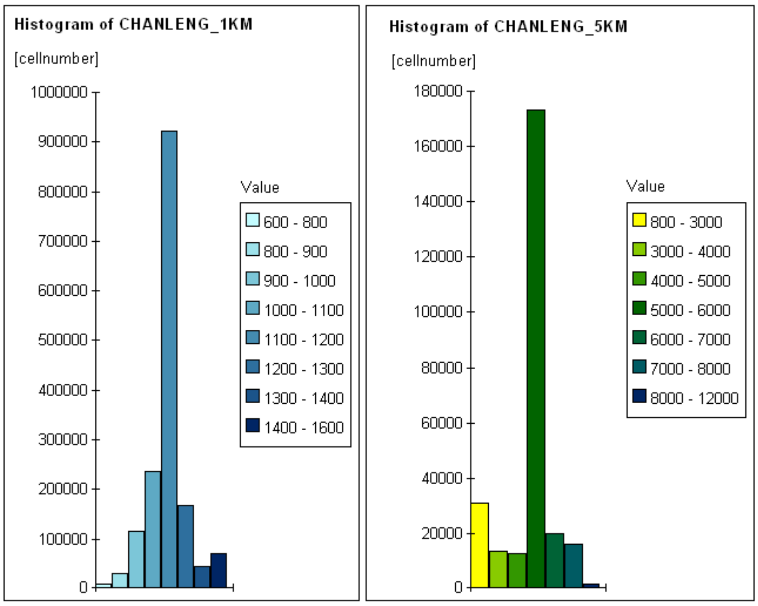

Figure 37 Frequency distribution of channel length values in the 1 km and 5 km model

The channel length can be smaller then the grid size if the flow path just 'touches' the pixel, or can exceed the grid size, to account for meandering rivers.

4.8 Channel Bottom Width Map and Bankfull Channel Depth Map

The channel bottom width values and bankfull channel depth were interpolated between measured information within the Danube River Basin and the Elbe River Basin. The values of other river basins were replaced by the values of previous data sets.

The main characteristics of the processed channel bottom width values [m] are the followings:

CHANBW_1KM.MAP - Minimum=3.000, Maximum=1500.000, Mean=8.357, StdDev=45.415
CHANBW_5KM.MAP - Minimum=3.000, Maximum= 999.520, Mean=7.036, StdDev=33.480

The main characteristics of the processed channel bottom width values [m] are the followings:

CHANBNKF_1KM.MAP - Minimum=0.500, Maximum=15.000, Mean=0.680, StdDev=1.096
CHANBNKF_5KM.MAP - Minimum=0.781, Maximum=16.000, Mean=1.348, StdDev=1.396

4.9 Local Drain Direction (LDD) Maps

The European 1 km gridded flow network, which was considered as a reference LDD in this resolution, has been developed for the Catchment-based Information System (CIS). The LDD_1km has been forming the essential part of the LISFLOOD hydrological model since it was published (Hiederer and de Roo, 2003). Only the LDD in 5 km resolution has been modified as described earlier in this phase of the project (*Figure 38*).

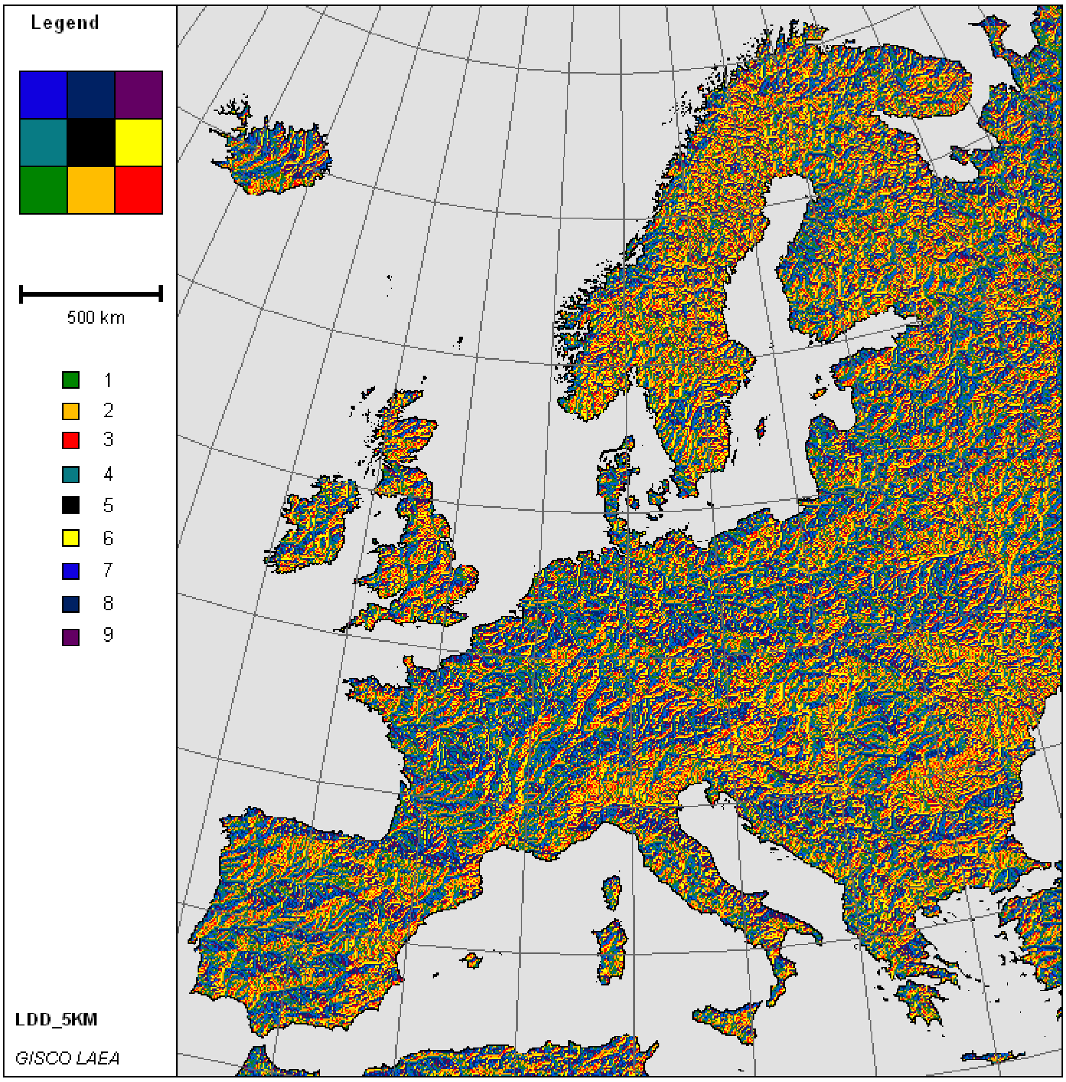

Figure 38 Channel gradient map in 5 km resolution based on SRTM elevation model

The applied D8 method shows an obvious bias towards the cardinal (orthogonal) directions against the intermediate (diagonal) directions. The pattern of processed European layers (*Figure 39*) shows similarity to the distribution based on the original data, or the pattern of selected sub-basins (*Figure 1*). The reason of this bias is that when differences in elevation are the same between neighbouring cells, the slopes towards the closet neighbours (orthogonal cells) are the steepest ones.

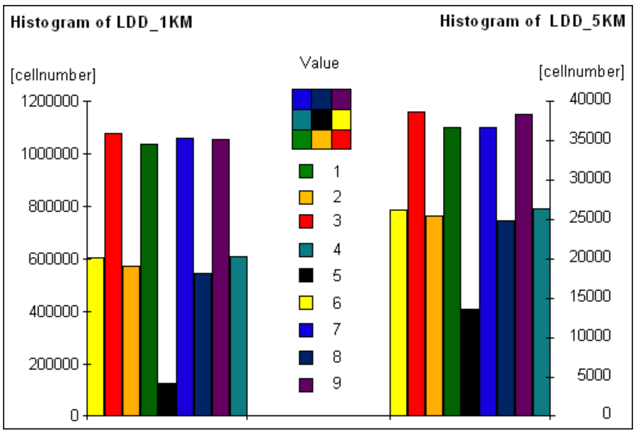

Figure 39 Frequency distribution of directions in LDDs

4.10 Land Cover Map

The processed European Land Cover data (ELC2000) in 100 m resolution as it forms an input data to the MOLAND model (Monitoring Land Use/Cover Dynamics) is presented in *Figure 27*. For LISFLOOD modelling the data was resampled in 1 km and 5 km resolution grid using two different techniques; central and dominant sampling. Considering the functions of 'land use map' in the hydrological model, the data generated by the spatially dominant condition is recommended for further modelling. The processed data in 5 km grid is given in *Figure 40*.

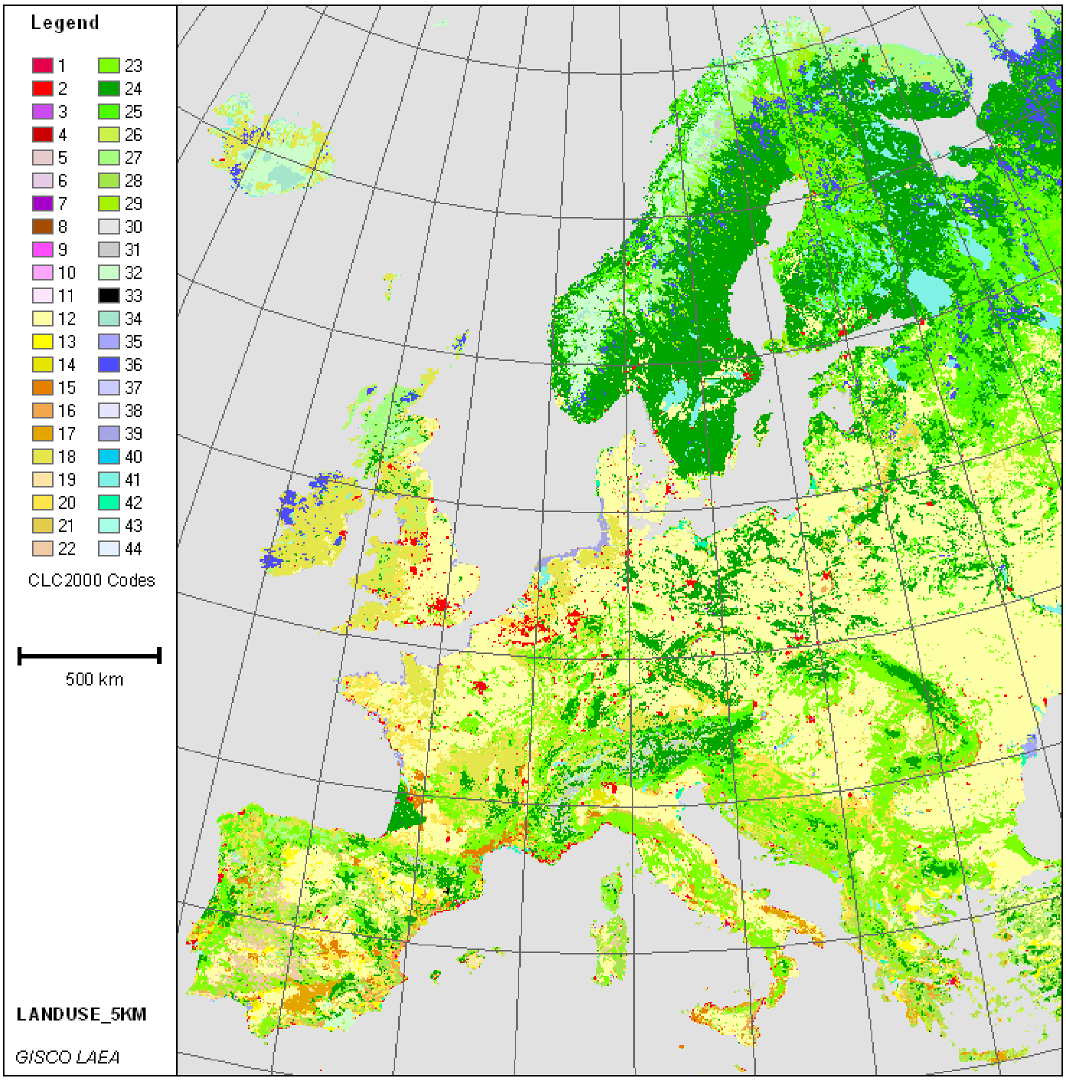

Figure 40 Land cover map in 5 km resolution based on merged CLC2000-GLC2000 data. Codes of applied CORINE land cover classes are given in Annex 2

The spatial resampling has naturally altered the cardinality of the input value set and there are areal differences in aggregated classes using the different techniques (*Figure 41*, see also *Annex 4*).

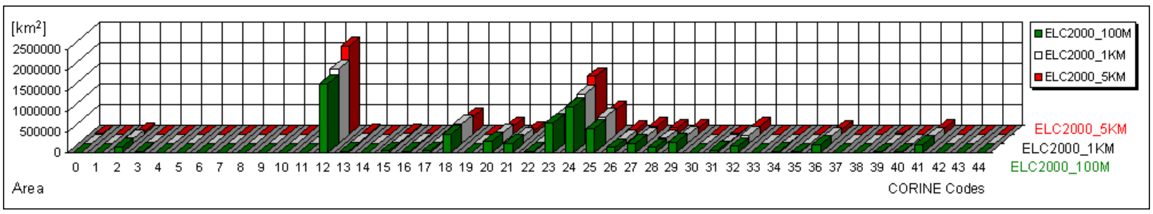

Figure 41 Total area of dominant land cover classes in three resolutions; 100 m, 1 km and 5 km

4.11 Forest Fraction Map

The gridded data contains the forest fraction for each cell. The classes 'broad-leaved forest', 'coniferous forest' and 'mixed forest' of combined ELC2000 were merged then the areal proportion of forest coverage defined for each cell in 1 km and 5 km grid (*Figure 42*).

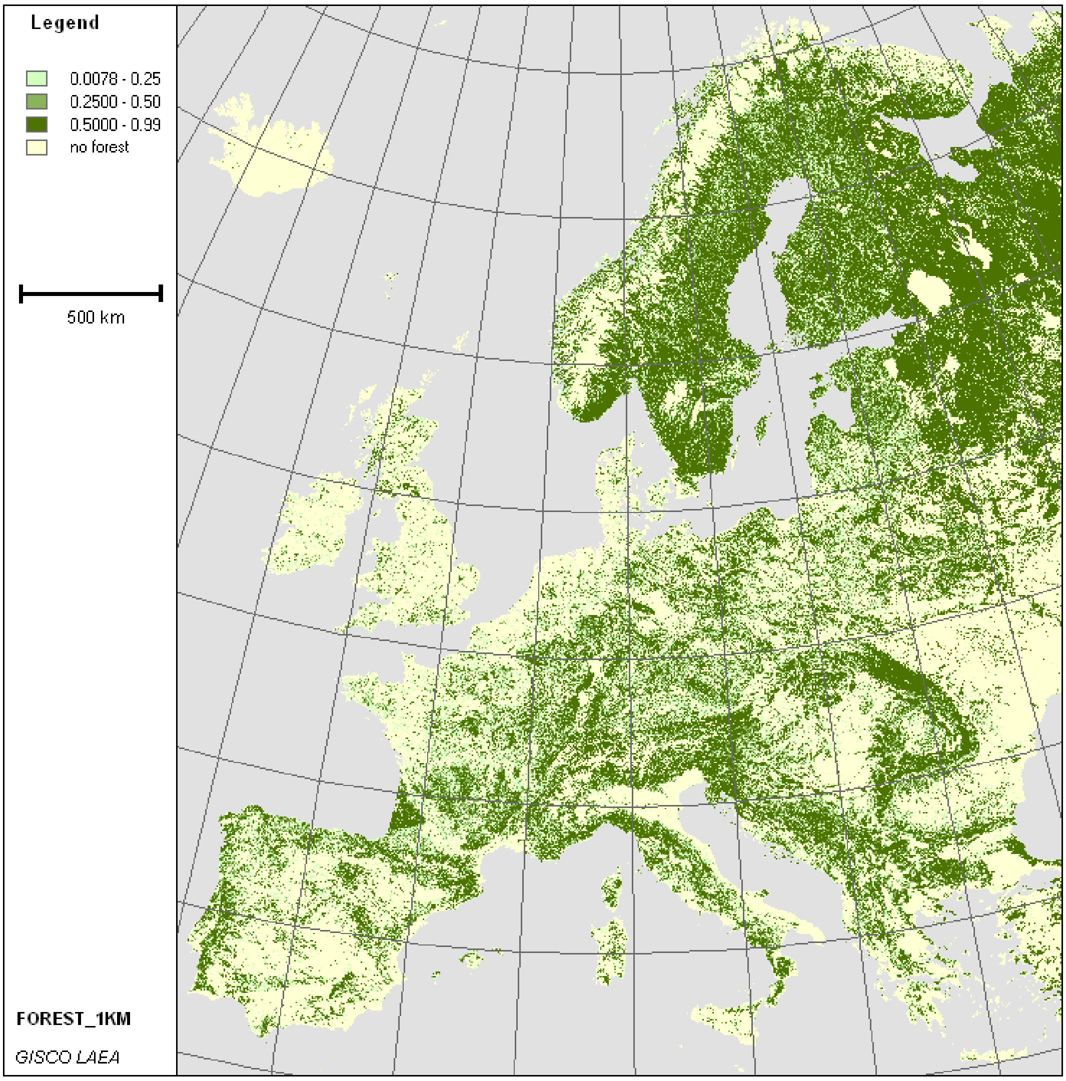

Figure 42 Map of forest coverage in 1 km resolution based on merged CLC2000-GLC2000 data. Values range from 0 (no forest at all) to 1 (pixel is 100% forest)

4.12 Direct Runoff Fraction Map

For the direct runoff fraction map a classification of permeability was applied assigning the land cover classes to five permeability classes (Laguardia, 2005) and calculating then the average permeability for each 1 km (*Figure 43*) and 5 km pixel (see also *Annex 5*).

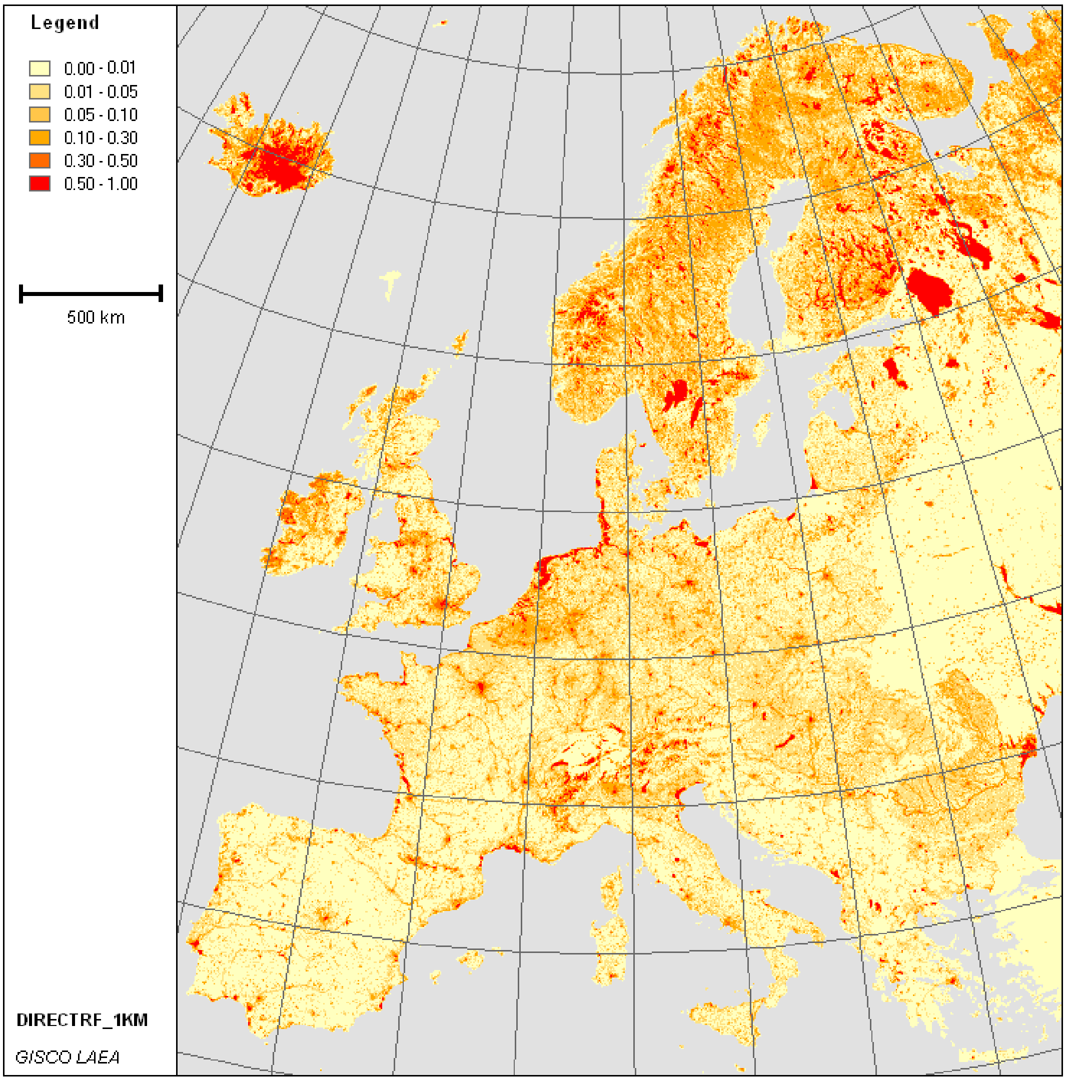

Figure 43 Percent of impermeable surface of Europe created assigning the land cover classes to permeability classes and calculating then the average permeability for each pixel. Values range from 0 (only permeable surface) to 1 (100 % urban area or water bodies)

The processed map contains wider information for permeability and water balance modelling than the previously applied classification of only two classes (build-up areas and water bodies). The applied methodology was developed and tested for soil moisture simulation related to a change of the evaporation rate of intercepted water (Laguardia, 2008).

5 Results – New African Input Maps

The sources of processed African data layers were the presented global geo-spatial databases. The African data set is kept in the source geographic coordinates with the WGS 84 datum. According to the model requirements against the data format, the African layers also were converted into PCRaster map format. The binary raster format does not store the definition or parameters of the projection. The geographic location is given only by the coordinates related to the above defined projections. The list of the processed African data layers is given in *Table 9*.

Table 9 *New African data layers related to topography, soil and land cover (0.1 degree)*

Name of New PCRaster Map	Default Name in LISFLOOD	Description
cellarea_01.map		Cell area in km^2 for each 0.1 x 0.1 cell
celldiag_01.map		Cell diagonal in km for each cell
cellheight_01.map		Cell height in km for each cell
cellwidth_01.map		Cell width (mid-line) in km for each cell
chanleng_01.map	chanleng.map	Channel length [m] based on LDD
dem_mean_01.map		Digital elevation model, average of values [m]
dem_cent_01.map		Digital elevation model, central value [m]
dem_max_01.map		Digital elevation model, maximum value [m]
dem_min_01.map		Digital elevation model, minimum value [m]
dem_rr_01.map		Digital elevation model, relative relief [m]
dem_skw_01.map		Digital elevation model, skewness of distribution
dem_std_01.map		Digital elevation model, standard deviation [m]
forest_01.map	forest.map	Forest fraction for each cell
directrf_01.map	directrf.map	Fraction of urban area for each cell
lai20080101.map, lai20080111.map, ... lai20090101.map		Leaf area index (LAI) - a sequence of LAI maps
ldd_01.map	ldd.map	Local drain direction map (with value 1-9)
glcclass_domi_01.map	landuse.map	Map of dominant land cover classes (GLC2000)
glcclass_variety_01.map		Number of present land cover classes for each cell
glcclass01pct.map, glcclass02pct.map, ... glcclass29pct.map		Percent of area of each land cover class
	gradient.map	Slope gradient [m m^{-1}]
soildep_01.map	soildep.map	Soil depth map [cm]
soiltex1_01.map	soiltex1.map	Soil texture maps - Subsoil
soiltex2_01.map	soiltex2.map	Soil texture maps - Topsoil
ups_01.map		Upstream area map for each cell [km^2]
zfactafr_01.map		Z-factor for African

5.1 Digital Elevation Model

The subset of global SRTM elevation data in 3 arcsec resolution was extracted and upscaled into 6 min resolution using two sampling techniques; the new values were defined by central sampling (*Figure 44*) and by the mean of corresponding original values.

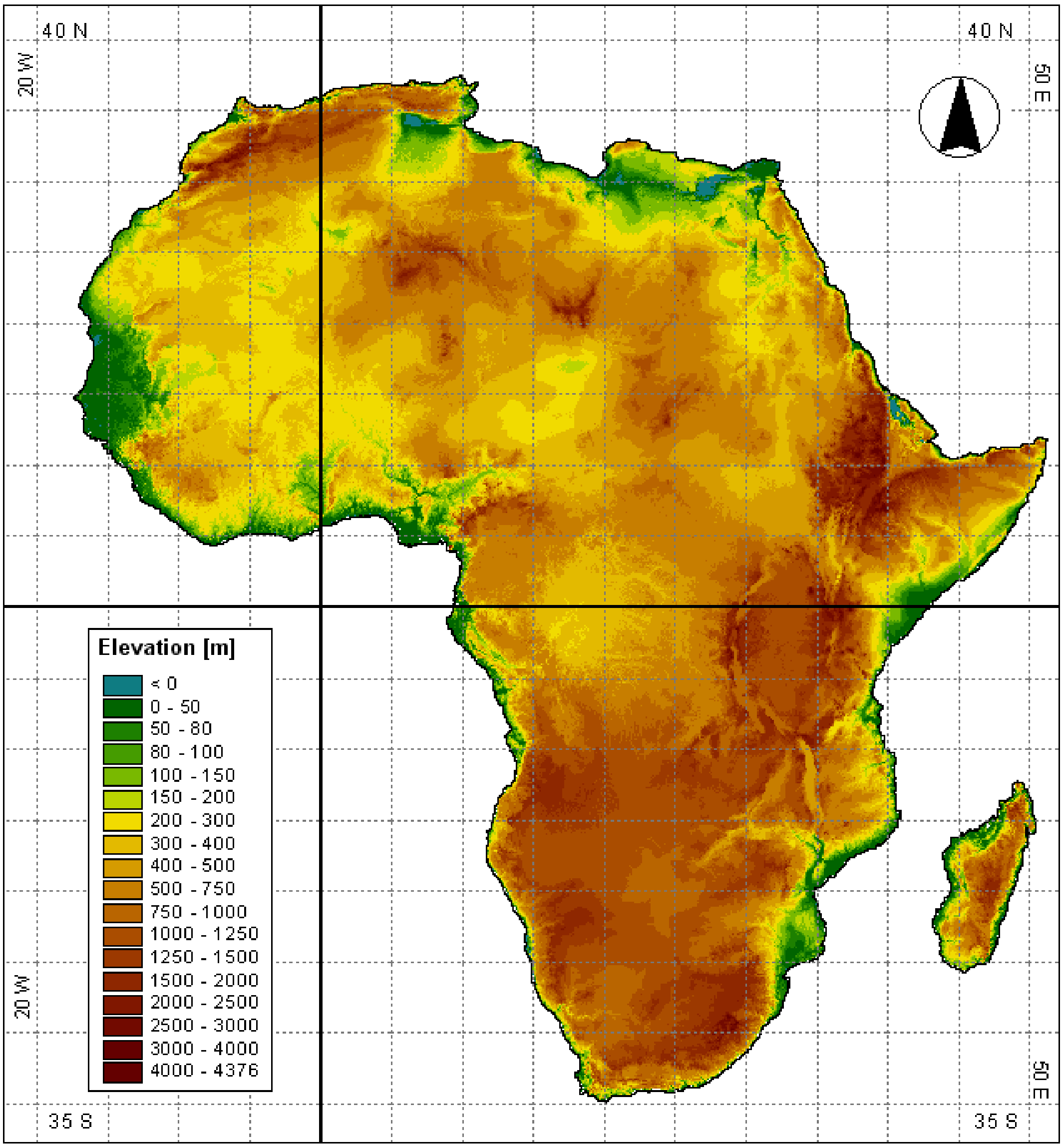

Figure 44 SRTM-based DEM in 0.1 degree (6 min) resolution using central resampling method

Naturally the original value set has been altered and the main statistical characteristics (maximum-minimum values, mean, standard deviation, etc.) of the derived data set are different from each other too (*Table 10*).

***Table 10** Characteristics of the processed value sets derived from SRTM data*

	source	dem_cent_01	dem_mean_01	dem_max_01	dem_min_01
Minimum Value	-174.000	-157.000	-120.750	-113.000	-174.000
Maximum Value	5866.000	4376.000	4207.415	5866.000	3579.000
Mean	630.153	629.200	629.238	734.120	563.483
Standard Deviation	448.680	449.001	444.750	518.775	404.241

5.2 Relative Relief Map, Standard Deviation Map and Skewness Map

The relative relief map (dem_rr_01) was calculated by the difference of defined minimum and maximum values based on the higher resolution elevation data (*Figure 45*). However the snow accumulation and melt modelling will probably not be in the main focus of the hydrological model runs in African river basins, the auxiliary maps – standard deviation (dem_std_01), skewness (dem_skw_01) – providing additional information regarding the surface have been also processed. Their main numerical characteristics are summarized in *Table 11*.

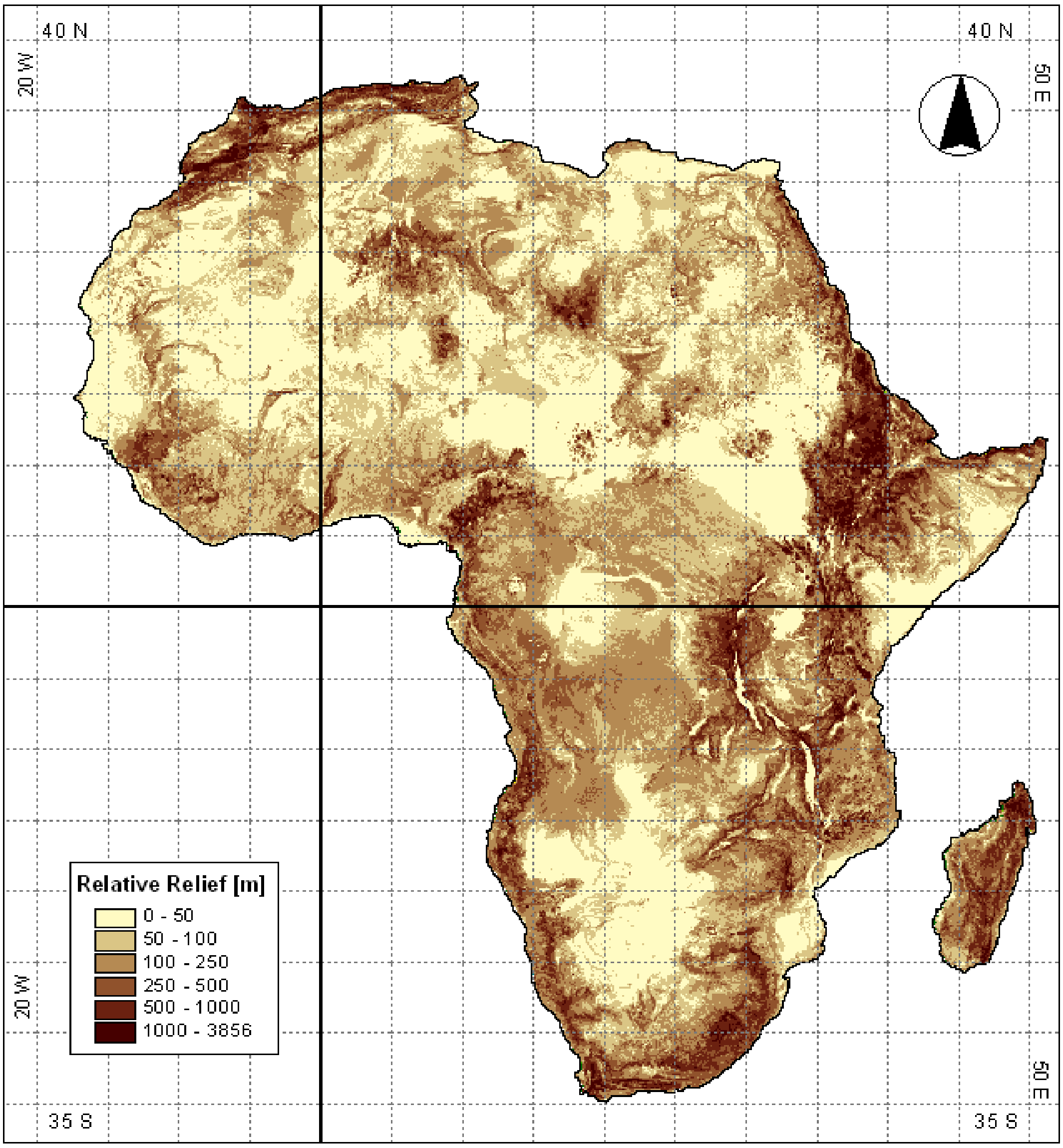

Figure 45 Relative relief map based on SRTM data resampled to 0.1 degree (6 min) resolution

Table 11 *Characteristics of auxiliary data related to topography derived from SRTM*

	source	dem_rr_01	dem_std_01	dem_skw_01
Minimum Value	-174.000	0	0	-24.105
Maximum Value	5866.000	3856.000	824.306	24.107
Mean	630.153	172.107	34.592	0.372
Standard Deviation	448.680	225.411	50.369	1.007

5.3 Geometrical parameters of each cell

The African data set is defined in the geographic coordinate system (latitudes and longitudes). In this reference system the length of a degree of longitude changes with latitude, thus the area of a cell given in degree-based resolution is also changing; the farther the pixel is from the Equator the smaller area it covers. The cell-based distance and areal measurements using the metrical scale (e.g. catchment area, length of flow path, gradient) require additional auxiliary information. The applied distances in kilometres and the cell-size in square kilometres belonging to the integer latitudes are given in *Annex 1*.

For the African map set the geometrical parameters of 0.1 degree resolution pixels were calculated using the semi-axes of WGS 1984 spheroid in the approximations of spherical distances. The 0.1x0.1 size sectors of sphere were simplified then as isosceles trapezoids and their length of mid-line was defined [cellwidth_01.map]. The height of the0.1x0.1 size sectors were defined [cellheight_01.map] by the semi-minor axis of the WGS 1984 (constant value). Their product is the area map of the pixels [cellarea_01.map]. For the later flow length estimations the length of the diagonals of the sectors was also defined [celldiag_01.map] using the Pythagorean position. The dimension of map values is kilometre, except in the case of the area map, where the dimensional unit is square kilometre. The main characteristics of the processed auxiliary maps are given in the *Table 12*.

***Table 12** Characteristics of the auxiliary maps of geometrical parameters of cells*

	Minimum	Maximum	Mean	Std. Deviation
cellwidth_01.map	8.521	11.132	10.338	0.714
cellheight_01.map	11.095	11.095	11.095	0
cellarea_01.map	94.541	123.504	114.696	7.923
celldiag_01.map	13.989	15.717	15.174	0.48

5.4 Slope Gradient Map

For the African basins only the surface gradient was estimated based on SRTM data. Since the length of a degree of longitude changes with latitude, and the surface z unit is expressed in unit (metre) which is different from the ground x,y unit (degree), the use of an appropriate z-factor [zfactafr_01.map] for latitudes is needed (see also *Annex 1*). The calculation was completed in three main steps using Arc/Info grid functions:

a) Slope calculation in degree using predefined z-factor for each 0.1 degree

```
slope03s_afr = slope ((srtm03s_afr * zfactafr_01), degree)
```

b) Rescaling the high resolution values to 0.1 degree assigning the mean value to the new cells

```
slope01d_avr = aggregate (slope03s_afr, 120, mean)
```

c) Gradient (rise/run) calculation by the tangent of the slope degrees in radian

```
gradient_01 = tan (slope01d_avr div deg)
```

DEG is an in-built constant (57.296) converting decimal degrees to radians. The ranges of value sets of the processed maps are given in *Table 13*. The result gradient map was converted to PCRaster map format [gradient_01.map].

***Table 13** Minimum and maximum values of the processed maps related to surface slopes*

	zfactafr_01.map	slope03s_afr	slope01d_avr	gradient_01.map
Minimum Value	0.000008983153	0.000	0.000	0.000
Maximum Value	0.000011726673	52.977	23.881	0.441

5.5 Local Drain Direction Map

The processed African LDD (v. 1.0) is presented in *Figure 24*. The defined flow directions provide the basis for delineation of large catchments and sub-catchments (*Figure 46*) in order to model hydrological phenomena. Preliminary research results and feasibility studies (Thiemig, 2009) show the applicability of the processed flow direction data.

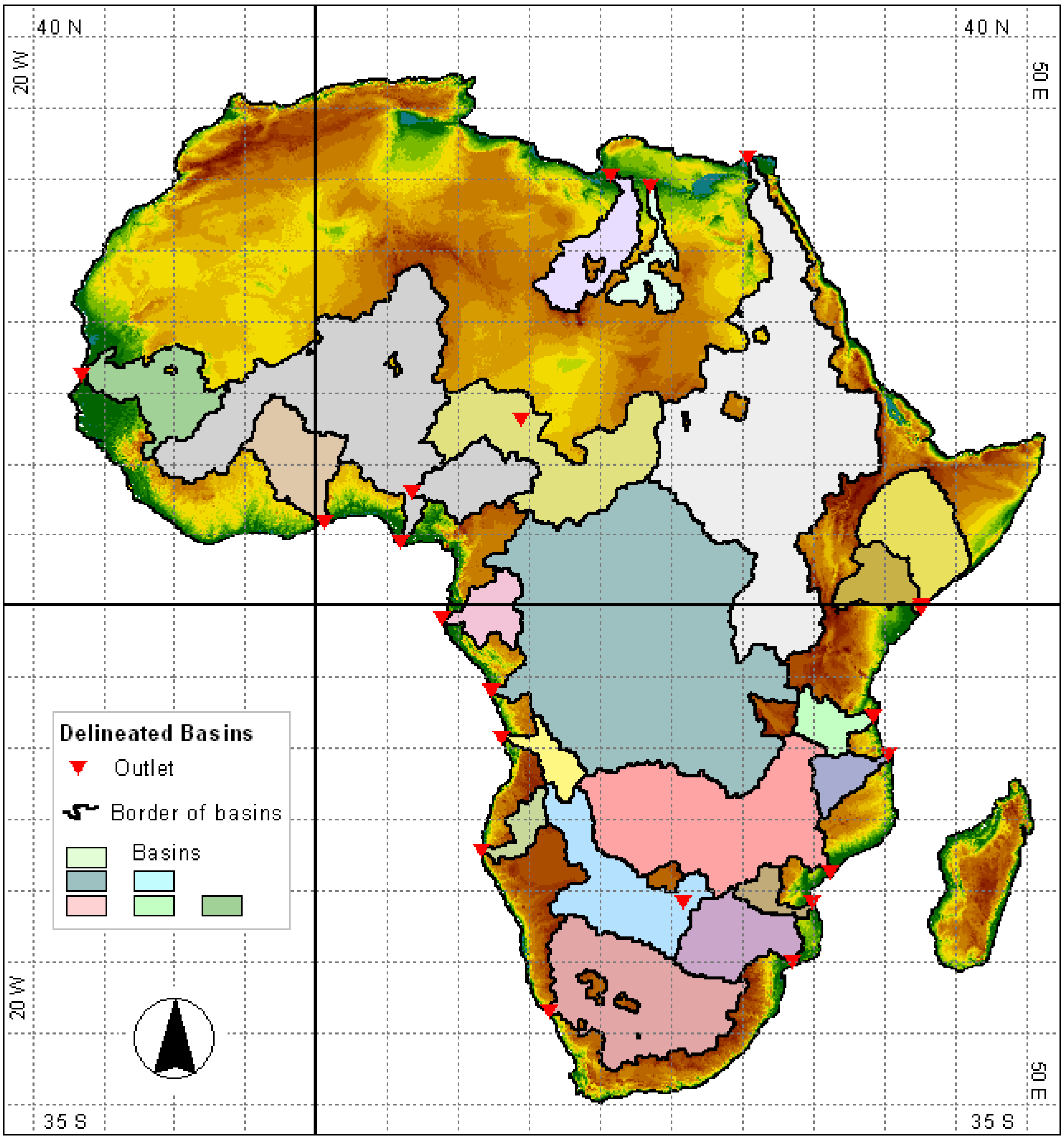

Figure 46 Delineated basins based on derived flow directions

5.6 Channel Length Map Based on LDD

The channel (flow) length could be approximated roughly by the cell-size of the gridded model taking the length of orthogonal and diagonal directions into account. In the case of the African data set the directions were defined by the processed LDD [ldd_01.map]. The flow length of cells with longitudinal flow direction (north-south) was defined by the geometrical auxiliary map of the height of the cells [cellheight_01.map]. The cell width values [cellwidth_01.map] were assigned to the cells with latitudinal (east-west) flow directions. Cells with diagonal flow directions got their flow length values from the calculated geometrical diagonals [celldiag_01.map]. An empirical multiplier could be applied to adjust the geometrical values of flow direction map [chanleng_01.map]. The map unit is metre.

The main characteristics of the processed channel length values [m] are the followings:

CHANLENG_01.MAP - Minimum=8837.476, Maximum=15716.551, Mean=12439.694, StdDev=2206.894

5.7 Land Cover Map, Forest Map, Direct Runoff Fraction Map

LISFLOOD input maps related to land cover of Africa were generated using the Global Land Cover 2000 data. The area-percentage of individual classes as well as the PCRaster map of the dominant land cover type and the variety of the classes (max 12) within the ~100km^2 pixels were calculated and rescaled to 0.1 degree resolution. The processed dominant land cover map is presented in *Figure 28*. The aggregated forest classes resulted in the input forest map of LISFLOOD (*Figure 47*). Similarly the area-percentage of urban area was defined for the direct runoff fraction map.

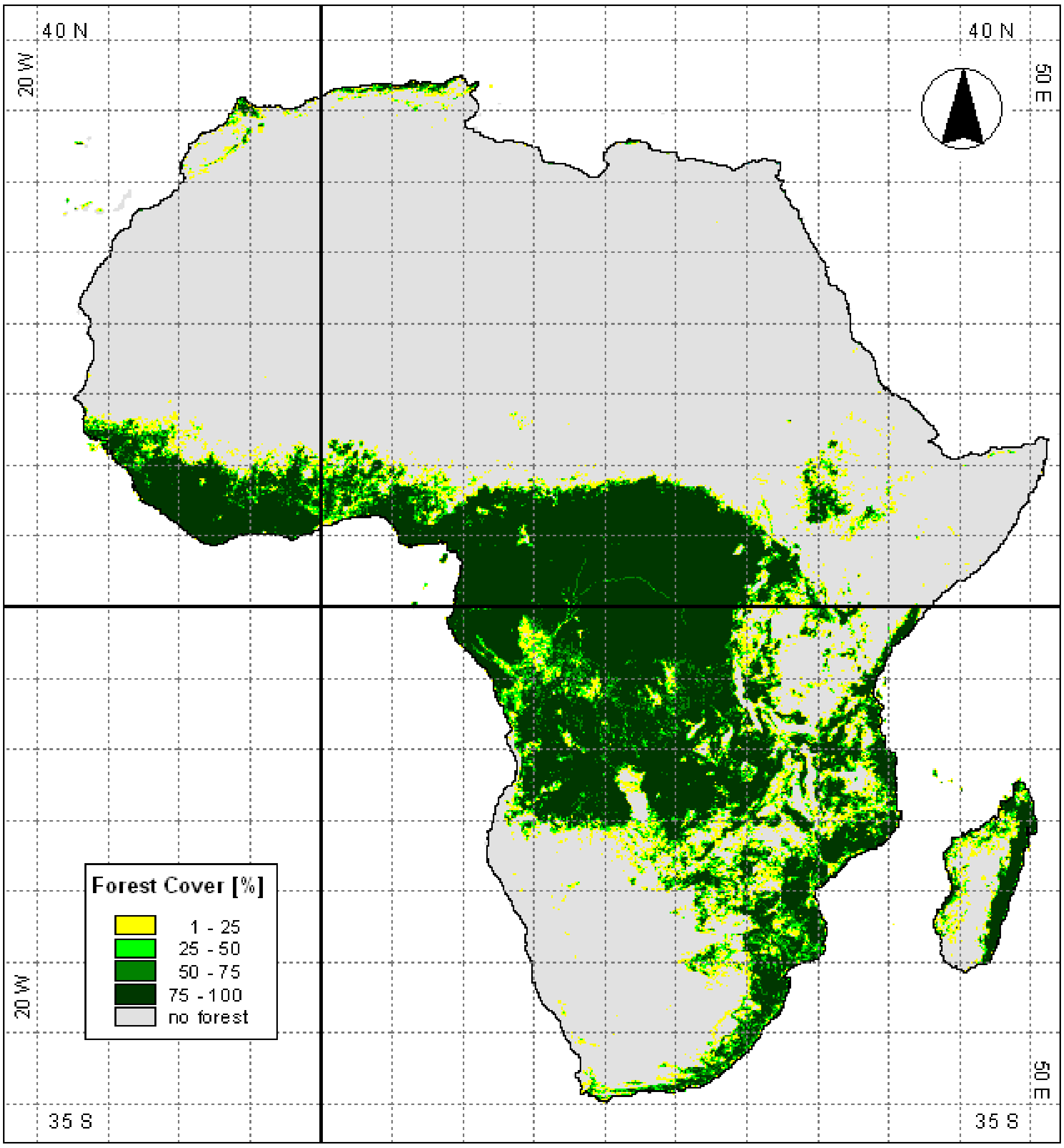

Figure 47 Forest cover map based on GLC2000 data resampled to 0.1 degree (6 min) resolution

5.8 Leaf Area Index Maps

In addition to land cover data a sequence of Leaf Area Index maps was processed. The source of the original data: VGT4AFRICA Project (MEDIAS/POSTEL). LAI data was extracted and converted based on the provided dataset. The prepared 0.1x0.1 degree data contain the average value of the higher resolution source grid data. After the data conversion (based on the documentation) the value-set is between 0 and 5.03333.

5.9 Soil Maps

The LISFLOOD hydrological model distinguishes between soil texture in two soil layers; soil texture class layer 1 and 2 (upper layer and lower layer).

5.9.1 Soil Texture Map

Soil texture layers of Africa were set up accordingly to the dominant soils based on the Harmonized World Soil Database v 1.0 (HWSD). The grid size was set to 0.1 degree. Sand, silt and clay content in percentage was derived on topsoil and subsoil levels with the condition that the sum of the three components was 100%:

For soiltex1.map (topsoil):
hwsda10_tsand.map - Topsoil Sand Fraction [%]
hwsda10_tsilt.map - Topsoil Silt Fraction [%]
hwsda10_tclay.map - Topsoil Clay Fraction [%]

For soiltex2.map (topsoil)
hwsda10_ssand.map - Subsoil Sand Fraction [%]
hwsda10_ssilt.map - Subsoil Silt Fraction [%]
hwsda10_sclay.map - Subsoil Clay Fraction [%]

The resulted soil texture classes (*Figure 48*) are based on the classification given in *Table 6*.

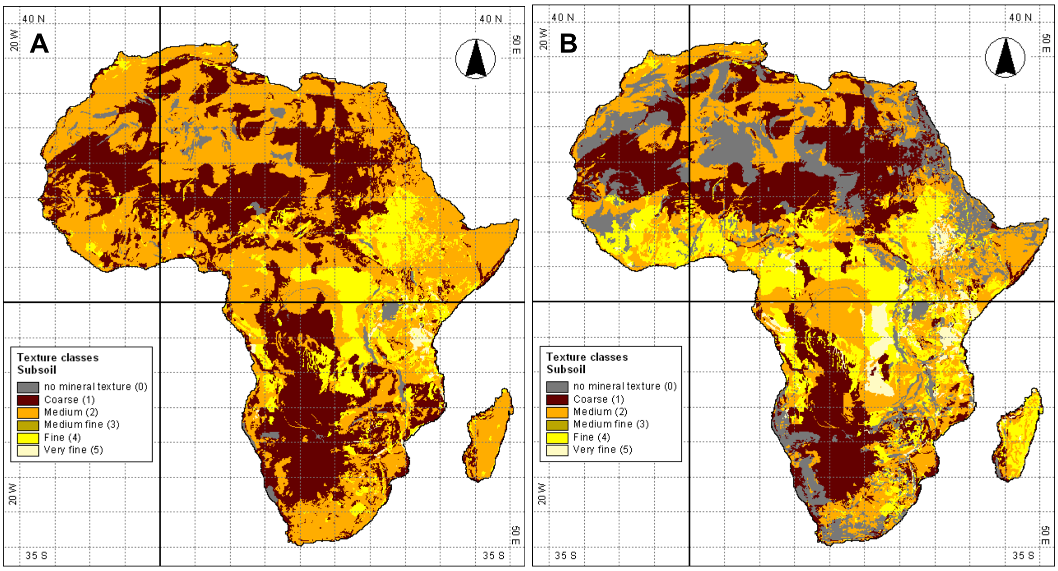

Figure 48 Soil texture classes as defined for topsoil (A, soiltex1.map) and subsoil (B, soiltex2.map)

5.9.2 Soil Depth Map

The soil depth map was extracted from the WHSD v. 1.0. According to the model requirements the most frequently occurring value of Reference Soil Depth [cm] was assigned to the new pixel. The data was resampled into 0.1 degree grid and converted into *soildep_01.map* PCRaster format.

6 Applications of the Data Set

The processed data set or parts of it provided input data for several researches on floods, and climate change effects on hydrology as well as supported research aiming land use modelling and spatial planning.

A few examples of applications of the data set are listed in this final chapter. The complete list of publications of the FLOODS Action of Land Management and Natural Hazards unit of the Institute for Environment and Sustainability, Joint Research Centre is available from the http://floods.jrc.ec.europa.eu/publications website.

a) Calibration of LISFLOOD Model

van der Knijff, J.M., J. Younis, J. and A.P.J. de Roo (2008) LISFLOOD: a GIS-based distributed model for river basin scale water balance and flood simulation, *International Journal of Geographical Information Science, 99999:1, DOI: 10.1080/13658810802549154*

Gierk, M., K. Bodis, J. Younis, J. Szabo, A. de Roo (2008) The impact of retention polders, dyke-shifts and reservoirs on discharge in the Elbe river, Hydrological modelling study in the framework of the Action Plan for the Flood Protection in the Elbe River Basin of the International Commission for the Protection of the Elbe River (ICPER), *European Commission, Directorate-General Joint Research Centre, Institute for Environment and Sustainability, Ispra, Italy, p. 110. EUR 23699 EN*

Szabó, J.A., M. Gierk, K. Wachter (2008) An approach for distributed parameter optimization of LISFLOOD hydrological model using efficient hybrid optimization procedure, *Geophysical Research Abstracts, Vol. 10, 2-2-2008*

Feyen, L., J.A. Vrugt, B.Ó. Nualláin, J. van der Knijff and A. De Roo (2007) Parameter optimisation and uncertainty assessment for large-scale streamflow simulation with the LISFLOOD model, *Journal of Hydrology, 332(1), 276-289.*

Kalaš, M., K. Wachter, J.A. Szabó, K. Bódis, S. Niemeyer, J. van der Knijff and A. de Roo (2005) Setup, calibration and testing of the LISFLOOD model for the Upper Danube River basin on 1km; *Geophysical Research Abstracts, Vol. 7, 09183, 2005, SRef-ID: 1607-7962/gra/EGU05-A-09183 © European Geosciences Union 2005*

Wachter, K., M. Kalaš, J. A. Szabó, S. Niemeyer, K. Bódis and A. de Roo (2005) Setup and testing of European Early Flood Alert System (EFAS) in the Danube River Basin; *Geophysical Research Abstracts, Vol. 7, 09297, 2005, SRef-ID: 1607-7962/gra/EGU05-A-09297 © European Geosciences Union 2005*

Kalaš, M., J.A. Szabó, J. van der Knijff, K. Bódis and A. De Roo (2004) Setup, calibration and testing of the Lisflood model for the Morava River basin on 1km, *In: 2nd EFAS workshop, Book of Abstracts, (Editors: J. Thielen, A. de Roo), European Communities, S.P.I. 04.187 (2004)*

Gierk, M., J. Younis, J.A. Szabó, M. Kalaš, K. Bódis and J. van der Knijff (2004) EFAS - Status of Data Collection for the Elbe River Basin and initial Results of hydrological Model Calibration for the German Elbe on 1 km *In: 2nd EFAS workshop, Book of Abstracts, (Editors: J. Thielen, A. de Roo), European Communities, S.P.I. 04.187 (2004)*

Younis, J., J.A. Szabó, M. Kalaš, M. Gierk, K. Bódis, A. de Roo, J. Thielen, J. and van der Knijff (2004), Calibration and Validation of the LISFLOOD Model to the Czech Part of Elbe and odra River Basins *In: 2nd EFAS workshop, Book of Abstracts, (Editors: J. Thielen, A. de Roo), European Communities, S.P.I. 04.187 (2004)*

b) Flood Forecasting and Early Flash Flood Warning

Thielen-del Pozo, J., J. Bartholmes, M.-H. Ramos and A. de Roo (2009) The European Flood Alert System. Part 1: Concept and development. *Hydrology and Earth System Sciences, 13, pp. 125-140.*

Younis, J., S. Anquetin and J. Thielen (2008) The Benefit of High-Resolution operational Weather Forecasts for Flash Flood Warning. *Hydrology and Earth System Sciences 12, pp. 1039-1051.*

Younis, J., M.-H. Ramos, J. Thielen (2008) EFAS Forecasts for The March-April 2006 Flood In The Czech Part Of The Elbe River Basin - A Case Study. *Atmospheric Science Letters, 9:88-94*

Thielen Del Pozo, J., P. Salamon, A. de Roo (2008) Geographical Information Systems - An Integral Part of the European Flood Alert System (EFAS). *Geo-Focus (8); 2008. pp. 12-16. JRC47743*

Younis, J. and J. Thielen (2008) Early Flash Flood Warning: A feasibility study with a distributed hydrological model and threshold exceedance. *European Commission, Directorate-General Joint Research Centre, Institute for Environment and Sustainability, Ispra, Italy, p. 55. EUR 23637 EN*

Thielen, J. and J. Bartholmes (Eds.) (2007) European Flood Alert System 4th Annual Report 2006; *European Commission, Directorate-General Joint Research Centre, Institute for Environment and Sustainability, Ispra, Italy, EUR 23044 EN*

c) Feasibility Studies in African River Basins

Thiemig, V. (2009) Early Flood Warning in Africa: Are the Methodologies of the European Flood Alert System (EFAS) Transferable to African Basins? – A Feasibility Study in the Juba-Shabelle River Basin. *Master's thesis. Radboud University Nijmegen & University Duisburg-Essen.*

Thiemig, V., F. Pappenberger, J. Thielen, H. Gadain, A. de Roo, K. Bodis, M. Del Medico and F. Muthusi (2009) Ensemble Flood Forecasting in Africa: A Feasibility Study in the Juba-Shabelle River Basin, *submitted to Atmospheric Science Letters*.

d) Flood Hazard and Risk Mapping

Barredo, J., P. Salamon, K. Bódis (2008) Towards an assessment of coastal flood damage potential in Europe. *European Commission, Directorate-General Joint Research Centre, Institute for Environment and Sustainability, Ispra, Italy, p. 30. EUR 23698 EN*

Barredo, J.I., P. Salamon, L. Feyen, R. Dankers, K. Bódis and A. de Roo (2008) Flood damage potential in Europe. Map. Institute for Environment and Sustainability, *European Commission - Joint Research Centre, Ispra. Catalogue number: LB-30-08-670-EN-C, ISBN: 978-92-79-09769-0, Luxembourg: Office for Official Publications of the European Communities.*

de Roo, A., J. Barredo, C. Lavalle, K. Bódis and R. Bonk (2007) Potential flood hazard and risk mapping at pan-European scale. *In: R. Peckham and G. Jordan (eds.), Digital elevation modelling. Development and applications in a policy support environment. pp. 183-202. Springer Verlag, Berlin, ISBN: 978-3-540-36730*

Barredo, J.I., A. de Roo and C. Lavalle (2007) Flood risk mapping at European scale. *Water Science and Technology, Vol. 56, 4, 11-17.*

e) Climate Change Impact on Floods

Feyen, L., R. Dankers, K. Bódis, P. Salamon and J.I. Barredo (2009) Climate warming and future flood risk in Europe, *submitted to Climatic Change*.

Dankers, R. and L. Feyen (2008) Climate change impact on flood hazard in Europe: An assessment based on high-resolution climate simulations, *Journal of Geophysical Research, 113, D19105, doi:10.1029/2007JD009719.*

Dankers, R. and L. Feyen (2009) Flood hazard in Europe in an ensemble of regional climate scenarios, *Journal of Geophysical Research, 114, D16108, doi:10.1029/2008JD011523*.

Dankers, R. and L. Feyen (2008) Climate change impact on flood hazard in Europe: An assessment based on high-resolution climate simulations, *Journal of Geophysical Research, 113, D19105, doi:10.1029/2007JD009719*.

Feyen L., J.I. Barredo and R. Dankers (2008) Implications of Global Warming and Urban Land Use Change on Flooding in Europe. *In: Water and Urban Development Paradigms - Towards an Integration of Engineering, Design and Management Approaches. Leiden (The Netherlands): CRC Press - Balkema; p. 217-225.*

Feyen, L., R. Dankers, J. Barredo Cano, A. de Roo and C. Lavalle (2006) Climate Change and Floods in Europe - *In: Climate Change Impacts on the Water Cycle, Resources and Quality Research-Policy Interface, Scientific and policy report (EUR 22422), Brussels, pages 37-43, Directorate-General for Research (Publ.), Brussels*

Feyen, L., R. Dankers, J.I. Barredo, M. Kalas, K. Bódis, A. de Roo and C. Lavalle (2006) PESETA, Projections of economic impacts of climate change in sectors of Europe based on bottom-up analysis, Flood risk in Europe in a changing climate. *European Commission, Directorate-General Joint Research Centre, Institute for Environment and Sustainability Ispra, Italy, p. 20. EUR 22313 EN*

Acknowledgements

The data set has been developed within the Weather Driven Natural Hazards, later FLOODS Action of the Land Management and Natural Hazards unit of the Institute for Environment and Sustainability, Joint Research Centre. I would like to thank all the colleagues in the ‘Flood Group’ and the ‘Spatial Planning Group’ for the supportive and dynamic working environment.
I would also like to thank Roland Hiederer for his introduction into the European coverage of various geo-spatial data sets and for the constructive discussions about river networks.

The source of processed digital elevation models was the Shuttle Radar Topography Mission (SRTM) elevation data. The global source data was available from the website of Consultative Group on International Agricultural Research - Consortium for Spatial Information (CGIAR-CSI). The projected European subset of the data has been prepared in the frame of the Catchment Characterisation and Modelling activity. Jürgen Vogt and Alfred de Jager (IES, DESERT Action) are thanked for providing the public DEM100.

The applied reference 1 km gridded flow network and vector river network database have been developed for the Catchment-based Information System (CIS) by Roland Hiederer and Ad de Roo.

The source data of European land cover maps have been provided by the European Environment Agency (EEA) in Copenhagen, Denmark. I would like to thank Philippe Mayaux (IES, Global Environment Monitoring unit) for the access to the applied global land cover data and for time series vegetation data of Africa, and Carlo Lavalle for his support and continuous feedback on applicability of processed data in land use modelling.

Furthermore, I would like to thank Luca Montanarella and Marc van Liedekerke (IES, SOIL Action) for the access to the soil database.

References

Annoni, A., C. Luzet, E. Gubler and J. Ihde (Eds.) (2001) Map Projections for Europe, *European Commission, Directorate-General Joint Research Centre, Institute for Environment and Sustainability, Ispra, Italy, p. 131. EUR 20120 EN*
URL: http://www.ec-gis.org/sdi/publist/pdfs/annoni-etal2003eur.pdf

Burrough, P. A. (1986): Principles of Geographical Information Systems for Land Resources Assessment (Monographs on Soil Resources Survey), *Oxford University Press, New York, p. 193.*

Döll, P. and B. Lehner (2002) Validation of a new global 30-min drainage direction map, *Journal of Hydrology 258 (2002), pp. 214-231.*

EEA (2000): CORINE land cover technical guide – Addendum 2000. *Technical report No 40, European Environment Agency, Copenhagen, pp. 105.*
Documentation: URL: http://reports.eea.europa.eu/tech40add/en
Data source: URL: http://dataservice.eea.europa.eu/dataservice/metadetails.asp?id=1103

Engelen, G., C. Lavalle, J. Barredo Cano, M. Van Der Meulen and R. White (2007) The MOLAND Modelling Framework for Urban and Regional Land-Use Dynamics, *In: Koomen, E., Stillwell, J., Bakema, A., Scholten, HJ. editors. Modelling Land-Use Change. Dordrecht (The Netherlands): Springer; 2007. p. 297-319.*

FAO/IIASA/ISRIC/ISSCAS/JRC (2009) Harmonized World Soil Database (version 1.1).
FAO, Rome, Italy and IIASA, Laxenburg, Austria.
URL: http://www.iiasa.ac.at/Research/LUC/luc07/External-World-soil-database/HTML

Farr, T. G., Rosen, P. A., Caro, E., Crippen, R., Duren, R., Hensley, S., Kobrick, M., Paller, M., Rodriguez, E., Roth, L., Seal, D., Shaffer, S., Shimada, J., Umland, J., Werner, M., Oskin, M., Burbank, D. and Alsdorf, D. (2007) The Shuttle Radar Topography Mission, *Reviews of Geophysics, Volume 45. RG2004, doi:10.1029/2005RG000183.*

GEM (2003) Global Land Cover 2000 database, *European Commission, Joint Research Centre, 2003*, Documentation and data URL: http://bioval.jrc.ec.europa.eu/products/glc2000/glc2000.php

Gierk, M., K. Bodis, J. Younis, J. Szabo and A. de Roo (2008) The impact of retention polders, dyke-shifts and reservoirs on discharge in the Elbe river, Hydrological modelling study in the framework of the Action Plan for the Flood Protection in the Elbe River Basin of the International Commission for the Protection of the Elbe River (ICPER), *European Commission, Directorate-General Joint Research Centre, Institute for Environment and Sustainability, Ispra, Italy, p. 110. EUR 23699 EN*

Grohman, G., G. Kroenung and J. Strebeck (2006) Filling SRTM Voids: The Delta Surface Fill Method, *Photogrammetric Engineering and Remote Sensing, Vol. 72, No. 3, pp. 213-216.*

Hagedorn, H. (1985) The relief of the earth's surface. *In: Landolt-Börnstein. Numerical Data and Functional Relationships in Science and Technology. New Series. Group V: Geophysics and space research. Volume 2: Geophysics of the solid earth, the moon and the planets. Subvolume b.. K.-H. Hellwege, O. Madelung (Editors-in-chief), K. Fuchs, H. Soffel (Editors). Springer-Verlag, Berlin - Heidelberg - New York - Tokyo, 1985, p. 14+468.*

Hiederer, R. and A. de Roo (2003) A European flow network and catchment data set.
Report of the European Commission, Joint Research Centre, p. 41. EUR 20703 EN

Hiederer, R. and R.J.A. Jones (2009) Development of a spatial European soil property data set, *European Commission, Directorate-General Joint Research Centre, Institute for Environment and Sustainability, Ispra, Italy, p. 30. EUR 23839 EN*

Laguardia, G. (2005) LISFLOOD input map documentation: Land cover map processing, *JRC internal report, Ispra, p. 12.*

Laguardia, G. (2008) Towards improved soil moisture simulations for drought and desertification monitoring and assessment, *WP 2008, Deliverable 4, Final Technical Report, JRC internal report, Ispra, p. 142.*

Lambert, J.J., J. Daroussin, M. Eimberck, C. Le Bas, M. Jamagne, D. King and L. Montanarella (Eds.) (2003) Soil Geographical Database for Eurasia & The Mediterranean: Instructions Guide for Elaboration at scale 1:1,000,000. Version 4.0., *Office for Official Publications of the European Communities, Luxembourg, pp. 64. EUR 20422 EN*

Luedeling, E., S. Siebert, and A. Buerkert (2007) Filling the voids in the SRTM elevation model - A TIN-based delta surface approach, *ISPRS Journal of Photogrammetry & Remote Sensing 62 (2007) 283–294.*

Maidment, D.R. (1996) GIS and hydrological modeling: An assessment of progress. *Paper presented at The Third International Conference on GIS and Environmental Modeling, Santa Fe, New Mexico, U.S.A., January 22-26, 1996*
URL: http://www.ce.utexas.edu/prof/maidment/GISHYdro/meetings/santafe/santafe.htm

O'Callaghan, J.F. and D.M. Mark (1984) The Extraction of Drainage Networks from Digital Elevation Data, *CVGIP(28), Computer Graphics and Image Processing, No. 3, December 1984, pp. 323-344.*

Panagos, P., M. Van Liedekerke, N. Filippi and L. Montanarella (2006) MEUSIS: Towards a new Multi-scale European Soil Information System. *ECONGEO, 5th European Congress on Regional Geoscientific Cartography and Information, Systems, Barcelona (Spain) June 13th-15th 2006. pp 175-177.*

Pistocchi, A. and D. Pennington (2006) European hydraulic geometries for continental SCALE environmental modelling, *Journal of Hydrology, Volume 329, Issues 3-4, pp. 553-567.*

Reuter H.I., A. Nelson and A. Jarvis (2007) An evaluation of void filling interpolation methods for SRTM data, *International Journal of Geographic Information Science, 21:9, pp. 983-1008.*

Rodriguez, E., Morris, C.S., Belz, J.E., Chapin, E.C., Martin, J.M., Daffer, W. and Hensley, S. (2005): An assessment of the SRTM topographic products, *Technical Report JPL D-31639, Jet Propulsion Laboratory, Pasadena, California, pp. 143.*

Rodriguez, E., C.S. Morris and J.E. Belz (2006) A Global Assessment of the SRTM Performance, *Photogrammetric Engineering and Remote Sensing, Vol. 72, No. 3, pp. 249-260.*

Slater, J. A., Garvey, G., Johnston, C., Haase, J., Heady, B., Kroenung, G. and Little, J. (2006) The SRTM Data Finishing Process and Products, *Photogrammetric Engineering and Remote Sensing, Vol. 72, No. 3, pp. 237-248.*

Soille, P., J. Vogt, J. and R. Colombo (2003) Carving and adaptive drainage enforcement of grid digital elevation models, *Water Resources Research, Volume 39, No. 12, 1366, pp. 1366-1375.*

Soille, P. (2004a): Morphological carving, *Pattern Recognition Letters 25 (2004), pp. 543–550*

Soille, P. (2004b) Optimal removal of spurious pits in grid digital elevation models, *Water Resources Research, Volume 40, W12509, doi:10.1029/2004WR003060.*

Thiemig, V. (2009) Early Flood Warning in Africa: Are the Methodologies of the European Flood Alert System (EFAS) Transferable to African Basins? – A Feasibility Study in the Juba-Shabelle River Basin. *Master's thesis. Radboud University Nijmegen & University Duisburg-Essen.*

Tóth, G., L. Montanarella, V. Stolbovoy, F. Máté, K. Bódis, A. Jones, P. Panagos, and M. Van Liedekerke (2008) Soils of the European Union, *European Commission, Directorate-General Joint Research Centre, Institute for Environment and Sustainability, Ispra, Italy, p.151, JRC Scientific and Technical Reports, EUR 23439 EN*

USGS (2009) GTOPO30 Documentation, *Customer Services, U.S. Geological Survey - Center for Earth Resources Observation and Science (EROS), 47914 252nd Street, Sioux Falls, SD 57198-0001, U.S.A.*, URL: http://edc.usgs.gov/products/elevation/gtopo30/README.html.

van der Knijff, J. and A. de Roo (2008) LISFLOOD Distributed Water Balance and Flood Simulation Model, Revised User Manual, *Joint Research Centre, Institute for Environment and Sustainability, Luxembourg: Office for Official Publications of the European Communities, p. 109. EUR 22166 EN/2*

van Liedekerke, M., P. Panagos, L. Montanarella and N. Filippi (2007) Towards a Multi-scale European Soil Information System. *13th EC-GIS Symposium, July 4th-6th 2007, Porto, (Portugal)*

Vogt, J. V., Soille, P., de Jager, A., Rimavičiūtė, E., Mehl, W., Foisneau, S., Bódis, K., Dusart, J., Paracchini, M.L., Haastrup, P., Bamps, C. (2007a): A Pan-European River and Catchment Database, *European Commission, Directorate-General Joint Research Centre, Institute for Environment and Sustainability, Ispra, Italy, p.119., JRC Reference Reports, EUR 22920 EN*
Documentation: URL: http://desert.jrc.ec.europa.eu/action/php/index.php?action=view&id=23
Data source: URL: http://desert.jrc.ec.europa.eu/action/php/index.php?action=view&id=24

Vogt, J. V., Soille, P., de Jager, A., Rimavičiūtė, E., Mehl, W., Haastrup, P., Paracchini, M. L., Dusart, J., Bodis, K., Foisneau, S., Bamps, C. (2007b): Developing a pan-European Data Base of Drainage Networks and Catchment Boundaries from a 100 Metre DEM, *In: Proceedings of 10th AGILE International Conference on Geographic Information Science, 8-11 May 2007, Aalborg, Denmark*

Wachter, K. (2006) Scientific support towards development of a European Flood Alert System, Pilot project: Danube River Basin using LISFLOOD Model, *Final Technical Report, JRC internal report, Ispra, p. 90.*

Wesseling, C.G., D. Karssenberg, P.A. Burrough and W. Van Deursen (1996) Integrating dynamic environmental models in GIS: the development of a Dynamic Modelling language, *Transactions in GIS, Vol 1: 40-48.* URL: http://pcraster.geo.uu.nl/

Annexes

Annex 1 Geographical Graticule and Metrical Units

Ellipsoid: WGS 1984
Semi-major Axis (a): 6378137.00000000 m
Semi-minor Axis (b): 6356752.31424518 m
One latitudinal degree: 110.946 km

Calculated distances in kilometre and a z-factor defined for surface gradient estimation

latitude [degree]	distance [km]	midline [km]	area [km^2]	z-factor
0	111.319	111.311014	12349.540384	0.000008983153
1	111.303	111.277107	12345.778595	0.000008984521
2	111.252	111.209305	12338.256161	0.000008988628
3	111.167	111.107627	12326.975376	0.000008995481
4	111.048	110.972104	12311.939674	0.000009005089
5	110.896	110.802779	12293.153636	0.000009017467
6	110.710	110.599702	12270.622984	0.000009032635
7	110.490	110.362935	12244.354582	0.000009050615
8	110.236	110.092550	12214.356431	0.000009071435
9	109.949	109.788630	12180.637668	0.000009095129
10	109.628	109.451268	12143.208565	0.000009121732
11	109.274	109.080566	12102.080523	0.000009151288
12	108.887	108.676636	12057.266071	0.000009183842
13	108.466	108.239603	12008.778858	0.000009219447
14	108.013	107.769599	11956.633655	0.000009258160
15	107.526	107.266767	11900.846345	0.000009300044
16	107.007	106.731260	11841.433923	0.000009345169
17	106.455	106.163243	11778.414484	0.000009393609
18	105.871	105.562887	11711.807227	0.000009445446
19	105.255	104.930375	11641.632440	0.000009500768
20	104.606	104.265901	11567.911499	0.000009559672
21	103.926	103.569666	11490.666859	0.000009622259
22	103.214	102.841883	11409.922052	0.000009688642
23	102.470	102.082773	11325.701672	0.000009758941
24	101.695	101.292568	11238.031373	0.000009833285
25	100.890	100.471508	11146.937861	0.000009911812
26	100.053	99.619844	11052.448883	0.000009994673
27	99.186	98.737835	10954.593223	0.000010082028
28	98.289	97.825748	10853.400688	0.000010174050
29	97.362	96.883864	10748.902101	0.000010270924
30	96.406	95.912467	10641.129295	0.000010372851
31	95.419	94.911855	10530.115098	0.000010480046
32	94.404	93.882331	10415.893325	0.000010592740
33	93.360	92.824210	10298.498771	0.000010711182
34	92.288	91.737814	10177.967194	0.000010835640
35	91.188	90.623474	10054.335310	0.000010966405
36	90.059	89.481529	9927.640778	0.000011103788
37	88.904	88.312327	9797.922190	0.000011248126
38	87.721	87.116224	9665.219060	0.000011399785
39	86.511	85.893585	9529.571811	0.000011559158
40	85.276	84.644782	9391.021762	0.000011726673
41	84.014	83.370195	9249.611117	0.000011902794
42	82.727	82.070213	9105.382950	0.000012088024
43	81.414	80.745231	8958.381196	0.000012282912
44	80.077	79.395654	8808.650632	0.000012488052
45	78.715	78.021891	8656.236868	0.000012704097

Calculated distances in kilometre and a z-factor defined for surface gradient estimation (cont.)

latitude [degree]	distance [km]	midline [km]	area [km^2]	z-factor
46	77.329	76.624363	8501.186330	0.000012931756
47	75.920	75.203494	8343.546249	0.000013171810
48	74.487	73.759718	8183.364642	0.000013425111
49	73.032	72.293473	8020.690304	0.000013692598
50	71.555	70.805207	7855.572785	0.000013975305
51	70.056	69.295374	7688.062383	0.000014274371
52	68.535	67.764432	7518.210122	0.000014591059
53	66.994	66.212848	7346.067742	0.000014926767
54	65.432	64.641096	7171.687679	0.000015283052
55	63.850	63.049653	6995.123050	0.000015661649
56	62.249	61.439005	6816.427638	0.000016064497
57	60.629	59.809641	6635.655877	0.000016493773
58	58.990	58.162059	6452.862831	0.000016951927
59	57.334	56.496761	6268.104180	0.000017441726
60	55.660	54.814253	6081.436204	0.000017966306
61	53.969	53.115048	5892.915764	0.000018529238
62	52.261	51.399663	5702.600284	0.000019134605
63	50.538	49.668622	5510.547737	0.000019787094
64	48.799	47.922451	5316.816624	0.000020492117
65	47.046	46.161683	5121.465957	0.000021255950
66	45.278	44.386853	4924.555242	0.000022085920
67	43.496	42.598503	4726.144460	0.000022990625
68	41.701	40.797176	4526.294048	0.000023980232
69	39.893	38.983423	4325.064883	0.000025066842
70	38.074	37.157795	4122.518262	0.000026264982
71	36.242	35.320848	3918.715881	0.000027592234
72	34.400	33.473142	3713.719822	0.000029070093
73	32.547	31.615240	3507.592528	0.000030725110
74	30.684	29.747707	3300.396787	0.000032590477
75	28.812	27.871113	3092.195713	0.000034708237
76	26.931	25.986030	2883.052726	0.000037132451
77	25.041	24.093030	2673.031534	0.000039933811
78	23.145	22.192692	2462.196110	0.000043206579
79	21.241	20.285593	2250.610678	0.000047079294
80	19.330	18.372316	2038.339688	0.000051731915
81	17.414	16.453442	1825.447799	0.000057424384
82	15.493	14.529556	1611.999862	0.000064546617
83	13.566	12.601244	1398.060894	0.000073711342
84	11.636	10.669094	1183.696063	0.000085939777
85	9.702	8.733694	968.970667	0.000103070120
86	7.765	6.795634	753.950113	0.000128778769
87	5.826	4.855503	538.699898	0.000171643999
88	3.885	2.913894	323.285590	0.000257400642
89	1.943	0.971396	107.772806	0.000514722876
90	0.000	0.000000	0.000000	-

Annex 2 CLC2000 Classes

Applied land cover classes of CORINE Land Cover 2000

GRID_CODE	LABEL1	LABEL3
1	Artificial surfaces	Continuous urban fabric
2	Artificial surfaces	Discontinuous urban fabric
3	Artificial surfaces	Industrial or commercial units
4	Artificial surfaces	Road and rail networks and associated land
5	Artificial surfaces	Port areas
6	Artificial surfaces	Airports
7	Artificial surfaces	Mineral extraction sites
8	Artificial surfaces	Dump sites
9	Artificial surfaces	Construction sites
10	Artificial surfaces	Green urban areas
11	Artificial surfaces	Sport and leisure facilities
12	Agricultural areas	Non-irrigated arable land
13	Agricultural areas	Permanently irrigated land
14	Agricultural areas	Rice fields
15	Agricultural areas	Vineyards
16	Agricultural areas	Fruit trees and berry plantations
17	Agricultural areas	Olive groves
18	Agricultural areas	Pastures
19	Agricultural areas	Annual crops associated with permanent crops
20	Agricultural areas	Complex cultivation patterns
21	Agricultural areas	Land principally occupied by agriculture, with significant areas of natural vegetation
22	Agricultural areas	Agro-forestry areas
23	Forest and semi natural areas	Broad-leaved forest
24	Forest and semi natural areas	Coniferous forest
25	Forest and semi natural areas	Mixed forest
26	Forest and semi natural areas	Natural grasslands
27	Forest and semi natural areas	Moors and heathland
28	Forest and semi natural areas	Sclerophyllous vegetation
29	Forest and semi natural areas	Transitional woodland-shrub
30	Forest and semi natural areas	Beaches, dunes, sands
31	Forest and semi natural areas	Bare rocks
32	Forest and semi natural areas	Sparsely vegetated areas
33	Forest and semi natural areas	Burnt areas
34	Forest and semi natural areas	Glaciers and perpetual snow
35	Wetlands	Inland marshes
36	Wetlands	Peat bogs
37	Wetlands	Salt marshes
38	Wetlands	Salines
39	Wetlands	Intertidal flats
40	Water bodies	Water courses
41	Water bodies	Water bodies
42	Water bodies	Coastal lagoons
43	Water bodies	Estuaries
44	Water bodies	Sea and ocean

Annex 3 GLC2000 Classes

Applied land cover classes based on Global Land Cover 2000

GLC2000	***Legend***
1	Tree Cover, broadleaved, evergreen
2	Tree Cover, broadleaved, deciduous, closed
3	Tree Cover, broadleaved, deciduous, open
4	Tree Cover, needle-leaved, evergreen
5	Tree Cover, needle-leaved, deciduous
6	Tree Cover, mixed leaf type
7	Tree Cover, regularly flooded, fresh water
8	Tree Cover, regularly flooded, saline water
9	Mosaic: Tree Cover / Other natural vegetation
10	Tree Cover, burnt
11	Shrub Cover, closed-open, evergreen
12	Shrub Cover, closed-open, deciduous
13	Herbaceous Cover, closed-open
14	Sparse herbaceous or sparse shrub cover
15	Regularly flooded shrub and/or herbaceous cover
16	Cultivated and managed areas
17	Mosaic: Cropland / Tree Cover / Other natural vegetation
18	Mosaic: Cropland / Shrub and/or grass cover
19	Bare Areas
20	Water Bodies
21	Snow and Ice
22	Artificial surfaces and associated areas
23	Irrigated Agriculture

Annex 4 Land Cover Classes after Resampling

Aggregated Area [km^2] of Land Cover Classes after Resampling (Based on CLC2000 Classes)

CLC Code	ELC100M source cells	ELC1KM central cells	ELC1KM dominant cells	ELC5KM central cells	ELC5KM dominant cells	ELC100M source Area [km^2]	KM2_1KM dominant Area [km^2]	KM2_5KM dominant Area [km^2]
1	591389	5905	5255	225	134	5913.89	5255	3350
2	14283267	141667	120058	5579	3051	142832.7	120058	76275
3	2034093	19744	14741	792	119	20340.93	14741	2975
4	194081	1959	506	78	8	1940.81	506	200
5	109223	1029	1683	48	65	1092.23	1683	1625
6	298750	2910	2770	126	27	2987.5	2770	675
7	628747	6210	4250	253	59	6287.47	4250	1475
8	109817	1102	863	48	9	1098.17	863	225
9	115948	1115	664	47	7	1159.48	664	175
10	300113	2961	1705	105	11	3001.13	1705	275
11	857108	8100	6361	319	78	8571.08	6361	1950
12	166460177	1686202	1813191	67615	85687	1664602	1813191	2142175
13	3522187	35283	35531	1373	1448	35221.87	35531	36200
14	588185	5832	6005	235	245	5881.85	6005	6125
15	3930109	39190	39363	1623	1492	39301.09	39363	37300
16	2501280	24997	24117	981	777	25012.8	24117	19425
17	3994029	39956	41725	1578	1810	39940.29	41725	45250
18	43999708	486444	480027	19530	17351	439997.1	480027	433775
19	957693	9612	9596	374	354	9576.93	9596	8850
20	27432433	271010	258348	10629	8572	274324.3	258348	214300
21	22872814	217399	169257	8825	3322	228728.1	169257	83050
22	3193487	31918	32820	1310	1427	31934.87	32820	35675
23	72516914	680407	689504	27263	28391	725169.1	689504	709775
24	110541707	1128927	1205668	44802	56239	1105417	1205668	1405975
25	57136813	629636	630579	25224	24097	571368.1	630579	602425
26	12491260	121387	118673	4882	4607	124912.6	118673	115175
27	22865612	165964	171843	6622	7744	228656.1	171843	193600
28	12322744	123652	130399	4969	6444	123227.4	130399	161100
29	25215715	246910	207837	9927	5531	252157.2	207837	138275
30	704017	3724	4400	162	205	7040.17	4400	5125
31	6608685	20893	21373	876	951	66086.85	21373	23775
32	15125163	186925	188997	7499	8221	151251.6	188997	205525
33	139503	1322	1387	47	30	1395.03	1387	750
34	1785637	19995	19786	752	700	17856.37	19786	17500
35	1276925	12282	9934	506	276	12769.25	9934	6900
36	18760508	184438	174686	7370	5056	187605.1	174686	126400
37	316323	3083	3452	120	121	3163.23	3452	3025
38	75988	758	820	37	39	759.88	820	975
39	1169506	10392	14767	411	880	11695.06	14767	22000
40	1229660	11028	5388	454	46	12296.6	5388	1150
41	18743440	179863	177529	7238	6283	187434.4	177529	157075
42	590089	5616	5939	234	320	5900.89	5939	8000
43	332138	3282	3340	123	142	3321.38	3340	3550
44	14198	164	134	7	3	141.98	134	75
Area [km^2]	*6,789,372*	*6,781,193*	*6,855,271*	*6,780,450*	*7,082,575*	*6,789,372*	*6,855,271*	*7,059,475*

ELC100M – merged CLC2000 and GLC2000 in 100 m resolution
ELC1KM – resampled ELC100M in 1 km m resolution
ELC5KM – resampled ELC100M in 5 km m resolution

Annex 5 Classes of Permeability Based on CLC2000

Classification Used for Processing the Direct Runoff Fraction Maps of Europe

CLC2000 Code	Legend	Permeability Class	Impermeable Area [%]
1	Continuous urban fabric	3	0.75
2	Discontinuous urban fabric	2	0.5
3	Industrial or commercial units	3	0.75
4	Road and rail networks and associated land	2	0.5
5	Port areas	3	0.75
6	Airports	2	0.5
7	Mineral extraction sites	2	0.5
8	Dump sites	1	0.25
9	Construction sites	1	0.25
10	Green urban areas	1	0.25
11	Sport and leisure facilities	1	0.25
12	Non-irrigated arable land	0	0
13	Permanently irrigated land	0	0
14	Rice fields	0	0
15	Vineyards	0	0
16	Fruit trees and berry plantations	0	0
17	Olive groves	0	0
18	Pastures	0	0
19	Annual crops associated with permanent crops	0	0
20	Complex cultivation patterns	0	0
21	Land principally occupied by agriculture, with significant areas of natural vegetation	0	0
22	Agro-forestry areas	0	0
23	Broad-leaved forest	0	0
24	Coniferous forest	0	0
25	Mixed forest	0	0
26	Natural grasslands	0	0
27	Moors and heathland	0	0
28	Sclerophyllous vegetation	0	0
29	Transitional woodland-shrub	0	0
30	Beaches, dunes, sands	0	0
31	Bare rocks	3	0.75
32	Sparsely vegetated areas	0	0
33	Burnt areas	0	0
34	Glaciers and perpetual snow	3	0.75
35	Inland marshes	2	0.5
36	Peat bogs	2	0.5
37	Salt marshes	3	0.75
38	Salines	4	1
39	Intertidal flats	4	1
40	Water courses	4	1
41	Water bodies	4	1
42	Coastal lagoons	4	1
43	Estuaries	4	1
44	Sea and ocean	4	1

Based on Laguardia, 2005.

Annex 6 Description of Processed PCRaster Maps

EUROPEAN DATA SET

Coordinate System: 'GISCO LAEA 0948'
Corner Coordinates:
Upper Left (-1700000.000, 2700000.000)
Lower Left (-1700000.000,-1350000.000)
Upper Right (1700000.000, 2700000.000)
Lower Right (1700000.000,-1350000.000)
Center (0.000, 675000.000)

CHANBW_1KM.MAP
Format: PCRaster/PCRaster Raster File
Size is 3400, 4050
Coordinate System is 'GISCO LAEA 0948'
Pixel Size = (1000.000,-1000.000)
Band 1 Block=3400x1 Type=Float32
Min=3.000 Max=1500.000
NoData Value=-3.40282346638529e+38

CHANLENG_1KM.MAP
Format: PCRaster/PCRaster Raster File
Size is 3400, 4050
Coordinate System is 'GISCO LAEA 0948'
Pixel Size = (1000.000,-1000.000)
Band 1 Block=3400x1 Type=Float32
Min=667.000 Max=1584.000
NoData Value=-3.40282346638529e+38

DEM_CENT_1KM.MAP
Format: PCRaster/PCRaster Raster File
Size is 3400, 4050
Coordinate System is 'GISCO LAEA 0948'
Pixel Size = (1000.000,-1000.000)
Band 1 Block=3400x1 Type=Float32
Min=-10.000 Max=4562.000
NoData Value=-3.40282346638529e+38

DEM_RR_1KM.MAP
Format: PCRaster/PCRaster Raster File
Size is 3400, 4050
Coordinate System is 'GISCO LAEA 0948'
Pixel Size = (1000.000,-1000.000)
Band 1 Block=3400x1 Type=Float32
Min=0.000 Max=1791.000
NoData Value=-3.40282346638529e+38

DEM_STD_1KM.MAP
Format: PCRaster/PCRaster Raster File
Size is 3400, 4050
Coordinate System is 'GISCO LAEA 0948'
Pixel Size = (1000.000,-1000.000)
Band 1 Block=3400x1 Type=Float32
Min=0.000 Max=524.997
NoData Value=-3.40282346638529e+38

CHANGRAD_1KM.MAP
Format: PCRaster/PCRaster Raster File
Size is 3400, 4050
Coordinate System is 'GISCO LAEA 0948'
Pixel Size = (1000.000,-1000.000)
Band 1 Block=3400x1 Type=Float32
Min=0.000 Max=0.656
NoData Value=-3.40282346638529e+38

CHANMAN_1KM.MAP
Format: PCRaster/PCRaster Raster File
Size is 3400, 4050
Coordinate System is 'GISCO LAEA 0948'
Pixel Size = (1000.000,-1000.000)
Band 1 Block=3400x1 Type=Float32
Min=0.030 Max=0.065
NoData Value=-3.40282346638529e+38

DEM_MEAN_1KM.MAP
Format: PCRaster/PCRaster Raster File
Size is 3400, 4050
Coordinate System is 'GISCO LAEA 0948'
Pixel Size = (1000.000,-1000.000)
Band 1 Block=3400x1 Type=Float32
Min=-10.000 Max=4443.010
NoData Value=-3.40282346638529e+38

DEM_SKW_1KM.MAP
Format: PCRaster/PCRaster Raster File
Size is 3400, 4050
Coordinate System is 'GISCO LAEA 0948'
Pixel Size = (1000.000,-1000.000)
Band 1 Block=3400x1 Type=Float32
Min=-9.949 Max=9.949
NoData Value=-3.40282346638529e+38

DIRECTRF_1KM.MAP
Format: PCRaster/PCRaster Raster File
Size is 3400, 4050
Coordinate System is 'GISCO LAEA 0948'
Pixel Size = (1000.000,-1000.000)
Band 1 Block=3400x1 Type=Float32
Min=0.000 Max=1.000
NoData Value=-3.40282346638529e+38

FOREST_1KM.MAP
Format: PCRaster/PCRaster Raster File
Size is 3400, 4050
Coordinate System is 'GISCO LAEA 0948'
Pixel Size = (1000.000,-1000.000)
Band 1 Block=3400x1 Type=Float32
Min=0.000 Max=1.000
NoData Value=-3.40282346638529e+38

GRADIENT_1KM.MAP
Format: PCRaster/PCRaster Raster File
Size is 3400, 4050
Coordinate System is 'GISCO LAEA 0948'
Pixel Size = (1000.000,-1000.000)
Band 1 Block=3400x1 Type=Float32
Min=0.000 Max=1.362
NoData Value=-3.40282346638529e+38

LANDUSE_CENT_1KM.MAP
Format: PCRaster/PCRaster Raster File
Size is 3400, 4050
Coordinate System is 'GISCO LAEA 0948'
Pixel Size = (1000.000,-1000.000)
Band 1 Block=3400x1 Type=Int32
Min=0.000 Max=44.000
NoData Value=-2147483648

LANDUSE_DOMI_1KM.MAP
Format: PCRaster/PCRaster Raster File
Size is 3400, 4050
Coordinate System is 'GISCO LAEA 0948'
Pixel Size = (1000.000,-1000.000)
Band 1 Block=3400x1 Type=Int32
Min=0.000 Max=44.000
NoData Value=-2147483648

LDD_1KM.MAP
Format: PCRaster/PCRaster Raster File
Size is 3400, 4050
Coordinate System is 'GISCO LAEA 0948'
Pixel Size = (1000.000,-1000.000)
Band 1 Block=3400x1 Type=Byte
Min=1.000 Max=9.000
NoData Value=255

CHANBNKF_5KM.MAP
Format: PCRaster/PCRaster Raster File
Size is 680, 810
Coordinate System is 'GISCO LAEA 0948'
Pixel Size = (5000.000,-5000.000)
Band 1 Block=680x1 Type=Float32
Min=0.781 Max=16.000
NoData Value=-3.40282346638529e+38

CHANBW_5KM.MAP
Format: PCRaster/PCRaster Raster File
Size is 680, 810
Coordinate System is 'GISCO LAEA 0948'
Pixel Size = (5000.000,-5000.000)
Band 1 Block=680x1 Type=Float32
Min=3.000 Max=999.520
NoData Value=-3.40282346638529e+38

CHANGRAD_5KM.MAP
Format: PCRaster/PCRaster Raster File
Size is 680, 810
Coordinate System is 'GISCO LAEA 0948'
Pixel Size = (5000.000,-5000.000)
Band 1 Block=680x1 Type=Float32
Min=0.000 Max=0.522
NoData Value=-3.40282346638529e+38

CHANLENG_5KM.MAP
Format: PCRaster/PCRaster Raster File
Size is 680, 810
Coordinate System is 'GISCO LAEA 0948'
Pixel Size = (5000.000,-5000.000)
Band 1 Block=680x1 Type=Float32
Min=768.000 Max=11669.000
NoData Value=-3.40282346638529e+38

DEM_CENT_5KM.MAP
Format: PCRaster/PCRaster Raster File
Size is 680, 810
Coordinate System is 'GISCO LAEA 0948'
Pixel Size = (5000.000,-5000.000)
Band 1 Block=680x1 Type=Float32
Min=-10.000 Max=4092.000
NoData Value=-3.40282346638529e+38

DEM_MEAN_5KM.MAP
Format: PCRaster/PCRaster Raster File
Size is 680, 810
Coordinate System is 'GISCO LAEA 0948'
Pixel Size = (5000.000,-5000.000)
Band 1 Block=680x1 Type=Float32
Min=-9.250 Max=3539.372
NoData Value=-3.40282346638529e+38

DEM_RR_5KM.MAP
Format: PCRaster/PCRaster Raster File
Size is 680, 810
Coordinate System is 'GISCO LAEA 0948'
Pixel Size = (5000.000,-5000.000)
Band 1 Block=680x1 Type=Float32
Min=0.000 Max=2999.000
NoData Value=-3.40282346638529e+38

DEM_SKW_5KM.MAP
Format: PCRaster/PCRaster Raster File
Size is 680, 810
Coordinate System is 'GISCO LAEA 0948'
Pixel Size = (5000.000,-5000.000)
Band 1 Block=680x1 Type=Float32
Min=-18.026 Max=35.327
NoData Value=-3.40282346638529e+38

DEM_STD_5KM.MAP
Format: PCRaster/PCRaster Raster File
Size is 680, 810
Coordinate System is 'GISCO LAEA 0948'
Pixel Size = (5000.000,-5000.000)
Band 1 Block=680x1 Type=Float32
Min=0.000 Max=709.146
NoData Value=-3.40282346638529e+38

DIRECTRF_5KM.MAP
Format: PCRaster/PCRaster Raster File
Size is 680, 810
Coordinate System is 'GISCO LAEA 0948'
Pixel Size = (5000.000,-5000.000)
Band 1 Block=680x1 Type=Float32
Min=0.000 Max=1.000
NoData Value=-3.40282346638529e+38

FOREST_5KM.MAP
Format: PCRaster/PCRaster Raster File
Size is 680, 810
Coordinate System is 'GISCO LAEA 0948'
Pixel Size = (5000.000,-5000.000)
Band 1 Block=680x1 Type=Float32
Min=0.000 Max=1.000
NoData Value=-3.40282346638529e+38

GRADIENT_5KM.MAP
Format: PCRaster/PCRaster Raster File
Size is 680, 810
Coordinate System is 'GISCO LAEA 0948'
Pixel Size = (5000.000,-5000.000)
Band 1 Block=680x1 Type=Float32
Min=0.000 Max=0.698
NoData Value=-3.40282346638529e+38

LANDUSE_CENT_5KM.MAP
Format: PCRaster/PCRaster Raster File
Size is 680, 810
Coordinate System is 'GISCO LAEA 0948'
Pixel Size = (5000.000,-5000.000)
Band 1 Block=680x1 Type=Int32
Min=0.000 Max=44.000
NoData Value=-2147483648

LANDUSE_DOMI_5KM.MAP
Format: PCRaster/PCRaster Raster File
Size is 680, 810
Coordinate System is 'GISCO LAEA 0948'
Pixel Size = (5000.000,-5000.000)
Band 1 Block=680x1 Type=Int32
Min=0.000 Max=43.000
NoData Value=-2147483648

LDD_5KM.MAP
Format: PCRaster/PCRaster Raster File
Size is 680, 810
Coordinate System is 'GISCO LAEA 0948'
Pixel Size = (5000.000,-5000.000)
Band 1 Block=680x1 Type=Byte
Min=1.000 Max=9.000
NoData Value=255

UPS_5KM.MAP
Format: PCRaster/PCRaster Raster File
Size is 680, 810
Coordinate System is 'GISCO LAEA 0948'
Pixel Size = (5000.000,-5000.000)
Band 1 Block=680x1 Type=Float32
Min=25.000 Max=797350.000
NoData Value=-3.40282346638529e+38

AFRICAN DATA SET

Coordinate System: Geographic Lat/Lon
Corner Coordinates:
Upper Left (-20.0000000, 40.0000000)
Lower Left (-20.0000000, -35.0000000)
Upper Right (60.0000000, 40.0000000)
Lower Right (60.0000000, -35.0000000)
Center (20.0000000, 2.5000000)

Pixel Size = (0.100000000000000,-0.100000000000000)

CELL_AREA_01.MAP
Format: PCRaster/PCRaster Raster File
Size is 800, 750
Coordinate System is 'Geographic Lat/Lon'
Band 1 Block=800x1 Type=Float32
Min=94.541 Max=123.504
NoData Value=-3.40282346638529e+38

CELL_DIAG_01.MAP
Format: PCRaster/PCRaster Raster File
Size is 800, 750
Coordinate System is 'Geographic Lat/Lon'
Band 1 Block=800x1 Type=Float32
Min=13.989 Max=15.717
NoData Value=-3.40282346638529e+38

CELL_WIDTH_01.MAP
Format: PCRaster/PCRaster Raster File
Size is 800, 750
Coordinate System is 'Geographic Lat/Lon'
Band 1 Block=800x1 Type=Float32
Min=8.521 Max=11.132
NoData Value=-3.40282346638529e+38

CELL_HEIGHT_01.MAP
Format: PCRaster/PCRaster Raster File
Size is 800, 750
Coordinate System is 'Geographic Lat/Lon'
Band 1 Block=800x1 Type=Float32
Min=11.095 Max=11.095
NoData Value=-3.40282346638529e+38

CHANLENG_01.MAP
Format: PCRaster/PCRaster Raster File
Size is 800, 750
Coordinate System is 'Geographic Lat/Lon'
Band 1 Block=800x1 Type=Float32
Min=8837.476 Max=15716.551
NoData Value=-3.40282346638529e+38

DEM_CENT_01.MAP
Format: PCRaster/PCRaster Raster File
Size is 800, 750
Coordinate System is 'Geographic Lat/Lon'
Band 1 Block=800x1 Type=Float32
Min=-157.000 Max=4376.000
NoData Value=-3.40282346638529e+38

DEM_MAX_01.MAP
Format: PCRaster/PCRaster Raster File
Size is 800, 750
Coordinate System is 'Geographic Lat/Lon'
Band 1 Block=800x1 Type=Float32
Min=-113.000 Max=5866.000
NoData Value=-3.40282346638529e+38

DEM_MEAN_01.MAP
Format: PCRaster/PCRaster Raster File
Size is 800, 750
Coordinate System is 'Geographic Lat/Lon'
Band 1 Block=800x1 Type=Float32
Min=-120.750 Max=4207.415
NoData Value=-3.40282346638529e+38

DEM_MIN_01.MAP
Format: PCRaster/PCRaster Raster File
Size is 800, 750
Coordinate System is 'Geographic Lat/Lon'
Band 1 Block=800x1 Type=Float32
Min=-174.000 Max=3579.000
NoData Value=-3.40282346638529e+38

DEM_RR_01.MAP
Format: PCRaster/PCRaster Raster File
Size is 800, 750
Coordinate System is 'Geographic Lat/Lon'
Band 1 Block=800x1 Type=Float32
Min=0.000 Max=3856.000
NoData Value=-3.40282346638529e+38

DEM_SKW_01.MAP
Format: PCRaster/PCRaster Raster File
Size is 800, 750
Coordinate System is 'Geographic Lat/Lon'
Band 1 Block=800x1 Type=Float32
Min=-24.105 Max=24.107
NoData Value=-3.40282346638529e+38

DEM_STD_01.MAP
Format: PCRaster/PCRaster Raster File
Size is 800, 750
Coordinate System is 'Geographic Lat/Lon'
Band 1 Block=800x1 Type=Float32
Min=0.000 Max=824.306
NoData Value=-3.40282346638529e+38

DIRECTRF_01.MAP
Format: PCRaster/PCRaster Raster File
Size is 800, 750
Coordinate System is 'Geographic Lat/Lon'
Band 1 Block=800x1 Type=Float32
Min=0.000 Max=1.000
NoData Value=-3.40282346638529e+38

FOREST_01.MAP
Format: PCRaster/PCRaster Raster File
Size is 800, 750
Coordinate System is 'Geographic Lat/Lon'
Band 1 Block=800x1 Type=Float32
Min=0.000 Max=1.000
NoData Value=-3.40282346638529e+38

GLCCLASS_DOMI_01.MAP
Format: PCRaster/PCRaster Raster File
Size is 800, 750
Coordinate System is 'Geographic Lat/Lon'
Band 1 Block=800x1 Type=Int32
Min=1.000 Max=29.000
NoData Value=-2147483648

GLCCLASS_VARIETY_01.MAP
Format: PCRaster/PCRaster Raster File
Size is 800, 750
Coordinate System is 'Geographic Lat/Lon'
Band 1 Block=800x1 Type=Float32
Min=1.000 Max=12.000
NoData Value=-3.40282346638529e+38

GRADIENT_01.MAP
Format: PCRaster/PCRaster Raster File
Size is 800, 750
Coordinate System is 'Geographic Lat/Lon'
Band 1 Block=800x1 Type=Float32
Min=0.000 Max=0.441
NoData Value=-3.40282346638529e+38

HWSDA10_REFSOILDEPTH.MAP
Format: PCRaster/PCRaster Raster File
Size is 800, 750
Coordinate System is 'Geographic Lat/Lon'
Band 1 Block=800x1 Type=Float32
Min=0.000 Max=101.000
NoData Value=-3.40282346638529e+38

HWSDA10_SCLAY.MAP
Format: PCRaster/PCRaster Raster File
Size is 800, 750
Coordinate System is 'Geographic Lat/Lon'
Band 1 Block=800x1 Type=Float32
Min=0.000 Max=95.000
NoData Value=-3.40282346638529e+38

HWSDA10_SSAND.MAP
Format: PCRaster/PCRaster Raster File
Size is 800, 750
Coordinate System is 'Geographic Lat/Lon'
Band 1 Block=800x1 Type=Float32
Min=2.000 Max=100.000
NoData Value=-3.40282346638529e+38

HWSDA10_SSILT.MAP
Format: PCRaster/PCRaster Raster File
Size is 800, 750
Coordinate System is 'Geographic Lat/Lon'
Band 1 Block=800x1 Type=Float32
Min=0.000 Max=54.000
NoData Value=-3.40282346638529e+38

HWSDA10_TCLAY.MAP
Format: PCRaster/PCRaster Raster File
Size is 800, 750
Coordinate System is 'Geographic Lat/Lon'
Band 1 Block=800x1 Type=Float32
Min=0.000 Max=91.000
NoData Value=-3.40282346638529e+38

HWSDA10_TSAND.MAP
Format: PCRaster/PCRaster Raster File
Size is 800, 750
Coordinate System is 'Geographic Lat/Lon'
Band 1 Block=800x1 Type=Float32
Min=1.000 Max=100.000
NoData Value=-3.40282346638529e+38

HWSDA10_TSILT.MAP
Format: PCRaster/PCRaster Raster File
Size is 800, 750
Coordinate System is 'Geographic Lat/Lon'
Band 1 Block=800x1 Type=Float32
Min=0.000 Max=68.000
NoData Value=-3.40282346638529e+38

LDD_01.MAP
Format: PCRaster/PCRaster Raster File
Size is 800, 750
Coordinate System is 'Geographic Lat/Lon'
Band 1 Block=800x1 Type=Byte
Min=1.000 Max=9.000
NoData Value=255

MANNING_01.MAP
Format: PCRaster/PCRaster Raster File
Size is 800, 750
Coordinate System is 'Geographic Lat/Lon'
Band 1 Block=800x1 Type=Float32
Min=0.040 Max=0.040
NoData Value=-3.40282346638529e+38

SOILDEP_01.MAP
Format: PCRaster/PCRaster Raster File
Size is 800, 750
Coordinate System is 'Geographic Lat/Lon'
Band 1 Block=800x1 Type=Float32
Min=0.000 Max=101.000
NoData Value=-3.40282346638529e+38

SOILTEX1_01.MAP
Format: PCRaster/PCRaster Raster File
Size is 800, 750
Coordinate System is 'Geographic Lat/Lon'
Band 1 Block=800x1 Type=Int32
Min=0.000 Max=5.000
NoData Value=-2147483648

SOILTEX2_01.MAP
Format: PCRaster/PCRaster Raster File
Size is 800, 750
Coordinate System is 'Geographic Lat/Lon'
Band 1 Block=800x1 Type=Int32
Min=0.000 Max=5.000
NoData Value=-2147483648

UPS_01.MAP
Format: PCRaster/PCRaster Raster File
Size is 800, 750
Coordinate System is 'Geographic Lat/Lon'
Band 1 Block=800x1 Type=Float32
Min=98.048 Max=3699470.500
NoData Value=-3.40282346638529e+38

ZFACTAFR_01.MAP
Format: PCRaster/PCRaster Raster File
Size is 800, 750
Coordinate System is 'Geographic Lat/Lon'
Band 1 Block=800x1 Type=Float32
Min=0.000 Max=0.000
NoData Value=-3.40282346638529e+38

European Commission

EUR 24087 EN – Joint Research Centre – Institute for Environment and Sustainability

Title: Development of a data set for continental hydrologic modelling. Input layers related to topography, channel geometry, land cover and soil characteristics of European and African river basins

Author(s): Katalin Bódis

Luxembourg: Publications Office of the European Union
2009 – 80 pp. – 21.0 x 29.7 cm
EUR – Scientific and Technical Research series – ISSN 1018-5593
ISBN 978-92-79-14149-2
doi:10.2788/46925

Abstract

The data set was created for the purpose of updating/processing static input layers for LISFLOOD model. The LISFLOOD model is a hydrological rainfall-runoff model that is capable of simulating the hydrological processes that occur in a catchment. The new data set contains gridded numerical and descriptive information related to topography, channel geometry, land cover and soil characteristics of European and African river basins.

This document gives a brief summary of the source geo-spatial data sets, the applied methodology and the main characteristics of resulted data.

How to obtain EU publications

Our priced publications are available from EU Bookshop (http://bookshop.europa.eu), where you can place an order with the sales agent of your choice.

The Publications Office has a worldwide network of sales agents. You can obtain their contact details by sending a fax to (352) 29 29-42758.

The mission of the JRC is to provide customer-driven scientific and technical support for the conception, development, implementation and monitoring of EU policies. As a service of the European Commission, the JRC functions as a reference centre of science and technology for the Union. Close to the policy-making process, it serves the common interest of the Member States, while being independent of special interests, whether private or national.

LB-NA-24087-EN-C

EUROPEAN COMMISSION

Publications Office

ISBN 978-92-79-14149-2

9 789279 141492